Giant polyoxomolybdates: Syntheses, structure and stability studies

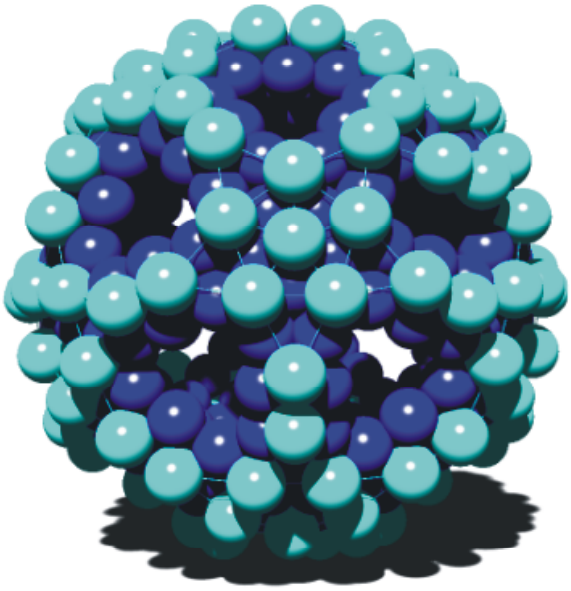

From syntheses of extended structures to novel host design, stability investigations in solution and perspectives for a future mechanistic study.

Soumyajit Roy

Department of Chemistry
University of Bielefeld

March 2005

This thesis is the result of research carried out during the period of July 2001 to March 2005 under the aegis of Prof. Dr. Dr. h. c. mult. Achim Müller, the chair of Anorganische Chemie I at the Universität Bielefeld.

Referee: Prof. Dr. Dr. h.c. mult. Achim Müller

Second referee: Prof. Dr. Lothar Weber

To all those who made my stay at Bielefeld beautiful.

Acknowledgement

2001. I suddenly stumbled upon a cover page of an issue of *Angewandte Chemie International Edition*. There was a picture of an unusually large and beautiful molecule with Kepler's early model of universe. I was lucky to be able to visit this 'land of beautiful molecules' and meet the 'master' of this molecular orchestra, Prof. Dr. Dr. h. c. mult. Achim Müller. Since then he has been my source of inspiration and encouragement. He has given me not only a position to pursue doctoral research but also plenty of freedom, support and exposure. This freedom taught me responsibility. I am thankful to him for extending me all these provisions.

On my first visit to this laboratory in Bielefeld, I was lucky to have unknowingly knocked on the door of Hartmut (Dr. H. Bögge) asking him "Dr. Bögge, do you want to go for a lunch?" Since then his door has always been cordially open to me, be it a scientific problem, a classic of Hesse, or discussion on Coetzeean 'existential crisis'. He has been my teacher in disguise.

Then there was marvellous Marc (Mr. M. Schmidtmann) who has been amiable to my worst crystals. This thesis would not have been possible without his cooperation and help that goes far beyond just mounting, measuring and 'mapping' of the molecular structures described in this thesis. I gratefully acknowledge his cooperation.

I am also extremely grateful to Karin (Ms. K. Lacey) and Dr. E. Diemann for being there always in my hours of need. I would like to remember: Dr. A. Mix for measuring countless NMR spectra; Ms. A. Merca for some fruitful collaborations; Dr. E. Beckmann for her advice in improving Chapter 6; Dr. A. Bell for very quickly leafing through Chapters 5 and 6; Dr. M. Fricke for LB-experiments; Dipl. Chem. A. Berkle, Ms. B. Michel for elemental analyses; Ms. G. Heinze-Brückner, Ms. U. Stuphorn for Raman and EAS measurements.

I am indebted further to numerous other friends and colleagues who made this stay in sojourn a beautiful one. They are endless, and I dare not to list their names. This thesis is dedicated to them all.

This thesis would not have been possible without the generous financial support of 'Graduiertenkolleg Strukturbildungsprozesse', University of Bielefeld. I would also like to express my gratitude to Prof. A. Dress and Prof. W.- J. Beyn, the directors of the 'GK' for their continuous support.

Final word of gratitude goes to my parents, Pei and Banty.

Abstract

In this dissertation investigation of one of the existing ring-shaped polyoxomolybdates led to the formation of extended structures and alluded to their potential host-functionalities. After realizing such potentials in ring-shaped as well as in spherical giant polyoxomolybdates, and studying the structure of water inside the spherical capsules; this dissertation investigated the stability of some selected spherical polyoxomolybdates in aqueous solution. From this study sites vulnerable to 'attack' by degrading agents and hence responsible for their decomposition were proposed and also the role of cations in stabilizing these clusters emerged. The dissertation concludes with a perspective for some open questions regarding the generation of the giant polyoxomolybdates from an ionic soup.

The Figure on the cover depicts an $[O_{372}]$ shell, formed by 132 terminal oxygen atoms (shown in cyan) and 240 bridging oxygen atoms (in blue) of a spherical giant $[Mo_{132}]$ type cluster. These oxygens play a key role in determining the Raman spectral feature of these cluster types. For details please refer to Chapter 6.

List of compounds central to this dissertation[1]

$$^{1}_{\infty}\{(UH^{+})_{14}[Mo^{VI}_{126}Mo^{V}_{28}O_{462}H_{14}(H_2O)_{68}]\}\cdot ca.350H_2O \quad (1)$$

$$^{1}_{\infty}\{(NH_4)_{14}[Mo^{VI}_{126}Mo^{V}_{28}O_{462}H_{14}(H_2O)_{68}]\}\cdot ca.350H_2O \quad (2)$$

$$^{1}_{\infty}\{(UH^{+})_{22-x}K_x[Mo^{VI}_{118}Mo^{V}_{28}O_{442}H_{14}(H_2O)_{57}]\}\cdot nH_2O \quad (3)$$

$$^{1}_{\infty}\{(GH^{+})_{8}Na_{14}[Mo^{VI}_{118}Mo^{V}_{28}O_{442}H_{14}(H_2O)_{57}]\}\cdot ca.300H_2O \quad (4)$$

$$^{1}_{\infty}\{Na_{24}[Mo^{VI}_{116}Mo^{V}_{28}O_{437}H_{14}(H_2O)_{56}]\}\cdot ca.250H_2O \quad (5)$$

$$(NH_4)_{42}[\{(Mo)Mo_5O_{21}(H_2O)_6\}_{12}\{Mo_2O_4(CH_3COO)\}_{30}]\cdot ca.300H_2O\cdot 10CH_3COONH_4 \quad (6)$$

$$(NH_4)_{42}[(H_2O)_{80}@\{(Mo)Mo_5O_{21}(H_2O)_6\}_{12}\{Mo_2O_4(H_2PO_2)\}_{30}]\cdot ca.220H_2O \quad (7)$$

$$(NH_4)_{72-n}[\{(H_2O)_{81-n}+(NH_4)_n\}@\{(Mo)Mo_5O_{21}(H_2O)_6\}_{12}\{Mo_2O_4(SO_4)\}_{30}]\cdot ca.200H_2O \quad (8)$$

$$(GH^{+})_{32}[\{(H_2O)_{100}+(GH^{+})_{20}\}@\{(Mo)Mo_5O_{21}(H_2O)_6\}_{12}\{Mo_2O_4(H_2PO_2)\}_{20}\{Mo_2O_4(SO_4)\}_{10}]\cdot ca.100H_2O \quad (9)$$

$$(GH^{+})(NH_4)_{51-n}[\{(H_2O)_{81/2-n}+(GH^{+})_{20}+(NH_4)_n\}@\{(Mo)Mo_5O_{21}(H_2O)_6\}_{12}\{Mo_2O_4(SO_4)\}_{30}]\cdot ca.180H_2O \quad (10)$$

$$(UH^{+})_{20}(NH_4)_{32-n}[\{(H_2O)_{81-n}+(UH^{+})_{20}+(NH_4)_n\}@\{(Mo)Mo_5O_{21}(H_2O)_6\}_{12}\{Mo_2O_4(SO_4)\}_{30}]\cdot ca.120H_2O \quad (11)$$

$$(UH^{+})_{28}Na_{11}[\{(H_2O)_{60}+(UH^{+})_{20}+Na_{13}\}@\{(Mo)Mo_5O_{21}(H_2O)_6\}_{12}\{Mo_2O_4(SO_4)\}_{30}]\cdot ca.140H_2O \quad (12)$$

$$(GH^{+})_{6}(NH_4)_{20}Na_{13}[\{(H_2O)_{60}+(GH^{+})_{20}+Na_{13}\}@\{(Mo)Mo_5O_{21}(H_2O)_6\}_{12}\{Mo_2O_4(SO_4)\}_{30}]\cdot ca.190H_2O \quad (13)$$

$$(UH^{+})_{22}(NH_4)_{16}[\{(H_2O)_{60}+(UH^{+})_{20}+Ca_7\}@\{(Mo)Mo_5O_{21}(H_2O)_6\}_{12}\{Mo_2O_4(SO_4)\}_{30}]\cdot ca.140H_2O \quad (14)$$

[1]The compounds which have been synthesized by the author, and also those which have not been synthesized by the author but have been referred to in this thesis have been enlisted for easy reference. Hence those compounds which have been referred to in the Chapter 1 necessary only for the background information on the topic of this dissertation are *not* enlisted here.

The cluster compounds have been frequently referred to with the above numbering scheme in Chapters 2, 3 and 4 and 7. In Chapters 5 and 6 the cluster compounds have been abbreviated catering to the respective themes of those chapters and hence have been referred to in those chapters accordingly.

However, for complete information on any of the compounds enlisted here, the reader is requested also to look up the appendix together with the text of this thesis.

Here GH^{+} and UH^{+} stand for $\{(NH_2)_3C^{+}\}$ and $(NH_3^{+}CONH_2)$ respectively.

Note, compound **3** could not be reproduced by the author, and its formula reported here is not exact. The compound has however interesting structural features, and hence is included in spite of irreproducibility. For details, please refer to Chapter 2. Formula of the compound **10** might be subjected to small change as its single crystal X-ray structure data has not been completely refined and hence its *.cif file is also not included in the Appendix of this dissertation.

Contents

Chapter 1

Introduction

"I stand at the seashore, alone, and start to think. There are rushing waves... mountains of molecules, each stupidly minding its own business ...yet forming white surf in unison.[...]Deep in the sea, all molecules repeat the patterns of one another till complex new ones are formed. They make others like themselves... and a new dance starts. Growing in size and complexity... living things, masses of atoms, DNA, protein... dancing a pattern ever more intricate.

Out of the cradle onto the dry land... here it is standing... atoms with consciousness... matter with curiosity.

Stands at the sea... wonders at wondering... I... a universe of atoms an atom in the universe."

R. P. Feynman [1]

The film rolls back.

> "An atom in the universe... a universe of atoms ... wonders at wondering...."

1959. December 29. Feynman found "there is plenty of room at the bottom". Unexplored, yet pregnant with potential. Nanoscience was born. [1] Since then, the science at the level of nanometer, at the interface of quantum and classical interactions, has grown in leaps and bounds. 1974. Norio Taniguchi coined the word nanomachines to signify machining with tolerances less than a micron. 1981. Gerd Binnig and Heinrich Rohrer created a machine to image atoms, scanning tunnelling microscope or STM as it is popularly called. Robert Kurl, Harold Kroto, and Richard Smalley in 1985 discovered fullerenes. In 1989 Donald Eigler wrote IBM using xenon atoms. Nanodesign in a sense was taking shape in two ways: the physicists were carving out nanostructure from macroscopic forms (top-down) whereas the chemists were building up nanoassemblies from even smaller molecular or sub-molecular entities (bottom-up).

In 'top-down' approach usually the desired nanostructure is designed starting from a macroscopic structure. The usual techniques in this approach are nano-lithography, scanning probe microscopy, laser ablation etc. [2, 3] In the 'bottom-up' approach the nanostructures are generated from a library of building blocks, which might be a group of atoms, molecules, ions or an iterative structural moiety. It is inevitably a zone where chemists can exhibit extreme creative prowess. Feynman realized this at the inception of the field and acknowledged, "ultimately we can do chemical synthesis... The chemist does a mysterious thing when he wants to make a molecule. He sees that it has got that ring so he mixes this and that, and he takes it and he fiddles around. And at the end of a difficult process, he usually succeeds in synthesizing what he wants." [1] With this end in view a recent trend in chemical research has not only been in designing novel nanoarchitecture but also in understanding the formation of existing exquisite natural designs and developing further principle for future applications.

1.1 The state of the art of the field

Crossing the frontier of covalent chemistry today chemists have stepped in an era of 'chemistry beyond bonds', where 'weak' gets stronger by multiplication to form unusual structures. [4] Whether it is to design sophisticated molecular machines [5, 6] or 'bio-mimetic' architecture [7] studying/exploiting nature helps. The question arises: is there a possibility to study/develop model systems for understanding the creation of large, complex molecular systems like proteins, under dissipative conditions and if possible in 'one pot' reactions? The unusual and absolutely unique chemistry of oxomolybdates (or rather polyoxomolybdates)[1] - under reducing conditions - offers the option to generate related nanosystems. (See e.g., [9].) In the solution of oxomolybdates, controlled linking of metal-oxide building blocks produces a large variety of structures - and provide the option to form exquisite molecular architecture [10] with unprecedented functionalities. This only became evident in recent years. [11] Specifically speaking the reasons for such a versatile behaviour of polyoxomolybdates are as following:

1. The easy change of coordination numbers as well as easy exchange of H_2O ligands at Mo sites.
2. The moderate strength of Mo-O-Mo type bonds allowing "split and link" type processes.
3. The easy change and especially increase of electron densities without the strong tendency to form metal-metal bonds.

[1] Polyoxomolybdates are those polyoxometalates where the metal centres are molybdenum. The polyoxometalates can in turn be defined as a class of cluster anions comprising of at least two or more single or mixed-valent metal centres, each covalently bonded with oxygen atoms as per the requirement of coordinative saturation of the central metal atoms. [8]

4. The presence of terminal Mo = O groups preventing in principle unlimited growth to extended structure. ([9], see also: [12].)

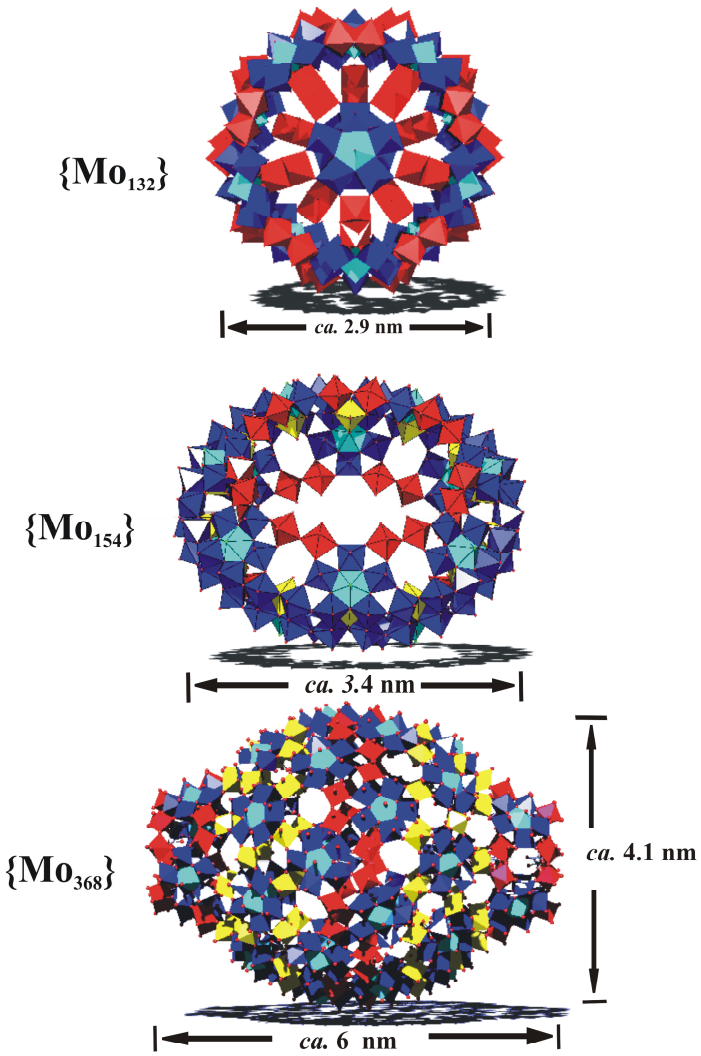

Figure 1.1: *The 'nanosociety' of polyoxomolybdates - three important types of clusters are depicted in polyhedral representations: [Mo_{132}] cluster (top), [Mo_{154}] (middle); [13] and [Mo_{368}] (bottom). [9] The central pentagonal bipyramidal ([$(Mo)Mo_5$]) unit is shown in cyan surrounded by five edge-shared octahedral units in blue; the edge and corner shared ([Mo_2]) units with different composition are shown in red; and [Mo_1] units in yellow polyhedral representation.*

In spite of an exotic architectural aspect, (see Figure 1.1) synthetically speaking, [13] all the giant polyoxomolybdate based systems are very easy to handle. As a starting point a synthetic principle for the cluster growth of the giant polyoxomolybdate based systems might be mentioned. This principle still continues to be the holy

grail of such giant cluster construction. The question comes: what is that principle?

1.1.1 Polyoxomolybdates: The growth-principle

Molecular growth guards the gateway to molecular complexity. In Nature complex molecular systems like proteins are formed under conditions far from equilibrium (natura naturans). Chemists cherish the dream of attaining complexity correspondingly under one-pot conditions without the problem of repetitive separation and purification of individual products.

In an aqueous molybdate solution α-Keggin type clusters with T_d symmetry can be formed, which upon reduction yield the highly nucleophilic ϵ-Keggin type clusters $[H_xMo^V{}_{12}O_{40}]^{(20-x)-}$as intermediates [14] (Figure 1.2) (See also [8] for different aspects of the ϵ-Keggin ion including the structure of the non-reduced species.) These species are stabilized by protonation and by the capture of four electrophilic $[Mo^{VI}O_3]$ groups, thus forming anions of the type $[H_xMo^V{}_{12}O_{40}(Mo^{VI}O_3)_4]^{(20-x)-}$one of which was isolated with a well-defined protonation and structurally characterized as the $NH_2Me_2{}^+$ salt. [15, 16] On further reduction, the Mo^{VI} centres of the originally electrophilic $[Mo^{VI}O_3]$ groups become nucleophilic and, in addition, may assume a template function. In a sort of synergistic co-assembly the latter mentioned species further forms and attracts electrophilic polyoxometalate fragments with 10 and 11 molybdenum atoms $[Mo_{10}]$ or $[H_3Mo^V{}_4Mo^{VI}{}_6O_{29}]^+$ and $[Mo_{11}]$ or $[H_5Mo^V{}_6Mo^{VI}{}_5O_{31}]^{3+}$. The formation of the related $[Mo_{37}]$ type cluster can be regarded as a result of information stored in the intermediate of the type $[Mo_{16}]$, i.e. as a result of its template function. The asymmetric growth in this case may be attributed, in principle, to the asymmetric protonation of (only) three of the four μ_3-O atoms forming the central cavity, which may cause an asymmetric charge distribution and protonation on the surface of the intermediate. [14] This reaction where intermediates act as templates for the generation of other intermediates with which the former intermediates react, aptly points to the growth potential of molybdenum based polyoxometalate clusters.

A further related case is that of the $[Mo_{57}M_6]$ (where, M = $Fe^{II/III}$, VO^{2+}) type clusters [14] (see also reviews [12, 17, 18] and literature cited therein), where six cavities at the surface are capable of undergoing quasi-reversible molecular growth processes, which is controlled by the redox conditions. Under reducing conditions, which increases the nucleophilicity, the cavities can be filled with positively charged electrophilic units like $(MoO)^{4+}$ and can be emptied again under oxidizing conditions. [12] These reactions present a basic principle of cluster growth: a growing (nucleophilic) species forms and attracts an electrophilic group, thereby switching on a molecular cascade (see Figure 1.3). Such a model of cluster growth has enabled the construction of clusters of ever increasing complexity, and even the largest inorganic cluster anion with 368 molybdenum atoms is formed correspondingly; where a growing $[Mo_{288}]$ nucleophile is capped by two electrophilic $[Mo_{40}]$ caps giving rise to the unusual giant nano-cluster. [9, 12] Like the principle of cluster growth it is also

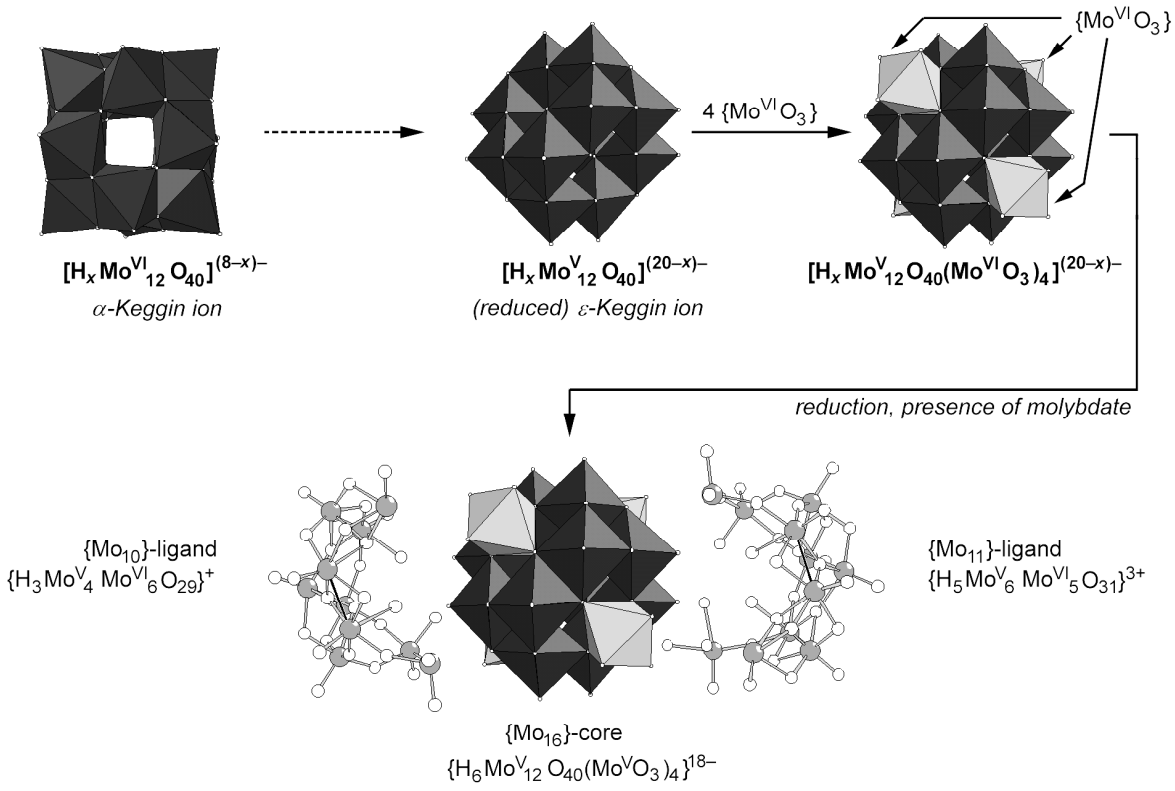

Figure 1.2: *Demonstration of the stepwise growth process leading to the remarkable cluster anion of* $(NH_4)_{14}[H_{14}Mo_{37}O_{112}] \cdot 35H_2O$ *with no symmetry. The central highly nucleophilic* ϵ*-Keggin type* $[H_xMo_{12}O_{40}]$ *core and the four captured* $[MoO_3]$ *groups are shown in black and grey polyhedra, respectively. The* $[Mo_{11}]$ *and* $[Mo_{10}]$ *type ligands are represented as ball-and-stick models (molybdenum, light grey; oxygen, white). Adapted from reference [12].*

important to have an overview of the structural principle of the clusters central to the key-concepts of this thesis. The following section will have a detailed look in the structural features of those clusters like $[Mo_{132}]$ and $[Mo_{154}]$.

1.1.2 Structural aspects of some giant polyoxomolybdate clusters

The giant spherical polyoxomolybdates

The construction of giant spherical systems, with icosahedral symmetry requires reaction systems where pentagonal building blocks can be first generated (mainly by a split and link process from a larger fragment), then be linked while getting placed at the 12 corners of an icosahedron. (Figure 1.4) Reaction mixture of molybdates under appropriate pH values and reducing conditions house a potential library ideal for such constructions. In these giant spherical clusters, the pentagonal $[(Mo)Mo_5]$

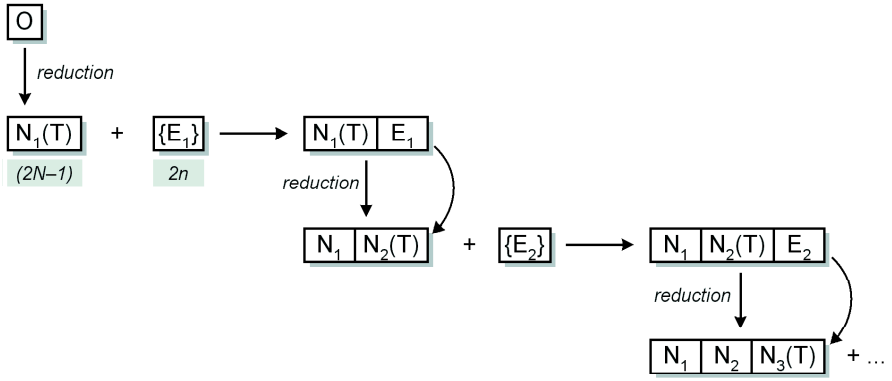

Figure 1.3: *Reaction scheme corresponding to the growth process shown in Figure 1.2, demonstrating principally the step-by-step procedure in which nucleophiles (such as the reduced ϵ-Keggin ion) attract electrophiles $[MoO_3]$. Remarkably these can become nucleophiles ($[Mo^VO_3]$ units) on the surface of the cluster upon reduction. O denotes species at the beginning of a growth process (formally the non-reduced ϵ-Keggin ion). $[N_i(T)]$ denotes a nucleophilic intermediate/fragment produced under reducing conditions (of the type 2N - 1 according to Scheme 1, e.g. the reduced ϵ-Keggin ion) with a potential template function for the generation of the electrophilic intermediate $[E_i(T)]$.* Adapted from reference [12].

building blocks are placed at the 12 vertices of an icosahedron and linked by a set of 30 mono- or dinuclear spacers, such as $[Fe(H_2O)]^{3+}$ [19], $[MoO(H_2O)]^{3+}$ [20] or $[Mo_2O_4(CH_3COO)]^+$. [21] Of these, the 30 mononuclear linkers for example define an Archimedean solid, the icosidodecahedron with 30 vertices and 32 faces. (Figure 1.5)

Changing the linkers on the one hand provides a means of tuning the size of these nanoscopic objects, and on the other enables, e.g. in the case of Fe^{3+} the construction of a giant spherical molecular magnet with 150 uncorrelated electrons on its surface! [19] Moreover this cluster can also act as a host for encapsulation of a suitably sized guest. [22] All such spherical clusters, which can be described by the general formula $[(Mo)Mo_5]_{12}[L]_{30}]$ or $[(pentagon)_{12}(linker)_{30}]$, [2] belong to the family of 'Keplerate' type molecules because of their striking similarity to Kepler's early model of the universe, as described in his speculative opus Mysterium Cosmographicum. [17, 23] A related mathematical study of the family of Keplerates has been published. [24]

The clusters described above are interesting for materials science and nanotechnology aspects because of their stability, size, solubility (in several solvents), giant cavities, 'nanosized' changeable pores, unique surfaces, unusual electronic structure, abundance of magnetic centres in a variety of topologies, etc. Moreover, most of the clusters especially the spherical ones can be manipulated keeping the robust

[2] From now onwards $[(pentagon)_{12}(linker)_{30}]$ will be written as $[(pent)_{12}(link)_{30}]$ for the sake of brevity.

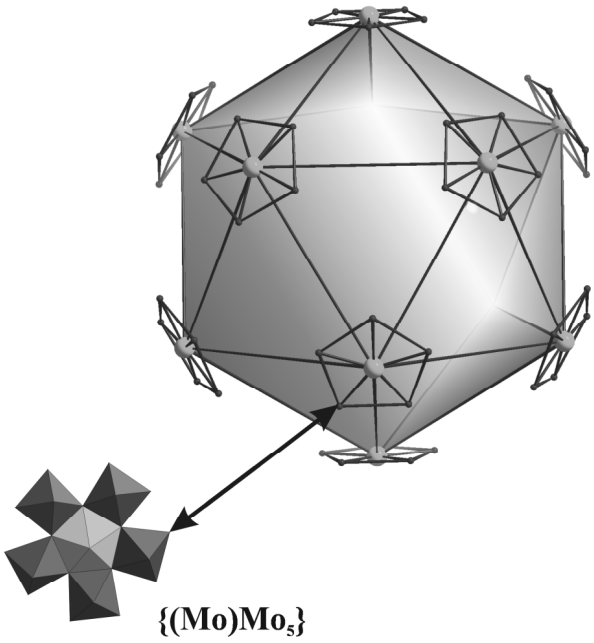

Figure 1.4: *Construction principle for clusters with icosahedral symmetry. The* $[(Mo)Mo_5]$ *units (polyhedral model with central pentagonal bipyramid in light grey) are the basis for the formation of the* $[(pent_{12}(link)_{30}]$ *type clusters, where the* $[(Mo)Mo_5]$ *units define the icosahedron vertices. Adapted from reference [12].*

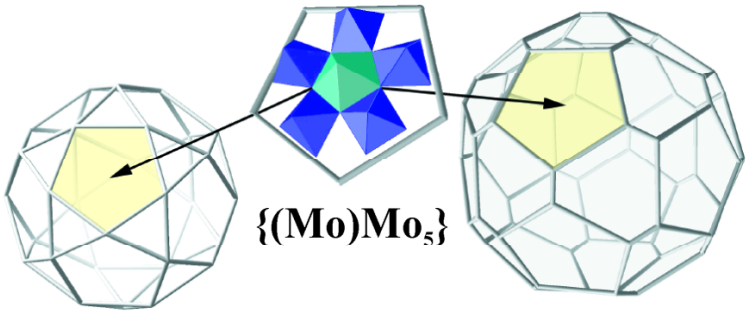

Figure 1.5: *"Sizing" the nanospheres is possible. Structure only formed by the linkers: Left: the icosidodecahedron with 12 pentagons and 20 triangles formed by mononuclear* $(link)_{30}$ *of the* $[(pent)_{12}(link)_{30}]$ *type clusters. Right: the (distorted) truncated icosahedron with twelve pentagons and twenty hexagons formed by 30 dinulear* $[Mo_2]$ *linkers. Colour code: central pentagonal bipyramidal* $[MoO_7]$ *of* $[(Mo)Mo_5]$ *in cyan and other octahedra in blue. Adapted from reference [12].*

nanoscopic oxomolybdate skeleton intact. Encapsulation of the giant clusters with surfactant molecules allows production of LB films and monolayers with implications

for design of new materials. For further details the reader may look up a collection of papers in reference [25].

The ring shaped molecular big-wheels and their derivatives

The above mentioned spherical 'Keplerates' are results of the "spherical disposition" of pentagonal $[(Mo)Mo_5]$ building blocks with a C_5 symmetry whereas a "circular disposition" of the deformed $[(Mo)Mo_5]$ unit leads to the formation of $[Mo_{154}]$ and $[Mo_{176}]$ type clusters, commonly known as the big-wheel and giant-wheel type species, respectively. Their structure can formally be represented as $([(Mo)Mo_5][Mo_2'][Mo_1])_m$, where m = 14, 16 for $[Mo_{154}]$ and $[Mo_{176}]$. (Figure 1.6) The $[Mo_{154}]$ cluster has an external diameter of 3.4 nm while that of $[Mo_{176}]$ is 4.1 nm. [12] It is now also possible to obtain the $[Mo_{176}]$ type cluster starting from the $[Mo_{132}]$ type Keplerate via a mild oxidation reaction catalyzed by metal cations (this represents the best available method). [26]

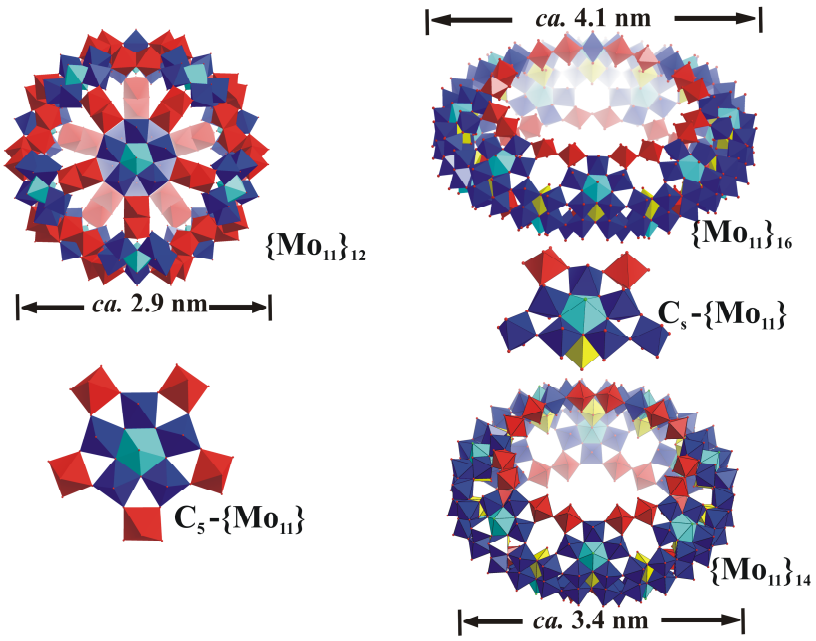

Figure 1.6: *Molybdenum 'brown' and 'blue': Left: The spherical molybdenum 'brown' type* $[Mo_{132}]$ *cluster is shown highlighting the constituent pentagonal* $[(Mo)Mo_5]$ *units (in cyan and blue) and* $[Mo_2]$ *units in red. Right: The wheel shaped molybdenum 'blue' type* $[Mo_{154}]$ *and* $[Mo_{176}]$ *clusters are shown with the abundance of pentagonal* $[(Mo)Mo_5]$ *units (in blue and cyan) (Both types of* $[Mo_2]$ *units in red,* $[Mo_1]$ *units in yellow). Note the two different types of* $[Mo_{11}]$ *units highlighted.*

Derivatives of the wheels

In addition to the pentagonal $[(Mo)Mo_5]$ unit, the wheel type polyoxomolybdates contain as mentioned above $[Mo_2']$ $(= [Mo_2O_5(H_2O)_2]^{2+})$ together with $[Mo_1]$ type units. Employing simple chemical techniques (for instance raising the pH, or prolonging crystallization time) it was possible to design new clusters with defects, i.e. with some missing $[Mo_2']$ units. [27, 28] In those 'defect' clusters it has even been possible to incorporate other metal ions like Cu^{2+} into the 14 or 16 tetrahedral cavities marked by four O atoms, normally occupied by protons in the parent cluster. [29] It is worth mentioning that all wheel type clusters like $[Mo_{154}]$ or $[Mo_{176}]$ contain electronically uncoupled 14 or 16 incomplete double cubane type $[Mo_5O_6]$ compartments with two delocalized Mo (4d) electrons. [11]

Likewise incorporation of different inorganic cations like K^+, Pr^{3+}, Eu^{2+} has also been shown to be possible (for details see [30, 31, 32] respectively).

The unusual giant $[Mo_{132}]$ type spherical clusters, the wheel-shaped $[Mo_{154}]$ and even the largest inorganic cluster anion $[Mo_{368}]$ (Figure 1.1) together with the principle for their generation were already known and well-developed before the inception of this thesis. [9, 13] This section however is the prelude to the dissertation and defines the state of the art of the field. The next section defines the problem to be discussed in this dissertation.

1.2 Defining the problem

This thesis crystallized from a course of research that started with the synthetic examination of one of the existing ring-shaped large polyoxomolybdate clusters. The investigation carried out in course of this thesis revealed potential host functionalities of the ring-shaped polyoxomolybdates. Inevitable challenge for this dissertation was to develop related model host-systems with spherical clusters. After realizing the host potential of the spherical clusters in course of the work carried out in this project next challenge was to understand the dynamics of the host-guest processes in (aqueous) solution. With this end in view as a ground work to such understanding, in this project, the stability of four selected spherical clusters in aqueous solution against variation of important chemical parameters were investigated. The underlying objective of this thesis was not only to identify their host-potential, the regime of their stability but also to understand the probable site(s) of the clusters 'vulnerable' to decomposition in solution.

Chapter 2

Connecting ring-shaped giant polyoxomolybdates to 1-D extended structures

2.1 Introduction

[1] The deliberate synthesis of multifunctional nanosized materials from well-defined building blocks which are abundant in a virtual library is one of the most challenging problems in contemporary chemistry. Pertinent targets include the synthesis of materials with especially desirable properties. In solution of oxoanions of the early transition elements, especially molybdates under reducing conditions, an enormous variety of compounds can be formed by linking together metal-oxide building blocks. In the first half of this Chapter: a one day facile synthesis of such a molybdenum-oxide based compound **1**, exhibiting a chain of nanosized ring shaped cluster units with unique receptor properties, is described. The second half demonstrates the application of the above synthetic principle to isolate related compounds with extended chain type structure and suitable guest sites also from the so-called molybdenum-blue solution. In this context it should be mentioned that for nearly 200 years it was not possible to obtain pure compounds from the related molybdenum blue solution mainly due to the high solubility of the abundant species. (Figure 2.1) [11, 12] Progress in the present case corresponds to the use of urea which forms interesting crystalline supramolecular compounds due to N-H...O=C hydrogen bonding, a property which is used technologically to separate hydrocarbons. Interestingly, urea shows complementary sites for hydrogen bonding comparable to the cluster itself. [2]

Compound $^{1}_{\infty}\{(UH^{+})_{14}[Mo^{VI}_{126}Mo^{V}_{28}O_{462}H_{14}(H_2O)_{68}]\} \cdot ca.350H_2O$ **1** as described in detail below was obtained by addition of urea to the reaction mixture from which normally discrete nanosized wheel shaped cluster species such as

[1] A major part of this Chapter has been published as reference [33]: A. Müller, S. Roy, M. Schmidtmann, H. Bögge, Chem. Commun. (2002) 2000. Some Figures of this Chapter have been adapted from the published article.

[2] Note: In this chapter UH^{+} and GH^{+} stand for $(NH_3^{+}CONH_2)$ and $\{(NH_2)_3C^{+}\}$ respectively.

$[Mo^{VI}_{126}Mo^{V}_{28}O_{462}H_{14}(H_2O)_{70}]^{14-} \equiv [\{Mo_9O_{26}(\mu_3{-}O)_2H(H_2O)_3\}_{14}\{Mo^{VI}_2O_5(H_2O)_2\}_{14}]^{14-}$ $\equiv [\{Mo_1Mo_8\}_{14}\{Mo_2\}_{14}]^{14-}$ [11] is formed (referred to here as $[Mo_{154}]$) and was characterized by elemental analysis, thermogravimetric analysis (to determine the crystal water content), cerimetric titrations [for the determination of the (formal) number of Mo^V centres], bond valence sum (BVS) calculations [34] (to determine the number of H_2O ligands and OH groups as well as the number of Mo^V centres), [17] spectroscopic methods (IR, resonance-Raman, VIS-NIR) and single crystal X-ray structure analysis. In this context it might also be mentioned that the formula of the $[Mo_{154}]$ type cluster given by Yamase and co-workers as reported in reference [35] agrees completely with ours except for the larger number of protons. This is due to an overinterpretation of the lowest BVS values at terminal O atoms, which are indeed caused by the H_2O/O disorder.

2.2 Synthesis and characterization of $^{1}_{\infty}\{(UH^+)_{14}[Mo^{VI}_{126}Mo^{V}_{28}O_{462}H_{14}(H_2O)_{68}]\} \cdot ca.350H_2O \equiv \mathbf{1}$

To a solution of $(NH_4)_6Mo_7O_{24} \cdot 4H_2O$ (1.00 g, 0.809 mmol) and urea (0.6 g, 10 mmol) in 40 ml distilled water in a 100 ml closed Erlenmeyer flask, $Na_2S_2O_4$ (0.1 g, 0.574 mmol) was added with constant stirring while the colour of the solution turned green. It was immediately acidified with 30 ml 1 M HCl (colour change to blue) and the solution was heated on a hot plate (60^0C) for 1 h under closed conditions. After 1 day while keeping the solution at 20^0C the precipitated dark blue stick shaped crystals of **1** were filtered off, washed quickly with a small volume of cold water and were dried at room temperature. Yield: 0.63 g (60% based on Mo) (Note: the crystals should be separated from the reaction mixture after 1 day, so as to avoid the co-precipitation of amorphous materials as an after effect.) Elemental analysis: Calc. C 0.5; H 2.9; N 1.4; Mo^V 9.4. Found: C 0.5; H 2.2; N 1.4; Mo^V 9.5%.

Note: Due to the fast loss of crystal water from this type of compound all the analytical calculations were done taking a loss of ca. 50 water molecules into consideration. This explains the difference in the M value used for analytical calculations and that obtained from the single crystal X-ray diffraction experiments. This also holds good for the analytical data of the cluster compounds **2** and **4** described later in this Chapter.

*Characteristic spectroscopic data for **1***: IR: ν/cm^{-1} (KBr disk, some characteristic bands 1700-400 cm^{-1}): ca. 1700sh [$\nu(C=O)$], 1624s [$\delta(H_2O)$], ca 1400w [$\delta(N-H)$], 1153w, ca. 995sh, 975s, 908m [$\nu(Mo=O)$], ca. 633s, 559s. Resonance-Raman: ν/cm^{-1} (solid, KBr dilution, λ_e = 1064 nm): 802s, 535m, 462s, 326s, 215s. VIS-NIR: λ_{max}/nm (solid state reflectance with cellulose as white standard): 700.

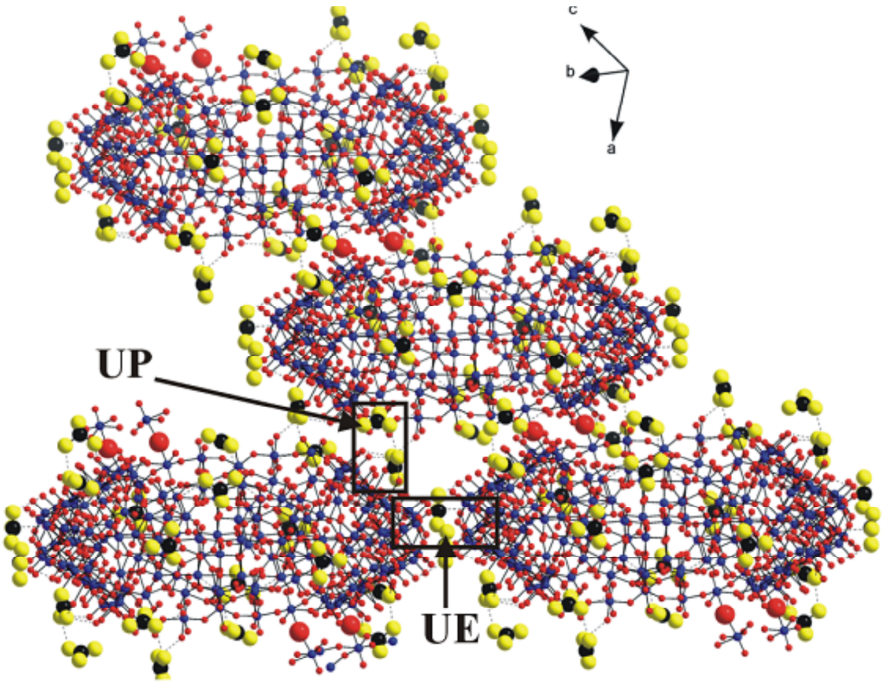

Figure 2.1: *Ball-and-stick representation of four* $[Mo_{154}]$ *type rings of* ***1*** *glued with two types of protonated urea molecules (viz., equatorial UE as well as polar UP). Colour code: molybdenum: blue; oxygen: red; carbon: black; nitrogen and oxygen atoms of urea units which could not clearly be distinguished using X-ray crystal structure analysis: yellow. The atoms of the urea (type) units and the oxygen atoms which covalently connect adjacent rings have been enlarged for clarity.*

2.3 Discussion of the structure

2.3.1 The unit cell and molecular connectivity

The monoclinic unit cell of **1** (space group C2/m) shows the abundance of two nanosized ring shaped $[Mo_{154}]$ units, which are related by a translation of (1/2, 1/2, 0). Along the smaller crystallographic c-axis, the rings appear to be arranged like a flight of stairs with protonated urea molecules attached to the surface of each of them (Figure 2.1). Every $[Mo_{154}]$ ring is connected to its next (chain) neighbours via two covalent Mo-O-Mo bonds at $[Mo'_2]$ type $(H_2O) - Mo = O$ position. [17] The urea units-protonated at the pH of the reaction and fixed to the cluster surface-act as counter ions and form a part of the overall supramolecular assembly. The observed protonation is consistent with numerous elemental analyses and with the fact that salts of protonated urea exist. [36]

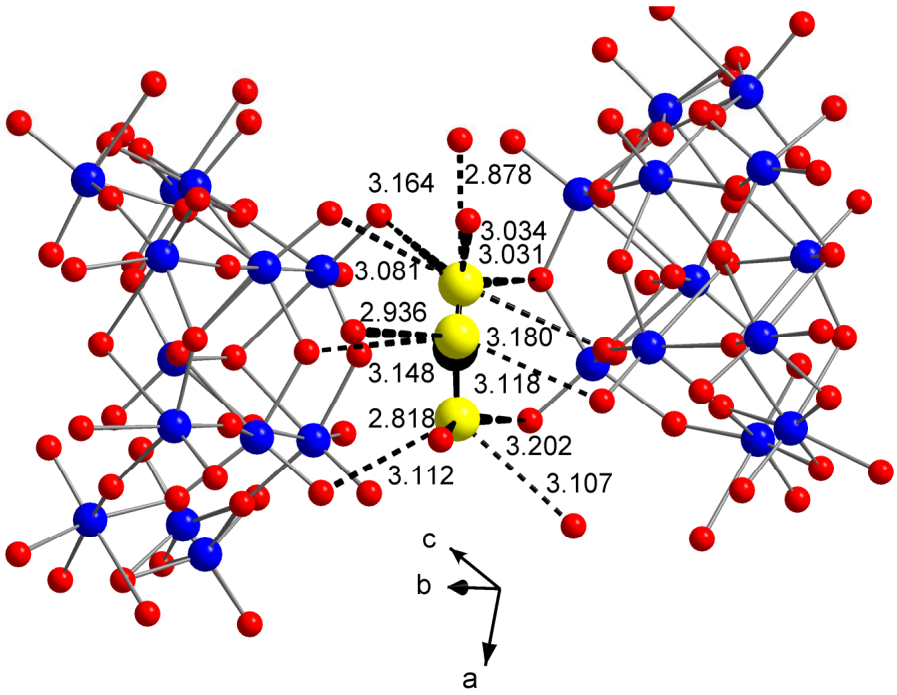

Figure 2.2: *Representation of ring atoms showing interaction with UE type urea units between two rings of two adjacent chains illustrating the glue function of the latter. Colour code as in Figure 2.1*

2.3.2 A detailed description of the cluster's local structures like $\{Mo_6O_6\}$ rings and the 'guests' like protonated urea present in the cluster: Description of the host-guest architecture

The urea (type) units associated with the chain of **1a** may be classified into two groups: those (four) found along the equatorial region of every $[Mo_{154}]$ ring (UE) and those (eight) found along the polar region (UP) on the upper and lower rims of the ring. The UE units glue the rings along the equator while the UP units link the polar parts of two $[Mo_{154}]$ units of different neighbouring chains as shown in Figure 2.2 and 2.3. Interestingly, the latter (UP) also show pairwise hydrogen bonding type interactions. The two other lattice urea cations, being not coordinated and therefore disordered, could not be located. The nitrogen and oxygen atoms of the UE units lie within a distance of 2.9 - 3.2 $\mathring{A}$ from the equatorial oxygen atoms of the metal-oxide backbones of two $[Mo_{154}]$ units of two neighbouring chains (Figure 2.2). The polar UP units are also located within similar distances from the surface atoms of the same $[Mo_{154}]$. (The disorder in the system prevents a clear distinction between N and O atoms of urea, see Figure 2.3). [34, 37] The given distances lie within the limits of moderate hydrogen bonds. [38, 39] (Note, that the negative charge density on the

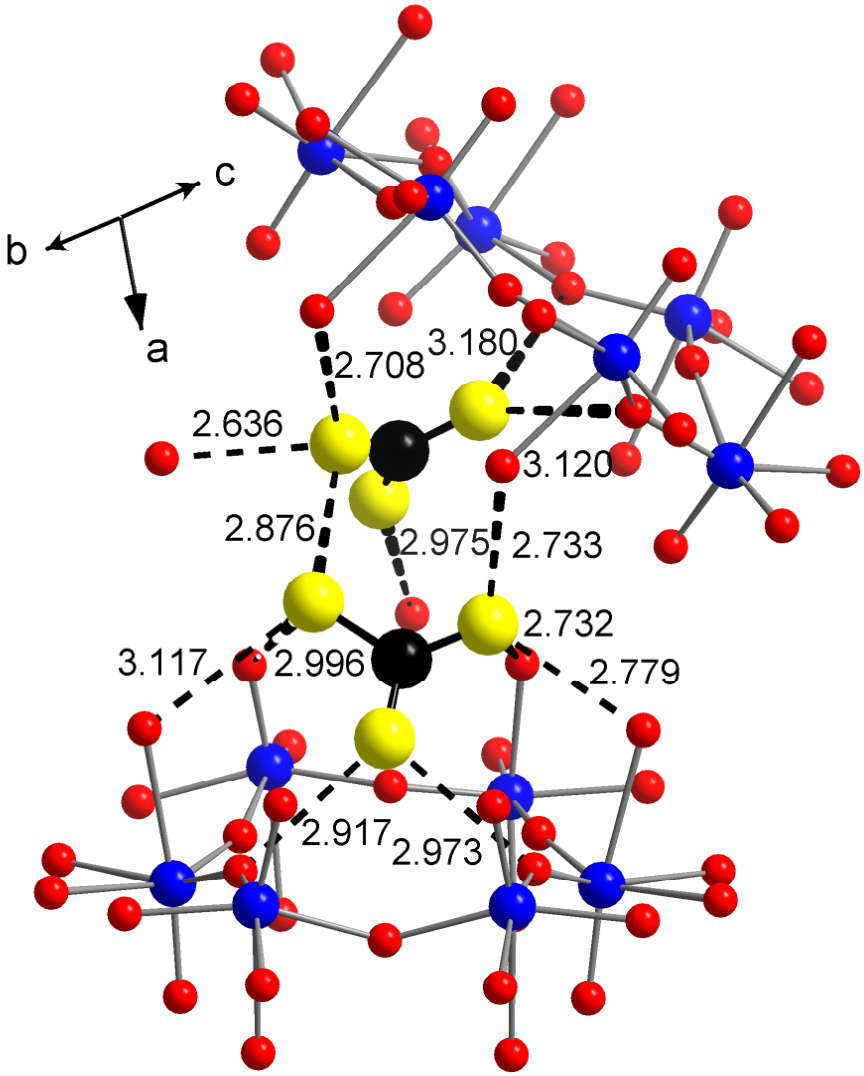

Figure 2.3: *Interaction between UP type units among themselves as well as with oxygen atoms of two hexagonal* $\{Mo_6O_6\}$ *ring sites with the potential receptor property of* ***1****. The difficulty to distinguish exactly between O and N atoms of UP is caused by a O=Mo-*H_2O *disorder at the cluster surface. Colour code as in Figure 2.1.* [34, 37]

ring units is rather small.) The UP units fit into the specific $\{Mo_6O_6\}$ hexagonal sites, [40] thereby indicating the possibility for these sites to act as a type of receptor (Figure 2.3). Another particularly important feature of **1a** is that the surface of the respective cluster ring has in principle the same positive or negative complementary hydrogen bonding sites as urea. Note the unique ability of urea to form remarkable cage structure with encapsulated alkanone, alkanedione, diaminoalkane, to act as

guests [41] or as a 'glue' [42] converge in the case of formation of **1a**. (See also [4, 43].) The observation of related extensive hydrogen bond formation by urea in the present compound is in accordance with the ability of urea to form four hydrogen bonds by two lone pairs of electrons on carbonyl oxygen, as was observed much earlier by Pauling. [44]

2.4 The essential features of the synthetic method and its application towards formation of related clusters of the family of extended structures

The reaction leading to the formation of crystalline **1a** shows the following feature: (1) the coordination of protonated urea destroys the cluster hydration shell (responsible for the high solubility and difficulty to precipitate the clusters) and simultaneously accelerates chain formation [33] by decreasing the negative charge density of the $[Mo_{154}]$ type constituent units thereby facilitating Mo-O-Mo bond formation. (2) The subsequent condensation reaction at two $[Mo_2']$ type $(H_2O) - Mo = O$ groups favours an entropy driven reaction with subsequent release of hydration shell and coordinated cluster water molecules into liquid bulk water . To summarize, urea acts as a glue in the formation of the crystalline compound while drastically reducing the crystallization time (one day). (Also note: after filtering the crystals from the blue solution, and leaving the solution undisturbed for 10 days, ring-shaped $[Mo_{176}]$ clusters were obtained. The details of which are not reported here.)

The knowledge acquired from the above reaction, was applied to tailor the synthesis of related structure. For example,

1. To 'connect' $[Mo_{154}]$ type rings in a one-dimensional chain as in **2**.
2. To study the $\{Mo_6O_6\}$ rings present in similar compounds like **3**, **4** and further to study their connectivity and compare their packing in the respective unit cells. (See also: [33, 45].)

$^1_\infty\{(NH_4)_{14}[Mo^{VI}_{126}Mo^{V}_{28}O_{462}H_{14}(H_2O)_{68}]\} \cdot ca.350H_2O$ **2**

$^1_\infty\{(UH^+)_{22-x}K_x[Mo^{VI}_{118}Mo^{V}_{28}O_{442}H_{14}(H_2O)_{57}]\} \cdot nH_2O$ **3**

$^1_\infty\{(GH^+)_8Na_{14}[Mo^{VI}_{118}Mo^{V}_{28}O_{442}H_{14}(H_2O)_{57}]\} \cdot ca.300H_2O$ **4**

2.4.1 Synthesis of $^1_\infty\{(NH_4)_{14}[Mo^{VI}_{126}Mo^{V}_{28}O_{462}H_{14}(H_2O)_{68}]\} \cdot ca.350H_2O \equiv$ **2**

A mixture of $(NH_4)_6Mo_7O_{24} \cdot 4H_2O$ (1.00 g, 0.809 mmol), $FeCl_2$ (2.0 g, 10 mmol) and 40 ml distilled water was warmed on a hot plate, in a 100 ml closed Erlenmeyer flask, till the solution was clear. To this dirty brown solution $Na_2S_2O_4$ (0.1 g, 0.574 mmol) was added with constant stirring and the colour of the solution turned green. It was immediately acidified with 30 ml 1 M HCl (colour change to blue) and the solution was heated on a hot plate (60^0C) for 1 h under closed conditions. After

1 day while keeping the solution at 20^0C the precipitated dark blue stick shaped crystals of **2** were filtered off, washed quickly with a small volume of cold water and were dried at room temperature. Yield: 0.54 g (52% based on Mo) (Note: the crystals should be separated from the reaction mixture after 1 day, so as to avoid the coprecipitation of amorphous materials as an after effect.) Elemental analysis: Calc. N 0.4, Mo^V 9.4. Found: N 0.4, Mo^V 9.5%.

*Characteristic spectroscopic data for **2***: IR: ν/cm^{-1} (KBr disk, some characteristic bands 1700-400 cm^{-1}): 1624s [$\delta(H_2O)$], ca 1400w [$\delta(N-H)$], 1153w, ca. 995sh, 975s, 908m [$\nu(Mo=O)$], ca. 630s, 557s. Resonance-Raman: ν/cm^{-1} (solid-state, λ_e = 1064 nm): 802s, 535m, 463s, 325s, 215s. VIS-NIR: λ_{max}/nm (solid state reflectance with cellulose as white standard): 700.

2.4.2 $^1_\infty\{(UH^+)_{22-x}K_x[Mo^{VI}_{118}Mo^V_{28}O_{442}H_{14}(H_2O)_{57}]\}\cdot nH_2O \equiv$ **3**

A mixture of $Na_2MoO_4\cdot 2H_2O$ (3 g, 12.4 mmol), urea (0.6 g, 10 mmol), K_2SO_4 (0.6 g, 3.4 mmol), and 10 ml water was acidified with 35 ml 0.5 M H_2SO_4. To this light yellow solution $Na_2S_2O_4$ (0.15 g, 0.86 mmol) was added with constant stirring (immediate colour change to blue). The solution was heated at 60^0C for 15 mins and was then stored in a closed flask at room temperature. After 5 days the precipitated deep-blue crystals of **3** were filtered off and a crystal was studied by single crystal X-ray diffraction. In spite of several attempts, this synthesis could not be reproduced. The C, H, N analysis showed lesser number of carbon, nitrogen than obtained from single crystal X-ray structure determination and the chemical analysis data being erratic is not given here. An approximate formula of the compound is given for the discussion of the structure. The characteristic spectroscopic data are given below.

*Characteristic spectroscopic data for **3***: IR: ν/cm^{-1} (KBr disk, some characteristic bands 1700-400 cm^{-1}): ca. 1700sh [$\nu(C=O)$], 1624s [$\delta(H_2O)$], ca 1400w [$\delta(N-H)$], 1153w, ca. 995sh, 975s, 908m [$\nu(Mo=O)$], ca. 633s, 559s. Resonance-Raman: ν/cm^{-1} (solid, KBr dilution, λ_e = 1064 nm): 802s, 535m, 462s, 326s, 215s. VIS-NIR: λ_{max}/nm (solid state reflectance with cellulose as white standard): 700.

2.4.3 $^1_\infty\{(GH^+)_8Na_{14}[Mo^{VI}_{118}Mo^V_{28}O_{442}H_{14}(H_2O)_{57}]\}\cdot ca.300H_2O \equiv$ **4**

A mixture of $Na_2MoO_4\cdot 2H_2O$ (3 g, 12.4 mmol), guanidinium sulfate (0.2 g, 0.92 mmol) and 10 ml water was acidified with 35ml 0.5 M H_2SO_4. To this light yellow solution $Na_2S_2O_4$ (0.15 g, 0.86 mmol) was added with constant stirring (immediate colour change to blue). The solution was heated at 60^0C for 45 mins and was then stored in a closed flask at room temperature. After 2 weeks the precipitated deep-blue crystals of **4** were filtered off. Yield: 0.50 g. (21% based on Mo) Elemental analysis: Calc. C 0.3, N 1.2. Na 1.1, Mo^V 9.2; Found: C 0.3, N 1.1, Na 1.0, Mo^V 9.2%. [46]

*Characteristic spectroscopic data for **4***: IR: ν/cm^{-1} (KBr disk, some characteristic bands 1700-400 cm^{-1}): 1656s [$\delta(H_2O)/(NH_2)_3C^+$], 997sh, 974s, 912m [$\nu(Mo=O)$], ca. 630s, 555s. Resonance-Raman: ν/cm^{-1} (solid-state, λ_e = 1064 nm): 802s, 535m,

462s, 326s, 215s. VIS-NIR: λ_{max}/nm (solid state reflectance with cellulose as white standard): 700.

2.5 Comparison of the structural features of different 'chains'

This section depicts a detailed account of the structural features of all the 'chain' type compounds i.e., **1**-**4**. For the sake of comparison some structural aspects of **1** will be touched upon avoiding repetition. Reference will be made to the structure of a previously synthesized 'chain' type compound **5** reported in the literature, [45] further for comparison. i.e.,

$^{1}_{\infty}\{Na_{24}[Mo^{VI}_{116}Mo^{V}_{28}O_{437}H_{14}(H_2O)_{56}]\} \cdot ca.250H_2O \equiv \mathbf{5}$

The section has been divided in four subsections, describing, the unit cells of the chains, their inter-ring connectivity, together with the structure of each such constituent ring and comparison of the $\{Mo_6O_6\}$ rings of the chains. Some important structural features of the chains have been tabulated in Table 2.1 for easy reference.

Compound	**1**	**2**	**3**	**4**	**5**
Crystal system	monoclinic	monoclinic	orthorhombic	monoclinic	triclinic
Space group	C2/m	C2/m	Pnnm	P2(1)/n	P-1
Axis of chain propagation	c	c	b	a	a
Constituent ring	$[Mo_{154}]$	$[Mo_{154}]$	$[Mo_{146}]$	$[Mo_{146}]$	$[Mo_{144}]$
No. of inter-ring Mo-O-Mo bonds	2	2	5	5	4
No. of coordinated water molecules	68	68	57	57	56

Table 2.1: Some selected comparative structural features of the chains.

2.5.1 Comparative account of the unit cells and direction of chain propagation

The cluster compounds **1**, **2** and **4**, crystallize in monoclinic unit cells. In these cases the direction of chain propagation is usually along the smallest crystallographic axis. For instance, chains of **1** propagate along the c-axis, those of **2** and **4** along the crystallographic c- and a- axes all of which are smallest in their respective unit-cells. (Figures 2.4 and 2.5) The same tendency is observed for the chains of **5**, which extends along the crystallographic a-axis of its least symmetric triclinic unit cell. (Figure 2.6 and [45].) But on the other hand **3** crystallizes in more symmetric orthorhombic crystal system, and the chains propagate along not the smallest, b-axis, of its unit-cell.

The unit cells of **1**, **2**, **3**, **4** and **5** show a similarity in the sense that they possess two nanosized ring shaped $[Mo_{154}]$, $[Mo_{146}]$ or $[Mo_{144}]$ units respectively. The nature of these 'units' is however different. The unit cells of **1** and **2** contain only one crystallographically unique $[Mo_{154}]$ type ring, whereas those of **3** and **4** show the

presence of two crystallographically independent $[Mo_{146}]$ type rings. In this matter the last two compounds are similar to the previously published **5**, comprising two crystallographically independent $[Mo_{144}]$ type rings. [45]

2.5.2 Comparison of the 'inter-ring' connectivity of the chains

Connectivity in 1 and 2

The 'inter-ring' connectivity between the constituent $[Mo_{154}]$ rings of the cluster compounds **1** and **2** are similar. In both cases the constituent $[Mo_{154}]$ rings are connected to each-other by *2 Mo-O-Mo bonds* formed by the condensation at 2 $(H_2O)-Mo=O$ positions of 2 neighboured $[Mo'_2]$ type units flanking one $[(Mo)Mo_5]$ unit. (Figure 2.7) [17] It is also worth mentioning that because of such condensation two coordinated water molecules are 'lost' and consequently the cluster compounds have 68 coordinated water molecules, i.e., 2 less than the discrete $[Mo_{154}]$ cluster compound with 70 such molecules. [11]

Connectivity in 3 and 4

In the cases of compounds **3** and **4** the connectivity between the neighbouring constituent $[Mo_{146}]$ rings is a bit more intricate. In both cases the constituent $[Mo_{146}]$ rings are connected to each-other by *5 Mo-O-Mo bonds* formed by the condensation at 3 $(H_2O)-Mo=O$ positions of $[(Mo)Mo_5]$ and 2 $(H_2O)-Mo=O$ positions of $[Mo'_2]$ units of 2 neighbouring rings related by an inversion centre. The 3 apical $(H_2O)-Mo=O$ groups of a $[(Mo)Mo_5]$ unit of one ring condense with 1 $(H_2O)-Mo=O$ group of $[(Mo)Mo_5]$ of another neighbouring ring and 2 $(H_2O)-Mo=O$ groups of 2 $[Mo'_2]$ units flanking that $[(Mo)Mo_5]$ unit of the other ring. This pattern of connectivity is repeated in the other ring, the connecting sites being related by an inversion centre. (Figure 2.7) Also note that in course of 5 such Mo-O-Mo bond formation 5 coordinated water molecules are 'lost' and consequently the cluster compounds have 57 coordinated water molecules, 5 less than that of the constituent $[Mo_{146}]$, with 62 coordinated water molecules. (See later as well and [11].)

Connectivity in 5

In this case the constituent $[Mo_{144}]$ rings are connected to each-other by *4 Mo-O-Mo bonds* formed by the condensation at 2 $(H_2O)-Mo=O$ positions of a $[Mo'_2]$ type unit, positioned between 2 pentagonal $[(Mo)Mo_5]$ units, 2 of whose apical $(H_2O)-Mo=O$ positions form the remaining 2 Mo-O-Mo bonds. (Figure 2.7) Note as before that in course of 4 'inter-ring' Mo-O-Mo bond formation 4 coordinated water molecules are 'lost' and consequently the cluster compound has 56 coordinated water, 4 less than that of individual constituent $[Mo_{144}]$ with 60 coordinated water molecules. (See the next section and also [45].)

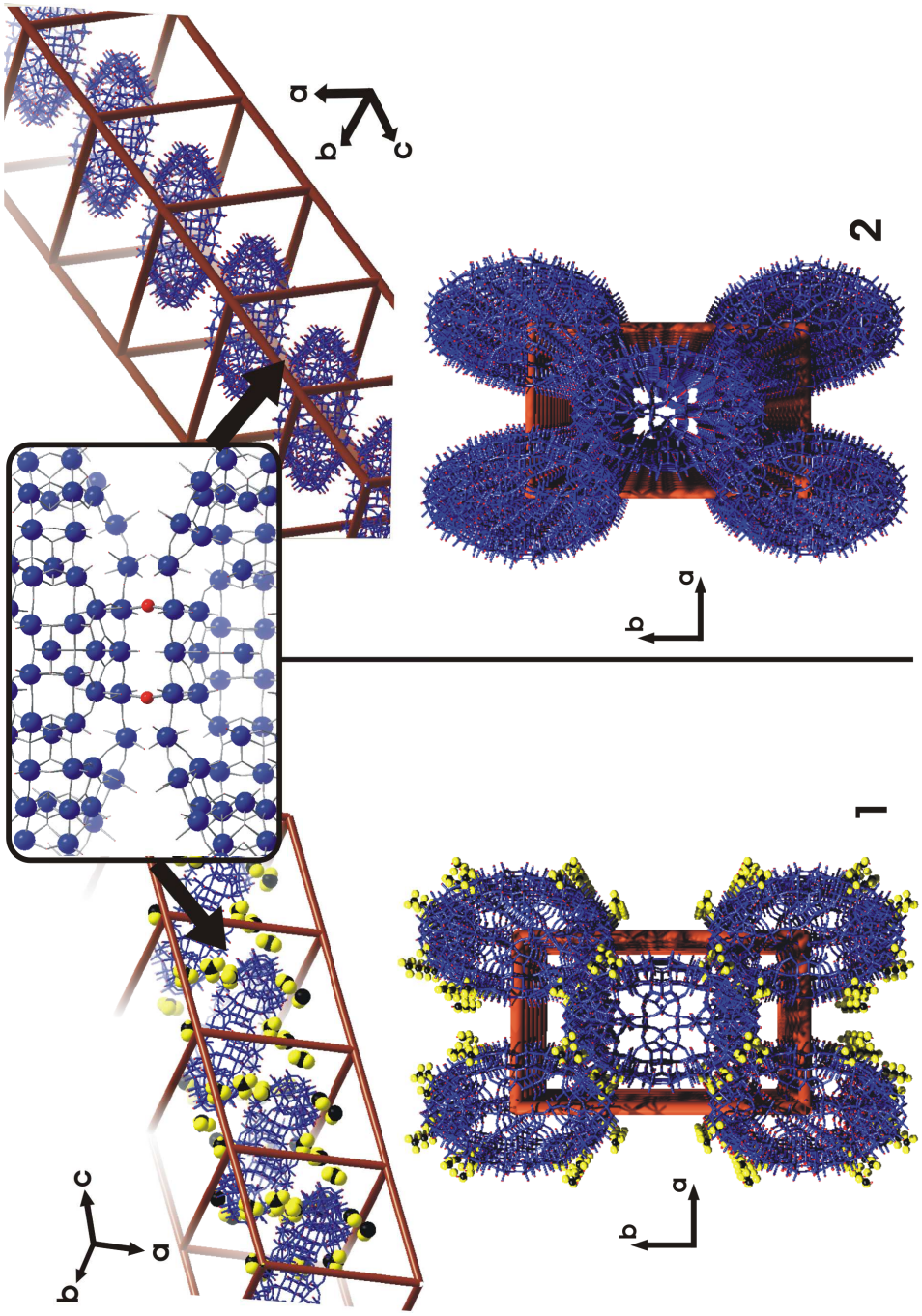

Figure 2.4: *Connecting the* $[Mo_{154}]$ *rings to chains: Isolated chains of* $[Mo_{154}]$ *(in wire-frame model) propagating along the crystallographic c-axes of* **1** *and* **2** *are shown (above) together with a perspective view along the axis of the chain propagation (below). In the inset the connecting region between the* $[Mo_{154}]$ *rings has been highlighted where two connecting oxygen atoms (in red) and all the molybdenum atoms (in blue) have been enlarged, whereas the other oxygen atoms have been diminished for clarity. For more on connectivity please see Figure 2.7. Colour code same as in Figure 2.1. See also [33].*

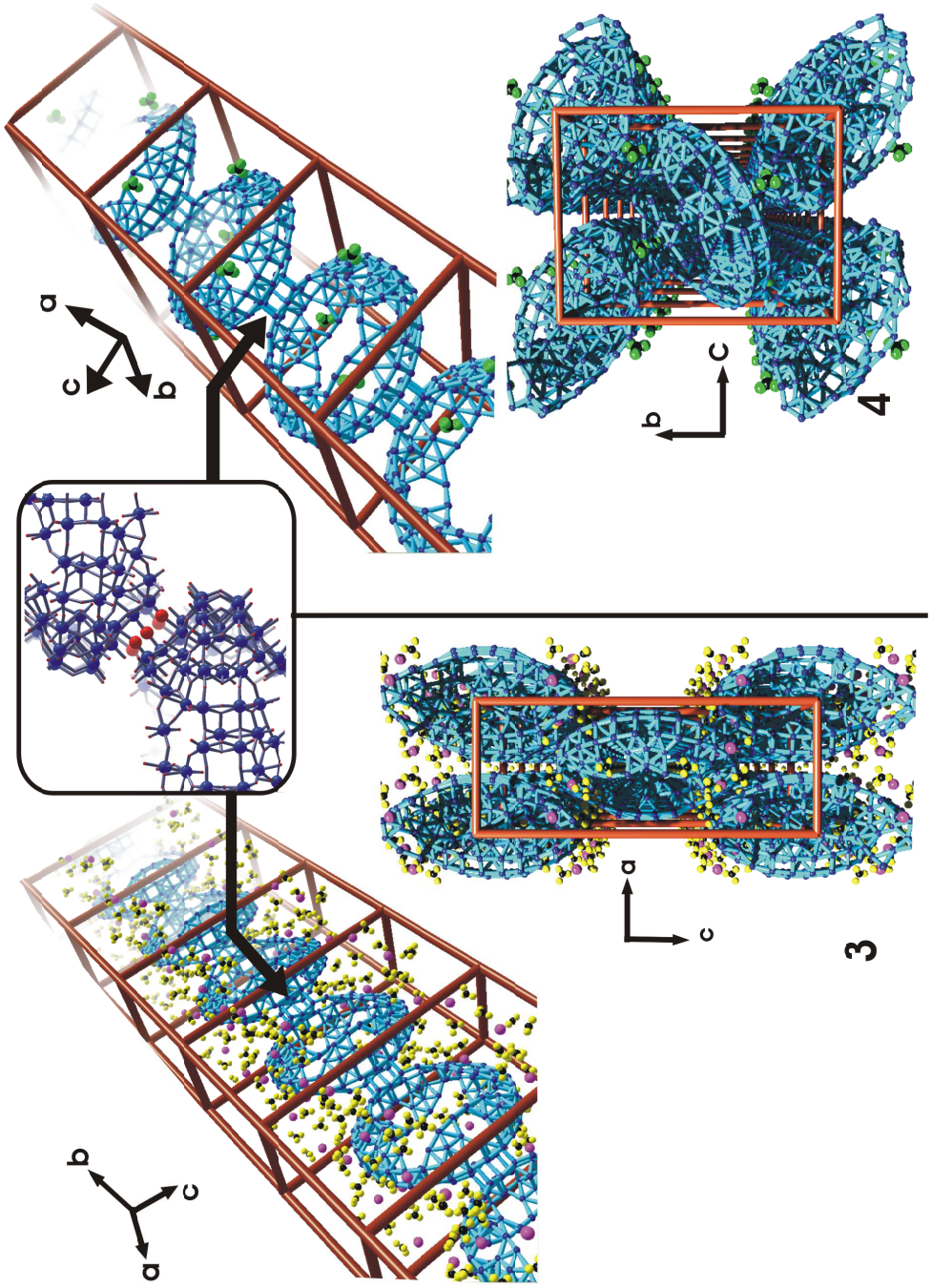

Figure 2.5: *Connecting the* $[Mo_{146}]$ *rings to chains: Chains of* $[Mo_{146}]$ *(depicting Mo-skeleton in cyan wire-frame) propagating along the crystallographic b and a-axes of* **3** *and* **4** *(above) together with a perspective view along the respective axes of chain propagation are shown (below). The potassium ions in the lattice of* **3** *are shown in lilac; carbon: black; nitrogen and oxygen atoms of urea units which could not clearly be distinguished using X-ray crystal structure analysis: yellow; nitrogen of guanidinium cations of* **4** *in green. The connecting region between the* $[Mo_{146}]$ *rings has also been highlighted in the inset as in Figure 2.4. For more on connectivity please see Figure 2.7. See also [33] and [45].*

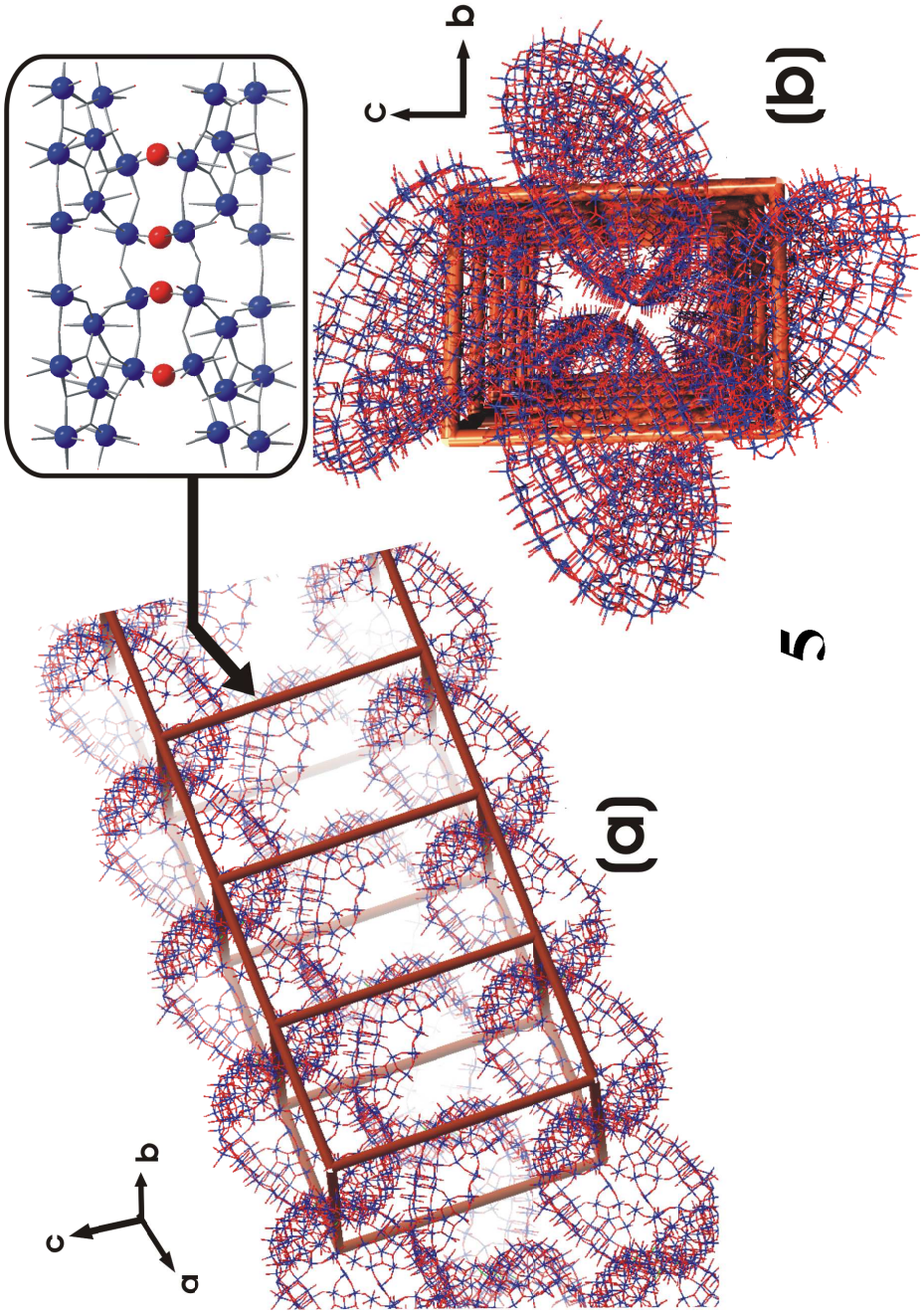

Figure 2.6: *Connecting the* $[Mo_{144}]$ *rings to chains: a) 3 chains of* $[Mo_{144}]$ *(in wire-frame representation, with molybdenum in blue, oxygen in red,) propagating along the crystallographic a-axis of* **5** *are shown (above) together with a perspective view along the axis of the chain propagation in b). The connecting region between the* $[Mo_{144}]$ *rings has also been highlighted in the inset as in Figure 2.4. For more on connectivity please see Figure 2.7. For details please look up reference [45].*

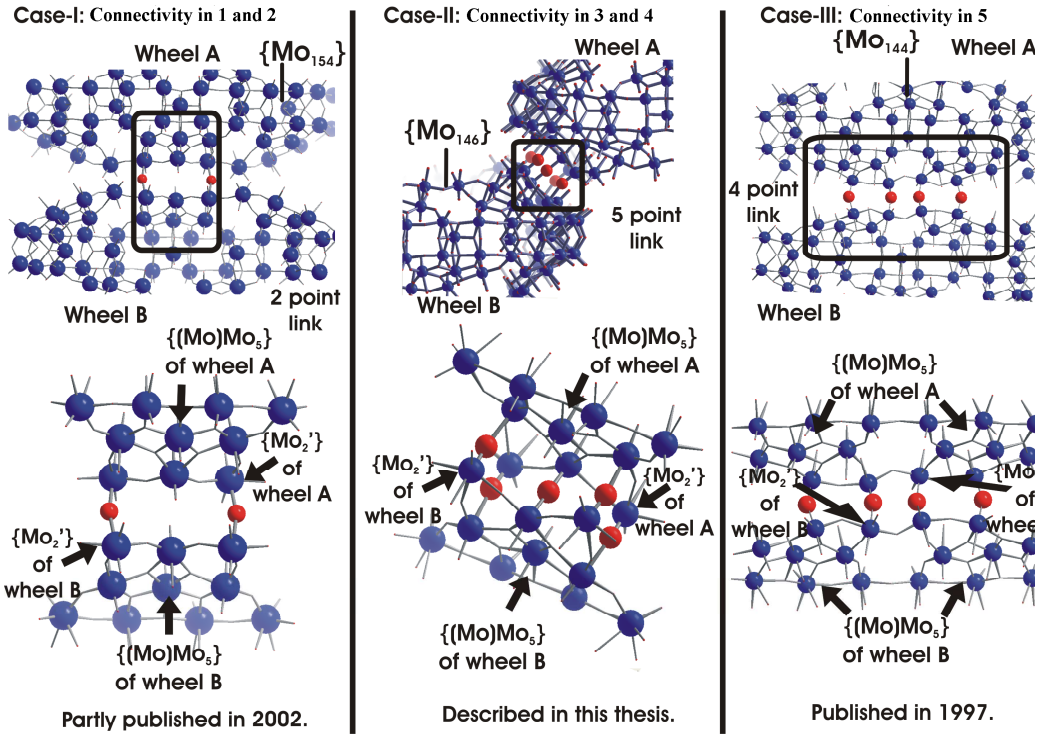

Figure 2.7: *Region of connectivity of three different type of chains: (Left) The connecting region between two rings/wheels (denoted as wheel A and B in the Figure) of the type* $[Mo_{154}]$*, forming the compounds* ***1*** *and* ***2****. 2 Mo-o-Mo bonds in this case are formed by the linking of 2* $(H_2O) - Mo = O$ *groups from 2 different* $[Mo_2']$ *type units flanking the* $[(Mo)Mo_5]$ *unit of every ring. (Middle) 5 Mo-O-Mo bonds connecting 2 neighbouring* $[Mo_{146}]$ *rings/wheels (marked as wheel A and B) of* ***3*** *and* ***4*** *are shown. Of these, 3 bonds connect 3 apical* $(H_2O) - Mo = O$ *of* $[(Mo)Mo_5]$ *unit of one ring/wheel (say wheel A) with 1 apical* $(H_2O) - Mo = O$ *of* $[(Mo)Mo_5]$ *unit and 2* $(H_2O) - Mo = O$ *groups from 2 different* $[Mo_2']$ *type units flanking that* $[(Mo)Mo_5]$ *unit of the neighbouring wheel B. The remaining 2 bonds connect 2* $(H_2O) - Mo = O$ *groups from 2 different* $[Mo_2']$ *units flanking the* $[(Mo)Mo_5]$ *unit of wheel A with 2 remaining apical* $(H_2O) - Mo = O$ *groups of* $[(Mo)Mo_5]$ *unit of wheel B. (Right) 4 Mo-O-Mo bonds connecting 2 neighbouring* $[Mo_{144}]$ *type rings/wheels (wheel A and B in the Figure) of* ***5*** *are formed by the condensation of 2* $(H_2O) - Mo = O$ *groups from 2 different* $[(Mo)Mo_5]$ *units of every ring/wheel, and the other 2* $(H_2O) - Mo = O$ *from* $[Mo_2']$ *type units between those 2* $[(Mo)Mo_5]$ *units. For more details please see the text, and references [33, 45]. Colour code: molybdenum, blue spheres; oxygen, red spheres; the connecting oxygen atoms have been enhanced for clarity.*

Figure 2.8: *Three different type of constituent rings of the chains. The* $[Mo_{154}]$ *ring of the compounds* **1** *and* **2** *(left);* $[Mo_{146}]$ *of* **3** *and* **4** *highlighting under-occupied Mo positions in grey (middle); and* $[Mo_{144}]$*, ring of the previously published compound* **5** *(right) are shown. The under-occupied/missing* $[Mo'_2]$ *units of* $[Mo_{146}]$ *(middle) and* $[Mo_{144}]$ *(right) with respect to* $[Mo_{154}]$ *(left) are shown in grey-polyhedra. Note the upper part of the figure shows the rings in ball-stick representation while the lower part shows only the upper halves of the corresponding rings in polyhedral represetation. For details please see the text and references [33, 45]. Colour code (ball-stick): molybdenum, blue spheres; oxygen, red spheres; (polyhedral representation):* $[(Mo)Mo_5]$ *unit in cyan and blue polyhedra;* $[Mo_2]$ *units in red polyhedra, (whereas the under-occupied* $[Mo'_2]$ *units in grey) and* $[Mo_1]$ *units in yellow polyhedra.*

2.5.3 Comparison of the constituent 'rings' of the chains

Like their connectivity, the chains also differ in the matter of their constituent units or 'rings'. For instance, compounds **1** and **2** show the abundance of $[Mo_{154}]$ as constituent rings. Whereas **3** possesses $[Mo_{146}]$ rings as constituents, lacking four $[Mo_2']$ units as compared to $[Mo_{154}]$. Compound **4** on the other hand shows the abundance of an 'deceptively' complete $[Mo_{154}]$ as constituents. Closer study reveals that 8 (4 on each surface) of the usual Mo_2 positions are under-occupied, with the occupancy factor lying in the range of 0.2-0.7. Consequently the constituent rings of compound **4** are found to be $[Mo_{146}]$ instead of $[Mo_{154}]$. On a passing, it might be also mentioned that previously published **5** shows the presence of $[Mo_{144}]$ as constituents.

It is worth noting that the anions **1a**, **2a**, **3a**, **4a** and **5a** bear the same overall negative charge as the their single discrete constituent units. For example, **1a** and **2a** have an overall negative charge of 14-, same as that of discrete $[Mo_{154}]$. [13] Since each $[Mo_2']$ unit (= $[Mo_2O_5(H_2O)_2]^{2+}$) is bi-positive, absence of four such units in $[Mo_{146}]$ type clusters raise the cluster charge by 8 units with respect to $[Mo_{154}]$ type clusters. [12] This in turn also explains that although **1** and **2** with $[Mo_{154}]$ as constituent rings have 14 positively charged cations, **3** and **4** with $[Mo_{146}]$ as constituent rings have 22 cations in the lattice; i.e., 8 more than their non-defect counter-parts. Likewise it could be also explained why the previously published **5** with $[Mo_{144}]$ as constituent rings has 24 cations in its lattice. (Figure 2.8) [45]

Another interesting influence of the constituent rings refers to the number of coordinated water molecules associated with these cluster anions. From the Table 2.1 it becomes evident that, number of coordinated water molecules for any chain-type anion = number of coordinated water molecules for the discrete constituent ring type unit − the number of water molecules 'lost' in course of the 'inter-ring' Mo-O-Mo bond formation. Note: Cluster anions **1a** or **2a**, **3a** or **4a** [3] and **5a**, having $[Mo_{154}]$, $[Mo_{146}]$ and $[Mo_{144}]$ as constituent rings and with 2, 5 or 4 'inter-ring' Mo-O-Mo connectivity contain 68, 57 and 56 coordinated water molecules respectively. Also note: discrete $[Mo_{154}]$, $[Mo_{146}]$ and $[Mo_{144}]$ clusters have 70, 62 and 60 coordinated water molecules respectively.

2.5.4 Study of $\{Mo_6O_6\}$ rings of the chains

As demonstrated earlier, the $\{Mo_6O_6\}$ rings of **1a** can act as receptors (or hosts) to cationic substrates like protonated urea. Although **2a** shows a pristine 'guest-free' chain with 'empty' $\{Mo_6O_6\}$ rings; cationic substrates like K^+, and protonated urea even coordinated to $\{Mo_6O_6\}$ rings are observed in **3a**. (In this case the K...O

[3] The relation though holds good for **4a** it must be noted that **4a** has 16 under-occupied 'so-called' H_2O positions which altogether leads more strictly to an overall number of coordinated water molecules of 58.5 [(=70-6.5-5) where, 70 (the number of coordinated water molecules in non-defect $[Mo_{154}]$ type cluster), 6.5 (the number of water molecules to be diminished due to the under-occupancy of 16 of all 70 H_2O sites) and 5 (lost water molecules due to 5 Mo-O-Mo bond formation)]. For the sake of convenience of discussion and comparison the number of water molecules of **4a** has always been referred to in this Chapter as 57.

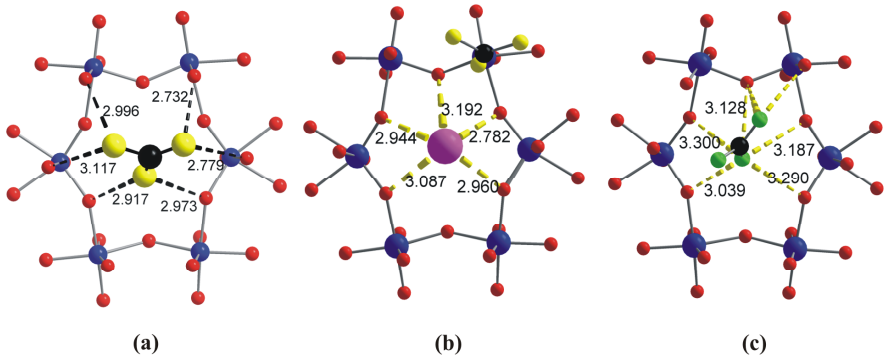

Figure 2.9: *(a) Protonated urea @ $\{Mo_6O_6\}$ ring of **1a** (b) potassium @ $\{Mo_6O_6\}$ ring together with coordinated urea of **3a** seen at the upper corner and (c) protonated guanidinium @ $\{Mo_6O_6\}$ ring of **4a** (Colour code: molybdenum, blue; carbon black; nitrogen in guanidinium green; potassium, lilac; nitrogen and oxygen atoms of urea units which could not clearly be distinguished using X-ray crystal structure analysis: yellow.) This difficulty to distinguish exactly between O and N atoms is caused by a O=Mo-H_2O disorder at the cluster surface. [34, 37]*

distances lie between 2.78 - 3.2 $\mathring{A}$.) (Figure 2.9) Comparable phenomenon is observed in the case of **4a** where protonated guanidinium cations are found with the N...O distances lying in the range of 3 - 3.3 $\mathring{A}$. (Figure 2.9) The nitrogen atoms of guanidinium cations form moderate hydrogen bonding with the oxygen atoms of some of the hexagonal $\{Mo_6O_6\}$ rings of the cluster. Unlike as in **3a**, where K^+ ions are found crystallographically at $\{Mo_6O_6\}$ rings of the cluster, the Na^+ ions of **4a**, could not be crystallographically located and their presence was ascertained from elemental analysis.

2.6 Synthetic commonality of the family of 1-D chains of ring-shaped giant polyoxomolybdates and the IR 'finger-print'

Although the exact *modus operandi* of the synthetic conditions, for the chain type clusters described so far in this Chapter is not fully understood; still it might be said that low pH (< 1) and a temperature around 60^0C are crucial for their crystallization. In addition to such synthetic commonality they show a finger-print pattern in the IR spectrum, also very typical for the discrete ring $[(Mo_{154})_{0.5}(Mo_{152})_{0.5}]$ type [13] molybdenum blue cluster compounds. (Figure 2.10)

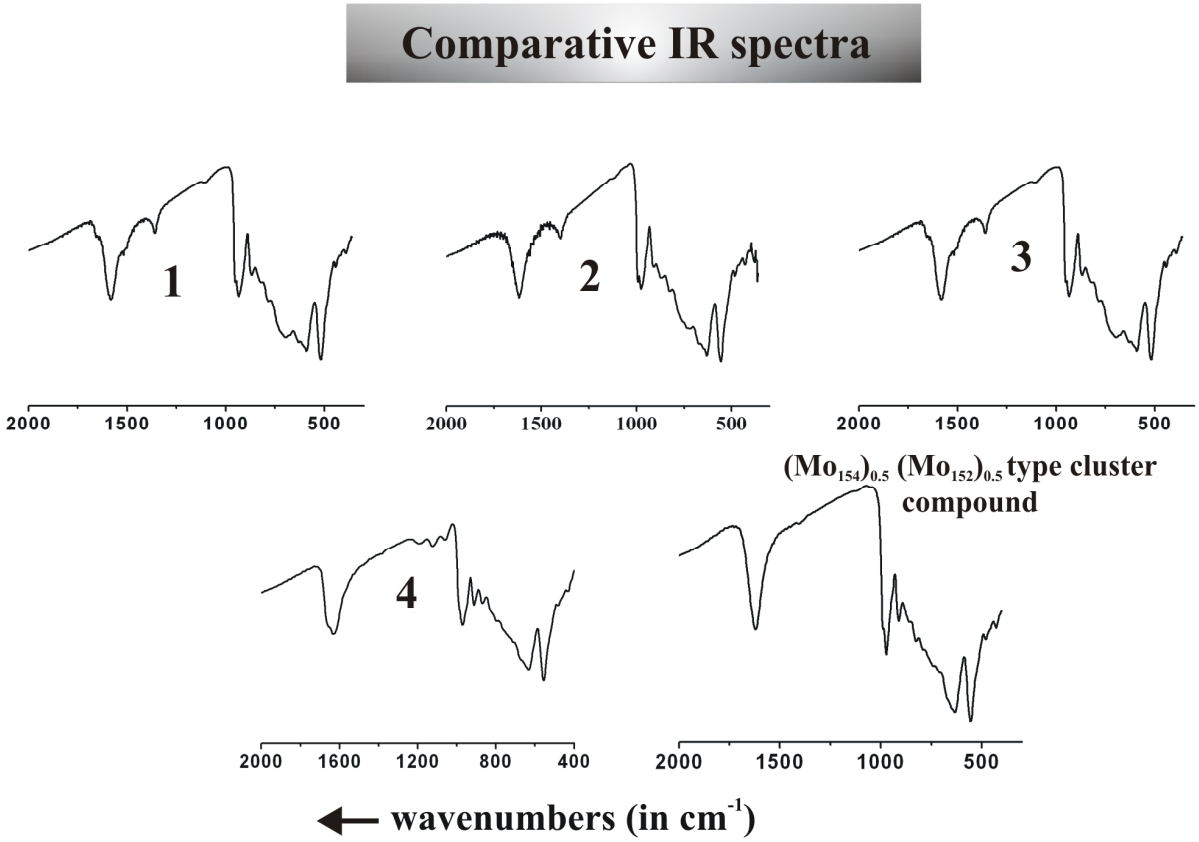

Figure 2.10: *A clear similarity in the IR spectra of **1**, **2**, **3** and **4** with the spectrum of a discrete* $[(Mo_{154})_{0.5}(Mo_{152})_{0.5}]$ *type cluster compound is worth noting. See also [13].*

2.7 Discussion and perspectives

The general perspectives from the obtained results may be the possibility to investigate a variety of reactions at different sites of a structurally well-defined nanoobject, which can regarding different functionalities (including complementary sites for hydrogen bonding) be considered as a nanostructured landscape. Furthermore, the special situation of specific receptors like $\{Mo_6O_6\}$ rings (i.e., to host guests) opens up new related avenues in host-guest and supramolecular chemistry, as will be seen in the following Chapters. Additionally, the options for improving the synthetic routes for extended structures are obvious.

Chapter 3

Syntheses of spherical giant polyoxomolybdates as 'substrate specific nanosponges'

3.1 Introduction

[1] A current challenge in nanotechnology is to mimic material constructions and molecular recognition type responsive sensing of biological systems. This becomes especially attractive if nanometer-sized objects can be constructed with tailor-made building blocks, which is possible with unique molybdenum-oxide based objects showing a huge variety of functionalities and reactivities as the fullerenes. [17, 24] In this Chapter a detour is made from the wheel-shaped circular systems with $\{Mo_6O_6\}$ rings to an unusual spherical molybdenum-oxide based nanoobject capable of responsive reactivity - like that of a nanosponge endowing sizeable $\{Mo_nO_m\}$ ring like pores - which may route to new techniques in supramolecular nanotechnology regarding efficient and specific recognition by a large number (up to now regarded as simply not possible) of pores/receptor sites, which are similar to those of macrocyclic ligands. [4] (The maximum pore diameter of a related $\{Mo_nO_m\}$ ring is now ca. 0.8 nm.) The pores are sizeable since fixed basic pentagonal $[(Mo)Mo_5]$ type units of the object $[(pent)_{12}(link)_{30}]$ can be connected with different linkers.

Beyond monotopic receptors polytopic receptors can bind several (different) substrates/guests simultaneously. This latter type of interaction depends - corresponding to cooperativity effects - not only on the type and number of binding sites but also on the overall object symmetry. In case of the present type of host system different investigations of cooperative, allosteric and regulatory effects are, in principle, possible. Additionally, there are in the reported compounds quite a large number of

[1] A major part of this Chapter has been published as reference [47]: A. Müller, E. Krickemeyer, H. Bögge, M. Schmidtmann, S. Roy, A. Berkle, Angew. Chem. Int. Ed. 41 (2002) 3604. Some Figures of this Chapter have been adapted from the published article.

In this Chapter GH^+ and UH^+ stand for $\{(NH_2)_3C^+\}$ and $(NH_3^+CONH_2)$ respectively.

different sets of equivalent atoms spanning, e.g. Platonic and Archimedean solids, some of which are the most complex ones and are observed now for the first time in chemistry. The present results can be considered as a starting point for a sphere-surface- and nanoporous cluster-chemistry with significant interdisciplinary aspects for modelling spherical virus surfaces, [48] for problems of discrete mathematics regarding spherical object tiling, [49] as well as catalytic and biomimetic processes because of the simultaneous presence of large pores providing access to the nano-sized cavities. It might be mentioned here, that spherical object tiling is important for understanding virus structure, for the construction of Buckminster Fuller domes and even fascinated M. C. Escher.

Spherical nanoobjects with icosahedral symmetry of the type $[(pent)_{12}(link)_{30}]$ can be constructed from 12 $[(Mo)Mo_5]$ type pentagonal units and 30 (different) linkers, [12] allowing not only overall object sizing but also a sizing of (because of symmetry reasons) the 20 abundant (tailor-made) pores. (The construction principle corresponds to that of icosahedral/spherical viruses. [48]) If the linker is built up, e.g., by a binuclear $[Mo_2]$ type unit. i.e. two edge-shared MoO_6 octahedra, the pores on the surface of the spherical system correspond to $\{Mo_9O_9\}$ rings (diameter ca. 0.8 nm), formed by three $[Mo_2]$ and three $[Mo_1]$ type units [12] (see Figure 3.1). In the case of mononuclear linkers M^{n+} (M = Fe^{3+}, [19] $[MoO(H_2O)]^{3+}$, [20] or $[VO(H_2O)]^{2+}/[MoO(H_2O)]^{3+}$ [50]) the correspondingly smaller Mo_6O_6 rings, respectively, are formed and are just large enough to "capture" K^+ cations. [50] Remarkably, each of such 20 pores/rings has in principle a receptor property comparable to that of the classical crown ethers of supramolecular chemistry [4] and those described in the last Chapter.

3.2 Syntheses and characterization of the cluster compounds

It could now be shown that the icosahedral clusters $[\{(Mo)Mo_5O_{21}(H_2O)_6\}_{12}\{Mo_2O_4(ligand)\}_{30}]^{n-}$ (e.g., with L = $H_2PO_2^-/SO_4^{2-}$) - known with different ligands stabilizing the $[\{Mo_2O_4\}^{2+}]$ linker groups - has e.g. the appropriate pore size to "encapsulate" rather large complementary substrates present in the solution - e.g., guanidinium cations and/or protonated urea cations, which can practically be completely removed from solution (Figure 3.1). Correspondingly, by reaction of **7a** (ligand = $H_2PO_2^-$) (prepared as per reference [13]) with guanidinium sulfate $[\{(H_2O)_{100}+(GH^+)_{20}\}@\{(Mo)Mo_5O_{21}(H_2O)_6\}_{12}\{Mo_2O_4(H_2PO_2)\}_{20}\{Mo_2O_4(SO_4)\}_{10}]^{32-}$ is formed and isolated as the crystalline guanidinium salt **9** (space group R-3m) in nearly quantitative yield.

$$(GH^+)_{32}[\{(H_2O)_{100}+(GH^+)_{20}\}@\{(Mo)Mo_5O_{21}(H_2O)_6\}_{12}\{Mo_2O_4(H_2PO_2)\}_{20}\{Mo_2O_4(SO_4)\}_{10}]\cdot ca.100H_2O$$

9

[2]

[2]The author though started working on the synthesis of this compound in continuation of the work with respect to the interaction of protonated urea with $\{Mo_6O_6\}$ ring-receptors of wheel-shaped $[Mo_{154}]$ type clusters as described

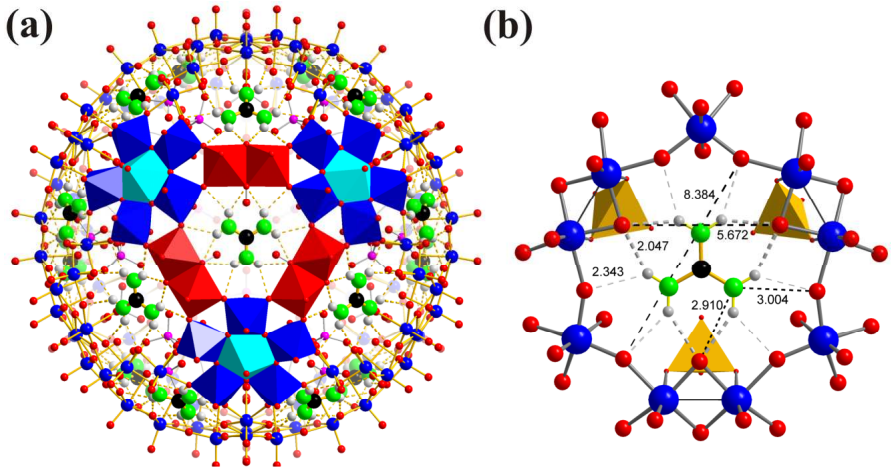

Figure 3.1: *Structural details of the spherical cluster anions* ***9a/10a*** *(diameter approximately 3 nm and cavity diameter around 2 nm) in ball-stick and polyhedral representations, in which three pentagonal* $[(Mo)Mo_5]$ *units (light and dark blue) and three* $[Mo_2]$ *linkers (red) forming an* $\{Mo_9O_9\}$ *ring/pore (highlighted in polyhedral representation) encapsulating* $[(NH_2)_3C]^+$ *ion (C black, N green) (in ball-stick model) has been illustrated as (a). (Note because of the similarity of the clusters* ***9a/10a*** *and* ***11a*** *only* ***9a*** *is shown as a representative case study.) One* $\{Mo_9O_9\}$ *ring of* ***9a/10a*** *together with interatomic distances reflecting the interaction between the receptors and substrates is shown as (b). These 'ring-receptors' are comparable with those known from related single host-guest systems with classical macrocycles. [4, 51] (Colour code: molybdenum, blue; oxygen, red; carbon, black; nitrogen, green; hydrogen, light grey; the* $PO_2H_2^-$ *and/or* SO_4^{2-} *ligands as yellow tetrahedra.) Adapted from reference [47]. The situation with* ***11a*** *can be easily visualized from this Figure just by imaginatively replacing one of the nitrogen atom of guanidinium cations with an oxygen atom.*

Likewise, guanidinium/protonated urea can also be 'up-taken' by icosahedral clusters of the type $[\{(Mo)Mo_5O_{21}(H_2O)_6\}_{12}\{Mo_2O_4(ligand)\}_{30}]^{72-}$ (e.g. with L=SO_4^{2-}) i.e., with only one type of ligand. [3] The uptake in these cases are also nearly quantitative and lead to the formation of **10** and **11**.

$$(GH^+)(NH_4)_{51-n}[\{(H_2O)_{81/2-n}+(GH^+)_{20}+(NH_4)_n\}@\{(Mo)Mo_5O_{21}(H_2O)_6\}_{12}\{Mo_2O_4(SO_4)\}_{30}]\cdot ca.180H_2O$$
10

$$(UH^+)_{20}(NH_4)_{32-n}[\{(H_2O)_{81-n}+(UH^+)_{20}+(NH_4)_n\}@\{(Mo)Mo_5O_{21}(H_2O)_6\}_{12}\{Mo_2O_4(SO_4)\}_{30}]\cdot ca.120H_2O$$
11

in Chapter 1, and also synthesized the compound. The compound in the crystalline state was obtained before the author by Mr. E. Krickemeyer. However the synthesis reported in this dissertation is of author's own, and hence differs from the published one.

[3] Note this cluster with sulfate as ligands can be thought to have been generated in-situ in this case. See the synthetic section later for details.

All these compounds were characterized by elemental analysis, spectroscopy (IR, Raman), single-crystal X-ray structure analysis (see Chapter on experimental details) and bond valence sum (BVS) [34] calculations (to determine the position of the H_2O molecules and to differentiate between the Mo^{VI} and Mo^{V} centers).

3.2.1 $(GH)_{32} \cdot \mathbf{9a} \cdot ca.100H_2O$

$\mathbf{9a} \equiv [\{(H_2O)_{100}+(GH^+)_{20}\}@\{(Mo)Mo_5O_{21}(H_2O)_6\}_{12}\{Mo_2O_4(H_2PO_2)\}_{20}\{Mo_2O_4(SO_4)\}_{10}]^{32-}$

A mixture of **7** (0.5 g, 0.02 mmol), (prepared as per reference [13]), guanidinium sulfate (0.38 g, 1.75 mmol) and 55 ml water was heated on an oil bath at 80^0C for 10 mins with stirring. The dark-brown solution was kept in an open beaker at room temperature for 10 days. The dark-brown crystals of **9** (rhombus type, truncated cubes and octahedra) were filtered over a glass frit and dried in air. Yield: 0.4 g. (80% based on **7**).Elemental analysis: Calc. C 2.2, N 7.8, Mo^V 9.2; Found: C 2.5, N 7.4, Mo^V 9.4%.

*Characteristic spectroscopic data for **9***: IR: ν/cm^{-1} (KBr disk, some characteristic bands 1700-400 cm^{-1}): 1655s $[\delta(H_2O)/(NH_2)_3C^+]$, 1188w, 1124(m-w), 1074vw $[\nu(SO_4)]$, 1038w $[\nu(H_2PO_2)]$, 976m, 945sh $[\nu(Mo=O)]$, 850m, 793s, 725s, 631(m-w), 567m are characteristic bands for the $[\{(Mo)Mo_5\}_{12}\{Mo_2\}_{30}]$ type cluster capsule. Raman: ν/cm^{-1} (solid-state, λ_e = 1064 nm): 950, 870, 374 and 314. VIS-NIR: λ_{max}/nm (in solution): 475.

3.2.2 $(GH^+)(NH_4)_{51-n} \cdot \mathbf{10a} \cdot ca.180H_2O$

$\mathbf{10a} \equiv [\{(H_2O)_{81/2-n}+(GH^+)_{20}+(NH_4)_n\}@\{(Mo)Mo_5O_{21}(H_2O)_6\}_{12}\{Mo_2O_4(SO_4)\}_{30}]^{(52-n)-}$

A mixture of **6** (1 g, 0.04 mmol), (prepared as per reference [13]), guanidinium sulfate (0.8 g, 3.7 mmol), $(NH_4)_2SO_4$ (10 g, 75 mmol) and 100 ml water was acidified with 16% HCl (8 ml) in a 250ml Erlenmeyer flask (covered with a watch-glass) and was heated with stirring at 70^0C for 20 mins. After 5 days brown rhombohedral crystals of **10** were filtered off, and dried in air. Yield: 0.75 g (75% based on **6**). Elemental analysis: Calc. C 0.9, N 5.2. Found: C 1.1, N 5.2%. [46]

*Characteristic spectroscopic data for **10***: IR: ν/cm^{-1} (KBr disk, some characteristic bands 1700-400 cm^{-1}): 1656s $[\delta(H_2O)/(NH_2)_3C^+]$, ca 1406w $[\delta(N-H)]$, 1197w, 1140(m-w), 1036w $[\nu(SO_4)]$ ca. 970s, 945sh $[\nu(Mo=O)]$, 851m, 800vs, 725s, 630(m-w), 570s are characteristic bands for the $[\{(Mo)Mo_5\}_{12}\{Mo_2\}_{30}]$ type cluster capsule. Raman: ν/cm^{-1} (solid-state, λ_e = 1064 nm): 950, 870, 374 and 314. VIS-NIR: λ_{max}/nm (in solution): 450.

3.2.3 $(UH^+)_{20}(NH_4)_{32-n} \cdot \mathbf{11a} \cdot ca.120H_2O$

$\mathbf{11a} \equiv [\{(H_2O)_{81-n}+(UH^+)_{20}+(NH_4)_n\}@\{(Mo)Mo_5O_{21}(H_2O)_6\}_{12}\{Mo_2O_4(SO_4)\}_{30}]^{(52-n)-}$

A mixture of **6** (1 g, 0.04 mmol), (prepared as per reference [13]) urea (3 g, 4.8 mmol), $(NH_4)_2SO_4$ (4 g, 32 mmol) and 100 ml water was acidified with 16% HCl (8 ml) in a 250ml Erlenmeyer flask (covered with a watch-glass) and was stirred for 45 mins. After 10 days brown rhombohedral crystals of **11** were filtered off, and dried

in air. Yield: 0.35 g (35% based on **6**). Elemental analysis: Calc. C 1.7, N 5.6. Found: C 1.7, N 5.6%. [46]

*Characteristic spectroscopic data for **11***: IR: ν/cm^{-1} (KBr disk, some characteristic bands 1700-400 cm^{-1}): 1701w [$\nu(C=O)$], 1632s [$\delta(H_2O)$], 1558w, [$\nu(NH_2)$ of urea], ca. 1400w [$\delta(N-H)$], 1200w, 1141(m-w), 1040 [$\nu(SO_4)$] ca. 970s, 945sh [$\nu(Mo=O)$], 852m, 795vs, 723vs, 632w, 570s are characteristic bands for the [$\{(Mo)Mo_5\}_{12}\{Mo_2\}_{30}$] type cluster capsule. Raman: ν/cm^{-1} (solid-state, λ_e = 1064 nm): 950, 880, 374 and 314. VIS-NIR: λ_{max}/nm (in solution): 450.

Note: The chemical formulas given above refer to the maximum possible number of water molecules in the crystal, which is in agreement with the cell volume. According to the observed loss of water the analytical data, however, refer to this number of crystal water molecules minus 50. [4]

3.3 Discussion of structural details of the host-guest cluster anions

3.3.1 Description of the local structures/'receptor sites' ($\{Mo_9O_9\}$ rings) of the cluster complexes

The integrated cations be it GH^+ ([$(NH_2)_3C^+$]) or UH^+ ([$NH_3^+CONH_2$]) regarding shape and symmetry - fit exactly into the pores, i.e., the $\{Mo_9O_9\}$ rings (similar to the K^+ into the $\{M_6O_6\}$ rings [50]), while the C_3 axes of the icosahedral point group (I_h) pass through their centers. The interaction between the macrocyclic ring, i.e. bridging oxygen atoms of the binuclear [Mo_2] units, and the three/two H_2N groups of the 20 guanidinum/protonated urea cations (Figure 3.1) is due to hydrogen bonding and corresponds to that observed in a monotopic receptor (see [51], also [50]). Reactions of the ball type cluster with its 20 receptors can be regarded as models for the manipulation of spherical icosahedral viruses. [52] A fragment of **9a**, **10a** or **11a** - based on the 12 pentagonal [$(Mo)Mo_5$] units with altogether 60 $\{MoO_6\}$ octahedra - is an inorganic analog of the most simple (so-called T = 1) virus type containing only 12 pentamers ($\equiv$ 60 proteins). [48] In both cases the 60 units are packed about the exact five-fold axes. More interesting: in case of the next larger (so-called T = 3) icosahedral virus type - like the Tomato Bushy Stunt Virus (TBSV) for instance - besides the 12 pentamers, additionally 20 hexamers or 120 proteins are placed around the local six-fold axes of an icosadeltahedron (Figure 3.2), [48] a situation comparable to the positioning of the 20 x 6 = 120 H atoms of the guanidinium cations of **9a** and **10a** on an icosadeltahedron (Figure 3.2; see also Figure 3.3)

[4] These compounds will be referred to in this Chapter after this section by numbers for the sake of convenience.

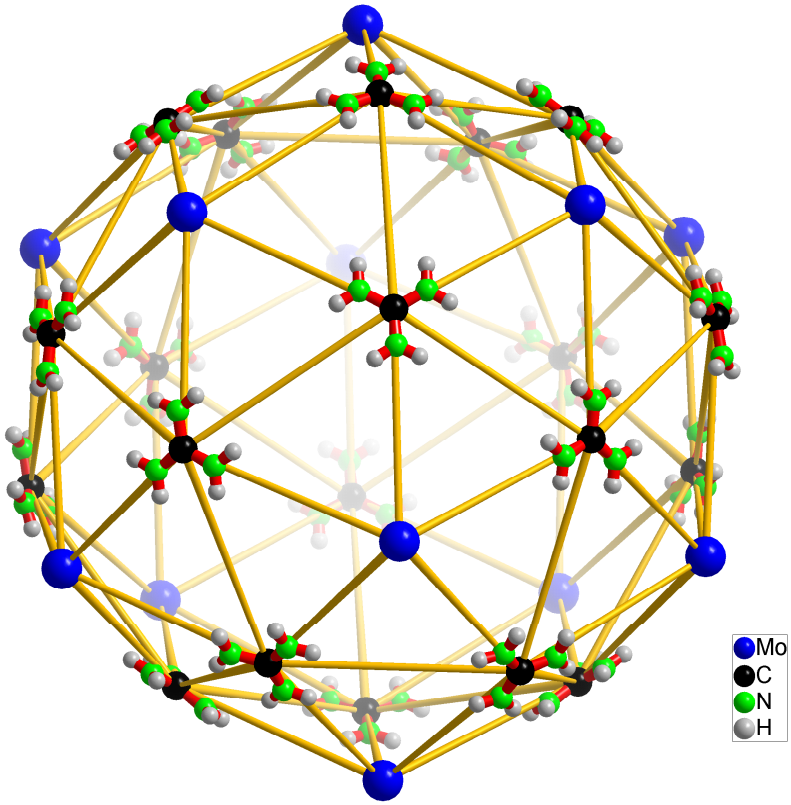

Figure 3.2: *The atoms of the guanidinium cations placed on an icosadeltahedron which is obtained by subdividing each triangular face of an icosahedron - formed by the 12 Mo centers of* ***9a/10a*** *- into three equilateral triangles. The icosadeltahedron has local six-fold symmetry elements relating its subunits/faces which are not elements of the icosahedral symmetry group. Interestingly, the 60 H atoms pack around the six-fold axes like proteins of an important (T = 3) spherical virus type, e.g., the TBSV (Tomato Bushy Stunt Virus). [48] The 12 x 5 MoO_6 octahedra of the pentagonal $[(Mo)Mo_5]$ groups of anion of* ***9a*** *or* ***10a*** *are correspondingly packed around the five-fold axes. A comparable and similar tiling of protonated urea in* ***11a*** *on an icosadeltahedron can be easily visualized replacing one nitrogen atom of guanidinium (as shown in this Figure) with an oxygen atom of protonated urea. Adapted from reference [47].*

3.3.2 Description of the structures of different encapsulated Platonic and Archimedean architecture inside the host-guest cluster complexes

Topologically speaking, **9a**, **10a** and **11a** are remarkable Keplerates [12] (for a mathematical interpretation/treatment see [24]) with several sets of equivalent atoms forming different types of Platonic and Archimedean solids (Figure 3.3 and table therein), i.e. chemistry can perform icosahedral tilings of the sphere. A nice sequence of truncation is observed by going from the dodecahedron spanned by the 20 carbon atoms

of the guanidinium cation via the (distorted) rhombicosidodecahedron formed by the related 60 N atoms to the (distorted) rhombitruncated icosidodecahedron spanned by the 120 H atoms. [But note: The truncation of the third leads to the second solid (Figure 3.3).] The 120-vertices solid represents the most complex Archimedean solid comprising 12 decagons, 30 tetragons and 20 hexagons. (According to our knowledge these two specific polyhedra have not been observed in chemistry until now.) Additionally, the 30 P/S atoms of **9a** or only 30 S atoms of **10a** and **11a** form an icosidodecahedron, the 12 Mo atoms an icosahedron, and the 30 $[Mo_2^V]$ linkers a (distorted) truncated icosahedron.

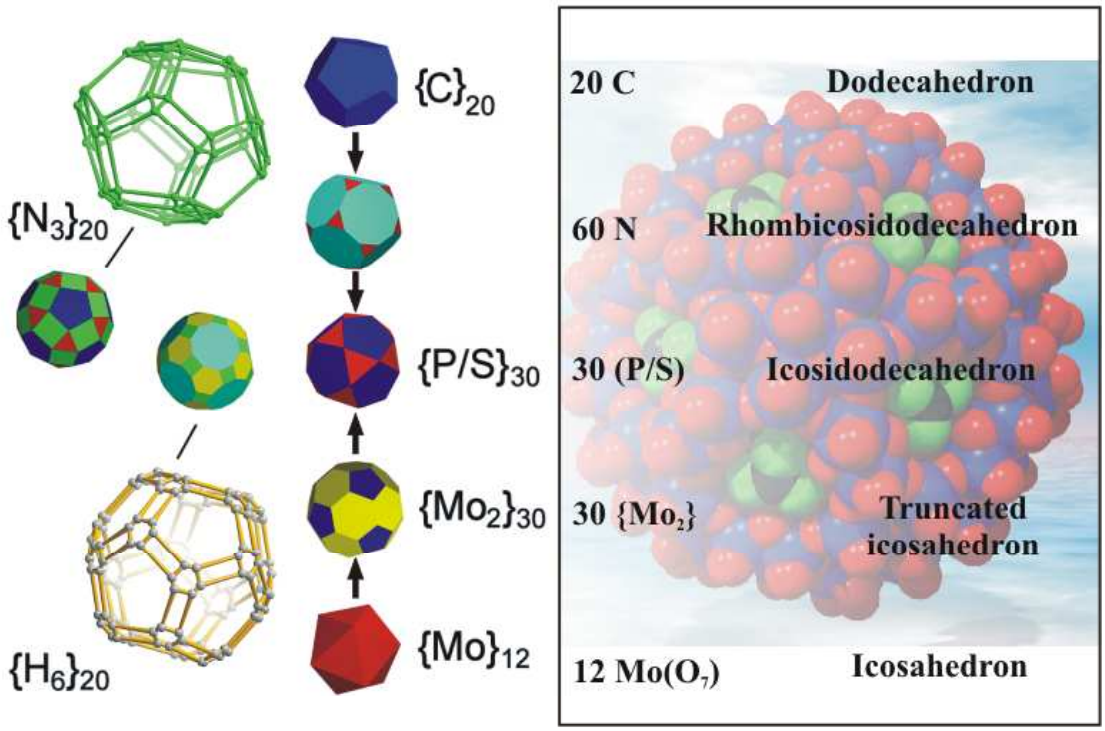

Figure 3.3: *Left: The stepwise truncation of the two Platonic solids - the dodecahedron and icosahedron - gives a series of Archimedean solids (truncated dodecahedron and the four others of the table depicted on the right); four of the Archimedean and two of the Platonic solids are spanned by equivalent sets of atoms of anion of* ***9a****. Additionally, the real (distorted) Archimedean solids* $\{N_3\}_{20}$ *and* $\{H_6\}_{20}$ *of anions of* ***9a*** *or* ***10a*** *are shown. Right: Chemistry creates icosahedral tilings of a sphere. Archimedean and Platonic solids formed by the sets of atoms of anion of* ***9a*** *or* ***10a****. The anion of* ***9a*** *or* ***10a*** *is shown in space-filling representation in the background of the table. Colour code: molybdenum, blue; oxygen, red; nitrogen, green; carbon, black. Adapted from reference [47].*

3.3.3 On the availability of space for the cations in the unit cells

It seems that the space in the lattice of the host-guest compounds **9-11** is limited. It is possible to accommodate at most 52 large monopositive organic cations like protonated urea or guanidinium. This proposal stems from the observation that the total number of guanidinium or protonated urea cations in the cluster compounds **9-11** is always found to be less than or equal to 52, even if the overall anionic charge is higher (72-) as in case of **10a** or **11a**. The available space is obviously determined by the extent and the nature of the stereo-electronic interactions operating in these clusters.

3.3.4 On the structuring of water and further encapsulation of cations inside some of these clusters

Unlike **9a** the formula of cluster anions **10a** and **11a** show encapsulated ammonium ions. But why? Moreover all the three cluster anions discussed in this Chapter, **9a**, **10a** and **11a** show structuring of water together with an interesting aspect of further cation (like ammonium) encapsulation. Is somehow structuring of water related with encapsulation of ammonium ions? All such questions have been separately discussed in Chapter 5.

3.4 General aspects

3.4.1 New host/receptor sites: $\{Mo_9O_9\}$ rings/pores and implications on closing those pores

Important aspects within the context of the these spherical 'Keplerates' are the possibility of closing their 20 pores with suitable 'organic cork' type substrates like guanidinium or protonated urea - and further the possibility of their removal from a solution by these 'Keplerates', a phenomenon comparable to the effective recognition by a nanosponge. (Guanidinium and urea play a central role in many processes of the chemical and pharmaceutical industry [53] while there is an extensive coordination as well as supramolecular chemistry of guanidinium which can act as sterically flexible ligand [54] and anion receptor; [4] urea plays a significant role in host-guest chemistry, [41] and also as 'supramolecular glue' in making of 'adhesive antibodies' [42] other than its regular roles in protein purification. [48])

Closing the pores decreases the negative charge of the cluster drastically, stabilizes it, and influences the structure of the remarkable $(H_2O)_n$ cluster (droplet of nanowater) incarcerated in the former open clusters. However the nature of the 'drop of water' inside **9a** and **11a** are different. (For more on structuring of water see [55, 56] and also Chapter 5.)

3.4.2 Chemistry on nanoobjects' spherical surfaces

Spherical shell type objects - where the subunits exist in identical environments -are interesting in several aspect: They are easily isolable and often the preferred target of self-assembly processes based on simple units because of their high stability (the surface area is minimum while the strain energy is evenly distributed along the surface). Consequently, this type of spherical shell object can be used as handleable/manipulateable molecular containers. They can be constructed with quite a different number of building blocks - as in the present situation - while allowing chemical reactions at quite different functional groups abundant at the surface. (Note: It is impossible to construct a spherical system from one chemical entity only.)

3.5 IR spectral features of the host-guest complexes

A small note in the context of vibrational spectra of the host-guest species discussed in this Chapter can be added here. It is worthy to note from Figure 3.4 that the incoming guest entity in each case leaves a low-intensity finger-print on the vibrational spectra of the host-guest moiety formed in each case, while the overall pattern of all the spectra are similar to that of the starting quasi-spherical icosahedral host, e.g., of **8**. The low intensity of the incoming guests' finger-print is expected keeping in mind the giant size of the clusters.

3.6 Discussion and perspectives

Supramolecular chemistry started with selective binding of alkali metal cations by natural and synthetic macrocyclic ligands, followed later by strong and selective binding of anionic as well as neutral complementary substrates. [4] Now it is possible to have a rather large multitude of receptor sites positioned on a stable nanoobject. While it became evident - mainly due to the initiative and work of J-M. Lehn - that a receptor-substrate supermolecule is characterized by its geometric (structure/conformation), thermodynamic (stability, entropy and enthalpy of formation), and kinetic (roles of formation and dissociation) features, which are markedly affected by the medium/solvent. Clearly new categories appear in the present type of polytopic super-supramolecule with the options to study a variety of relevant cooperativity effects. To summarize: The present results highlight that the spherical cluster type under investigation - having a large number of receptor sites - can exist with different linkers (for instance with mononuclear and dinuclear metal centers), and correspondingly with different pore sizes with the consequence that they can act as effective and specific nanosponges. Their reactivity should be different from the discrete type ones and can even be influenced by changing the electronic property of the host shells. This is a situation comparable to substrates placed on "classical", e.g. related industrially important metal-oxide surfaces [57] where the reactivity and even stability of the substrates can also be influenced by changing surface properties (with guests) as well. (See Chapter 4 for more on 'guest-activity' inside these spherical clusters.)

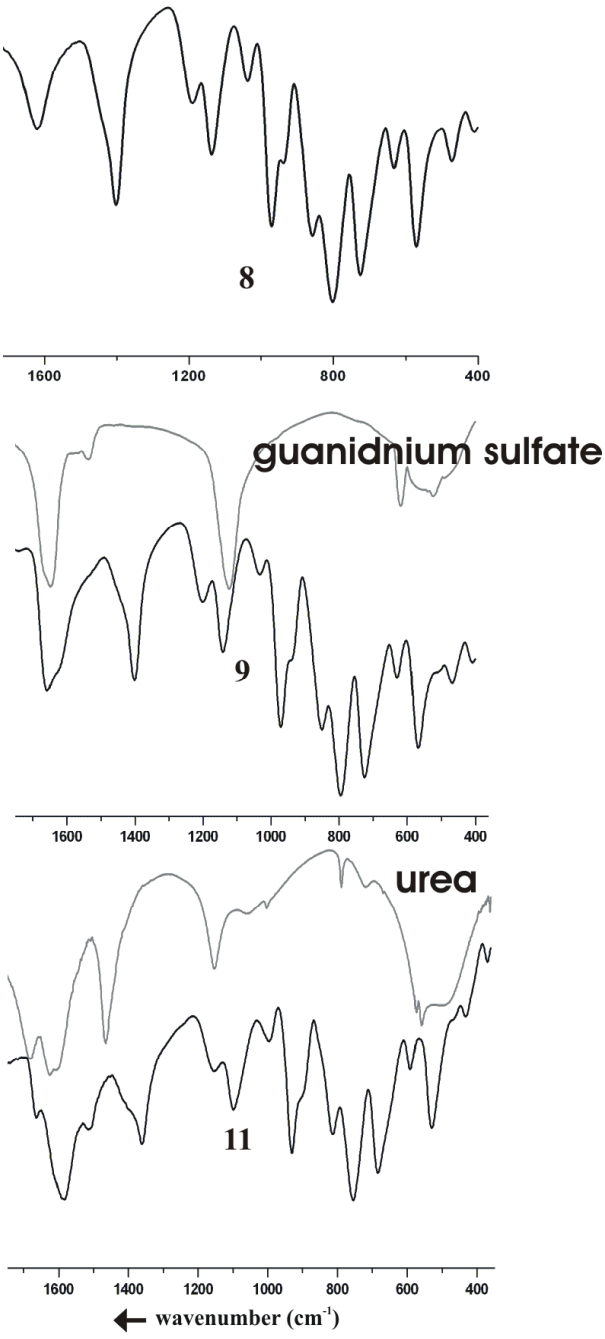

Figure 3.4: *Comparison of the IR spectra of the parent host complex i.e.,* ***8*** *with the host-guest complexes* ***9*** *and* ***11****. The spectra of* ***9*** *and* ***11*** *show clear signatures of the incorporated guests but also bear the overall structure of the spectrum of the parent host* ***8****. Note the relatively small intensity of the guest signature bands can be easily appreciated taking into account the large size and high overall cluster symmetry as compared to that of the guests. Due to obvious similarity in the spectra of* ***9*** *and* ***10*** *the spectrum of the former is given here only.*

Chapter 4

Preparation of spherical polyoxomolybdates as cation 'traps': New host sites for smaller inorganic cations inside the spherical cluster capsules

4.1 Introduction

[1]Molecular dimensioned holes can serve as filters and also trap molecules with well-defined shape. Whereas a large number of porous materials with cages and tunnels [59] exist as extended structure, as yet not much is known about well-defined related discrete (molecular) nanoporous type species. Processes that refer to the entrance of substrates, e.g. of cations, through pores and succeeding channels into cellular cavities are particularly of interest if the affinity of specific substrates to specific capsule areas can be predicted. It has been demonstrated in the preceeding Chapter that the spherical icosahedral clusters of the type $[Mo_{132}]$ are endowed with substrate responsive behaviour. This Chapter demonstrates the possibility for nanosized spherical capsules based on the robust fundamental skeleton $[(pent)_{12}(link)_{30}] \equiv \{(Mo)Mo_5O_{21}(H_2O)_6\}_{12}\{Mo_2O_4(ligand)\}_{30}$ [13, 56] having sizeable pores, finely sculpturable interiors and, in between, tuneable functionalized channels to show unprecedented molecular-scaled filter properties. Most importantly, the channel functionalities as well as the capsule size and charge can be extensively varied while charge modulations lead to related changes in the affinity to cations!

In this Chapter it is shown that different substrates/cations can get fixed at well-

[1]A major part of this Chapter has been published as reference [58]: A. Müller, S. K. Das, S. Talismanov, S. Roy, E. Beckmann, H. Bögge, M. Schmidtmann, A. Merca, A. Berkle, L. Allouche, Y. Zhou, L. Zhang, Angew. Chem. Int. Ed. 42 (2003) 5039. Some Figures of this Chapter have been adapted from the published article.

defined positions of the capsules and especially in the capsules' channels. (Please note in this study several other colleagues of the group were also involved, as evident from the original reference [58].) The situation further allows to study, in principle, new type of molecular transport phenomena on a nanoscale including osmotic type ones, and shows properties of a 'nano-ion chromatograph'. Additionally, one can construct new 'stable' geometries like 'interpenetrating solids' according to the fact that these clusters have a multitude of different as well as equivalent sites in the channels, pores, and in the interior (see also [60]). This further allows the study of matter under confined conditions.

4.2 Syntheses and characterization of the cluster compounds

For the uptake investigations the known capsule i.e., **6a** [13] was used to generate *in-situ* **8a**, [56] exhibiting the above mentioned skeleton. As the latter contains the neutral linker units $[\{Mo_2O_4(SO_4)\}]$, the overall cluster charge corresponds to the charge of the 12 pentagonal units, i.e. 12 x (6-) = 72-. The exposition of this cluster anion **8a** [56] to (i.e., react with) different substrates/cations like Na^+, Ca^{2+}, $[OC(NH_2)NH_3^+]$ and $[C(NH_2)_3]^+$ in aqueous solution leads to the formation of **12a - 14a** exhibiting well-defined cation separations at, above, or below the capsule's channel-landscapes ('nano-ion chromatography' principle). All compounds were characterized by elemental analyses, single-crystal X-ray diffraction analyses (including bond valence sum (BVS) calculations), [34] IR and Raman spectroscopy. [2]

$(NH_4)_{42}[\{(Mo)Mo_5O_{21}(H_2O)_6\}_{12}\{Mo_2O_4(CH_3COO_)\}_{30}] \cdot ca.300H_2O \cdot 10CH_3COONH_4$ [13]

6

$(NH_4)_{72-n}[\{(H_2O)_{81-n} + (NH_4)_n\}@\{(Mo)Mo_5O_{21}(H_2O)_6\}_{12}\{Mo_2O_4(SO_4)\}_{30}] \cdot ca.200H_2O$ [56]

8

$(UH^+)_{28}Na_{11}[\{(H_2O)_{60} + (UH^+)_{20} + Na_{13}\}@\{(Mo)Mo_5O_{21}(H_2O)_6\}_{12}\{Mo_2O_4(SO_4)\}_{30}] \cdot ca.140H_2O$

12

$(GH^+)_6(NH_4)_{20}Na_{13}[\{(H_2O)_{60} + (GH^+)_{20} + Na_{13}\}@\{(Mo)Mo_5O_{21}(H_2O)_6\}_{12}\{Mo_2O_4(SO_4)\}_{30}] \cdot ca.190H_2O$

13

$(UH^+)_{22}(NH_4)_{16}[\{(H_2O)_{60} + (UH^+)_{20} + Ca_7\}@\{(Mo)Mo_5O_{21}(H_2O)_6\}_{12}\{Mo_2O_4(SO_4)\}_{30}] \cdot ca.140H_2O$

14

[2] GH^+ and UH^+ stand for $\{(NH_2)_3C^+\}$ and $(NH_3^+CONH_2)$ respectively.

4.2.1 $(UH^+)_{28}Na_{11} \cdot \mathbf{12a} \cdot ca.140H_2O$

$\mathbf{12a} \equiv [\{(H_2O)_{60} + (UH^+)_{20} + Na_{13}\}@\{(Mo)Mo_5O_{21}(H_2O)_6\}_{12}\{Mo_2O_4(SO_4)\}_{30}]^{39-}$

A mixture of **6** (0.5 g, 0.02 mmol), (prepared as per reference [13]), urea (1.0 g, 16.7 mmol), $(NH_4)_2SO_4$ (2.5 g, 18.9 mmol) and 40 ml water acidified with 8 ml 16%HCl was heated at $60 - 70^0C$ in a 100-ml Erlenmeyer flask (covered with a watch-glass). After 90 min, NaCl (3.0 g, 51.3 mmol) was added and the solution was heated further for 90 min and then kept at room temperature for crystallization. After 3-4 days brown rhombohedral crystals of **12** were filtered off, and dried in air. Yield: 0.35 g (70% based on **6**). Elemental analysis: Calc. Na 1.9, C 1.9, N 4.6. Found: Na 2.1, C 1.8, N 4.6%.

*Characteristic spectroscopic data for **12***: IR: ν/cm^{-1} (KBr disk, some characteristic bands 1700-400 cm^{-1}): 1703w [$\nu(C = O)$], 1625s [$\delta(H_2O)$], 1554w [$\nu(NH_2)$ of urea], ca 1402w [$\delta(N - H)$], 1197w, 1145(m-w), 1039w [$\nu(SO_4)$], ca. 974s, 945sh [$\nu(Mo = O)$], 852m, 792vs, 725vs, 630w, 570s are characteristic bands for the $[\{(Mo)Mo_5\}_{12}\{Mo_2\}_{30}]$ type cluster capsule. Raman: ν/cm^{-1} (solid-state, λ_e = 1064 nm): 950, 880, 374 and 314. VIS-NIR: λ_{max}/nm (in solution): 450.

4.2.2 $(GH^+)_6(NH_4)_{20}Na_{13} \cdot \mathbf{13a} \cdot ca.190H_2O$

$\mathbf{13a} \equiv [\{(H_2O)_{60} + (GH^+)_{20} + Na_{13}\}@\{(Mo)Mo_5O_{21}(H_2O)_6\}_{12}\{Mo_2O_4(SO_4)\}_{30}]^{39-}$

A mixture of **6** (1g, 0.04mmol), NaCl (3g, 51 mmol), guanidnium sulfate (0.5g), $(NH_4)_2SO_4$ (2.5g, 18.9 mmol) and 40 ml water was acidified with 10ml 16% HCl in a 100ml Erlenmeyer flask (covered with a watch-glass). The resulting brown solution was stirred for 1 hour and left in an open beaker for crystallization. After 3-4 days brown rhombohedral crystals were obtained, which were filtered and dried in open air. Yield: 0.8 g (80% based on **6**). Elemental analysis: Calc. C 1.1, N 4.8, Na 2.1. Found: C 1.1, N 4.8, Na 2.1%.

*Characteristic spectroscopic data for **13***: IR: ν/cm^{-1} (KBr disk, some characteristic bands 1700-400 cm^{-1}): 1655s [$\delta(H_2O)/(NH_2)_3C^+$], 1402 [$\delta(N - H)$], 1200w, 1147(m-w), 1039vw [$\nu(SO_4)$], ca. 976m, 945sh [$\nu(Mo = O)$], 850m, 793s, 725s, 631(w-m), 567m are characteristic bands for the $[\{(Mo)Mo_5\}_{12}\{Mo_2\}_{30}]$ type cluster capsule. Raman: ν/cm^{-1} (solid-state, λ_e = 1064 nm): 950, 880, 374 and 314. VIS-NIR: λ_{max}/nm (in solution): 475.

4.2.3 $(UH^+)_{22}(NH_4)_{16} \cdot \mathbf{14a} \cdot ca.140H_2O$

$\mathbf{14a} \equiv [\{(H_2O)_{60} + (UH^+)_{20} + Ca_7\}@\{(Mo)Mo_5O_{21}(H_2O)_6\}_{12}\{Mo_2O_4(SO_4)\}_{30}]^{38-}$

A mixture of **6** (0.5g, 0.02mmol), urea (0.6g, 10mmol), $(NH_4)_2SO_4$ (2.5g, 18.9 mmol), $CaCl_2 \cdot 2H_2O$ (1.5g, 10mmol) and 60 ml water was acidified with 8 ml 16% HCl in a 100ml Erlenmeyer flask (covered with a watch-glass). The resulting brown solution was kept on an oil bath at 65^0C for 3h without stirring. The solution was then filtered and kept in an open beaker for crystallization. After 10 days brown rhombohedral crystals were obtained. Yield: 0.5g. Elemental analysis: Calc. C 1.7, N 4.1, Ca 1.1. Found: C 1.7, N 4.8, Ca 1.0%.

*Characteristic spectroscopic data for **14***: IR: ν/cm^{-1} (KBr disk, some characteristic bands 1700-400 cm^{-1}): 1701w [$\nu(C=O)$], 1624s [$\delta(H_2O)$], 1550w [$\nu(NH_2)$ of urea], ca 1402w [$\delta(N-H)$], 1186sh, 1141(w-m), 1051w [$\nu(SO_4)$], ca. 977vs, 945sh [$\nu(Mo=O)$], 852w, 794s, 723s, 630m, 570s are characteristic bands for the [$\{(Mo)Mo_5\}_{12}\{Mo_2\}_{30}$] type cluster capsule. Raman: ν/cm^{-1} (solid-state, λ_e = 1064 nm): 950, 880, 374 and 314. VIS-NIR: λ_{max}/nm (in solution): 450.

Note: The chemical formulas given above refer to the maximum number of water molecules in the crystal, which is in agreement with the cell volume. According to the observed loss of water the analytical data, however, refer to this number of crystal water molecules minus 50. [3]

4.3 Description of the detailed comparative structural features of the cluster capsules containing organic guests on the cluster surface and inorganic cations inside

The capsules' basic skeleton $\{(Mo)Mo_5O_{21}(H_2O)_6\}_{12}\{Mo_2O_4(ligand)\}_{30}$ remain unchanged before and after cation uptake while as expected the interior gets differently modified (Figures 4.1, 4.2); this is a situation for molecular materials never observed before. Details of the cation position and the description of the channels where they are found are outlined below.

4.3.1 The positions of organic and inorganic guest cations inside the host cluster capsule

The uptake of various cations by the cluster capsules leads to stoichiometric preferences when the cations get fixed in the higher channel areas, i.e. if the $\{Mo_9O_9\}$ pores can act corresponding to their crown-ether function. Non-stoichiometric situations preferably occur especially below the pore area (see Figures 4.1 and 4.2). (In these cases the uptake can be increased by increasing related cation concentration and/or the capsule charge.) Although the comparatively large stoichiometrically bound protonated urea/guanidinium cations in the cluster anions of **12a**, **13a** or **14a** fit reasonably well into the $\{Mo_9O_9\}$ rings/pores (as mentioned in the last Chapter), the smaller Na^+ or Ca^{2+} cations are not found exactly at the pore centres, but slightly shifted inwards, to the channel interior. A detailed account of the relative positioning of Na^+ or Ca^{2+} cations is described later. [4] It is interesting to note here that the uptake of an inorganic cation like Na^+ and dissimilar yet related organic cations like protonated urea or guanidinium by the capsules result in similar structure: **12a** and **13a**. The coordinates of cations Na^+, protonated urea or guanidinium in these clusters **12a** and **13a** are nearly the same. (Note Na...C, Na...O,

[3] These compounds will be referred to in this Chapter after this section by numbers for the sake of convenience.

[4] Like the clusters described in the last Chapter, these clusters show structured water-assemblies. This issue of structuring of water inside these clusters has been described in detail in Chapter 5.

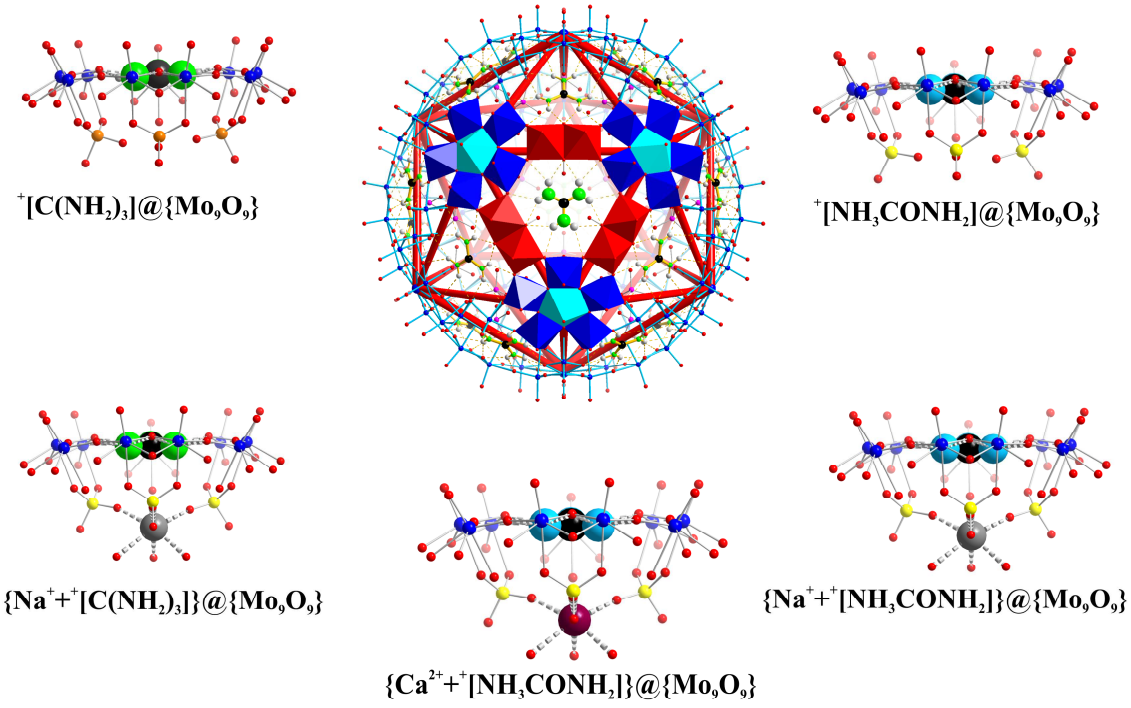

Figure 4.1: *The centre shows the main entering portion: one of the 20 $\{Mo_9O_9\}$ pores placed on one of the 20 faces of the icosahedron spanned by 12 Mo atoms in polyhedral representation (here with a guanidinium guest; see also last Chapter). Different substrates/cations get fixed specifically at different position of pores and adjoining channels leading to the interior of the "artificial cell" of the type $[\{(Mo)Mo_5O_{21}(H_2O)_6\}_{12}\{Mo_2O_4(ligand)\}_{30}]$: within the $\{Mo_9O_9\}$ rings/pores the protonated guanidinium and urea cations (of **9a/10a**, top left, and **11a**, top right), below, i.e. in the channels, e.g. Na^+ in an environment spanned by three O atoms of three sulphate ligands (**12a** and **13a** below right); the channel with Ca^{2+} lidded with urea is shown (**14a**, bottom middle). (Mo blue, O red, S yellow, P/S (of **9a**) brown; respective substrates/cations in different colours). Adapted from reference [58].*

Na...S distances are same in these clusters i.e., around 3.60 - 4.10 $\AA$, 2.31 - 2.82 $\AA$ and 3.68 - 3.84 $\AA$ respectively.) It might be proposed that such a similarity in the structure stems from comparable electrostatic interaction between the monopositive cations of these clusters: Na^+, protonated urea or guanidinium. So according to this proposal it is reasonable to think that there should be an effect on the structure of the cluster if one of these two cation type is changed. The 'organic corks', protonated urea or guanidnium, being stereo-electronically similar and indispensable for their 'cork-function' obviously cannot be changed. In order to test the above proposal that electrostatic repulsion between the cations affect their relative position inside the cluster a comparison of the structure of the clusters with Ca^{2+} and Na^+ (with

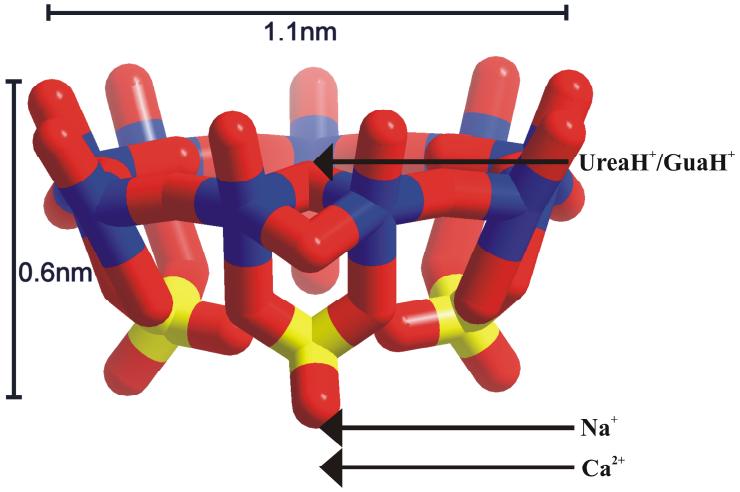

Figure 4.2: *The relative position of all the fixed substrates (described in this Chapter) in one of the 20 channels (wire-frame representation; color code as in Figure 4.1). Adapted from reference [58].*

same 'organic corks'), like **12a** and **14a**, is essential.

A note on the positions of Na^+ and Ca^{2+} cations in the host cluster capsule

The cations Na^+ or Ca^{2+} of **12a** or **14a** being located on the C_3 axis passing through the $\{Mo_9O_9\}$ pores of the clusters, when connected form $\{Na^+\}_{20}$ or $\{Ca^{2+}\}_{20}$ dodecahedron. The $\{Na^+\}_{20}$ dodecahedron of **12a** is a bit more inflated than $\{Ca^{2+}\}_{20}$ of **14a**. (The expanse of the dodecahedra are around 16 $\AA$ and 15.8 $\AA$ respectively.)

This in turn means that Ca^{2+} ions are located deeper inside the cluster than Na^+ ions. (Figure 4.3)

Such a differential positioning of the Na^+ or Ca^{2+} cations in the clusters **12a** or **14a** supports the previous proposal that relative cation position inside the clusters is determined by the effective electrostatic repulsion between them. The 'organic corks' on the surface of both these clusters being protonated urea: Ca^{2+} with higher charge density is 'pushed deeper' inside the cluster's channels in comparison to Na^+, with a lesser charge density. (Note the Ca...C and Na...C distances in **14a** and **12a** are 3.8-4.2 and 3.6-4.1 $\AA$ respectively.)

4.3.2 Description of the 'channels' of the host-guest complexes opening through $\{Mo_9O_9\}$ pores on the cluster surface

The channels of the clusters are lined with nucleo-/hydrophilic chemical groups conducive to the passage of electrophilic positively charged ions. There is a formal analogy of this channel type with biological membrane-channels. [61] In both cases the entrance region is important: in the biological membranes negatively charged

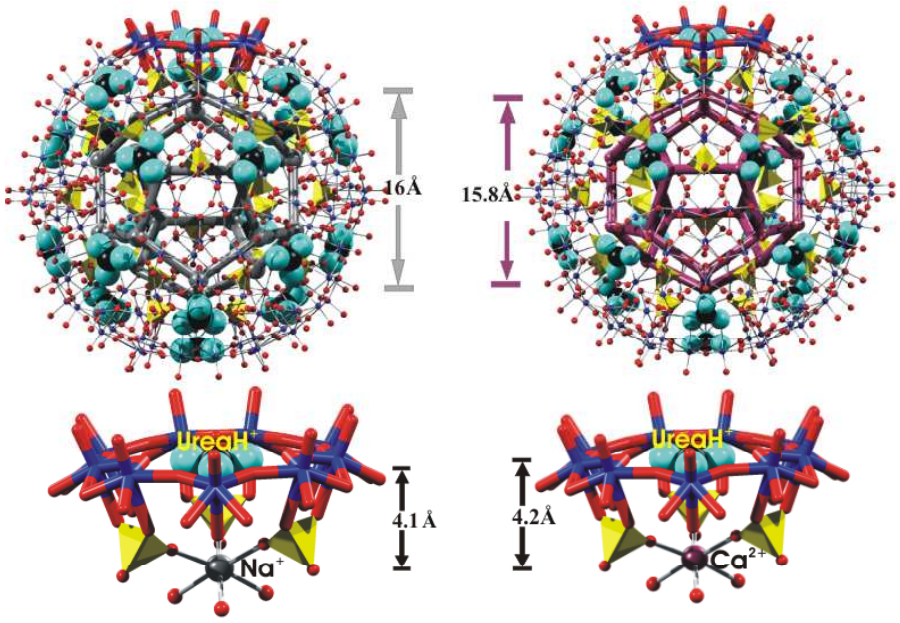

Figure 4.3: *A detailed comparison of position of Na^+ or Ca^{2+} cations in the host cluster capsules. The cluster anions* ***12a*** *(left) and* ***14a*** *(right) with encapsulated dodecahedra of Na^+ and Ca^{2+} ions in grey and plum. (The diameter of the spheres encapsulating those dodecahedra are shown correspondingly.) The related $\{Mo_9O_9\}$ ring/pore channels are highlighted in wire-frame representation below every cluster. Note the distances between the cations (Na^+ and Ca^{2+}) and the 'organic corks' (in these cases protonated urea) along those pore channels. See text for details. Colour code: Sulphate ligands are shown in yellow tetrahedra. Rest same as in Figure 4.1.*

amino acids, and in the present case the anionic ligands like sulphate promote cation diffusion leading to selectivity and gate mechanisms controlling the flux. There is also the option of different substrates coordinating simultaneously in the higher and lower parts of the 'channels' along the C_3 axes in the direction of the capsule centre if the cations are simultaneously present. This offers, in principle, also the possibility to study novel type of cooperativity interactions between different type of encapsulated fixed centres including paramagnetic ones. Unfortunately such a phenomenon has not been observed until now.

An interesting phenomenon of 'inorganic endosmosis' is observed when the usual reaction system forming **8a** [56] is treated with a strong electrolyte solution, i.e. $NaCl/CaCl_2$ in presence of urea, the cluster anion **8a** 'takes-up' Na^+ or Ca^{2+} cations before 'closing' the channel with protonated urea, hence forming **12a** or **14a** respectively. The remarkable preferential first trafficking depends specifically on the different capsules' functional-group activities involved. As the "channels' clothes" can be modified by exchanging ligands attached to the 30 linkers the option exists to use deliberately different related functionalities.

4.4 IR spectral features of the cluster compounds

It is interesting to note that the IR spectra of **11**, **12**, **13** and **14** are similar to that of the starting compound **8**, as depicted in Figure 4.4. Although the 'signature' of urea (i.e., two bands around 1700 [$\nu(C = O)$] and 1550 cm^{-1} [$\nu(NH_2)$ of urea], shown with two black arrows in the Figure 4.4) is observed in all the three compounds **11**, **12** and **14**, no significant change is noticeable in the sulfate bands of **12** and **13** as compared to the starting **8**, due to coordination of Na^+. A different phenomenon is observed with the compound **14**. In this case a 'slightly' red shifted sulfate band is observed at 1051 cm^{-1}. The reason as to why Ca^{2+} coordination alters the IR-spectra of these compound types and not Na^+ coordination is still debatable.

4.5 Discussion and perspectives

The capsules, described here, i.e. nanoscale laboratories ([62], see also: [3]) with a variety of functionalities enable the positioning of substrates/cations under controlled conditions. Additionally, trapping in the 20 pores and channels can be achieved stepwise and likewise the affinity of the positive substrates to the sites of the negative capsule changes with each trapping event, a phenomenon which can be regarded as one of the hallmarks of nanotechnology.

The results described in this Chapter might be considered as a new type of supramolecular situation showing perspectives for further investigations. Importantly, the separation of cations abundant in aqueous solution allows in principle the option of fabricating a 'nano-ion chromatograph'. The behaviour is perhaps comparable to "artificial cells" [5] in the sense that they respond to the change in their solution/solute environment in a specific way. (It seems that well-defined hydrated metal cations like the above given complexes because of their size are blocked at the pores.) As the reactions are performed under the conditions of nanocapsule confinement, whose size and charge can be precisely generated, new basic processes may emerge which need not necessarily agree with those observed in bulk materials though also offering new insights into related bulk reactions. For example, it was found very recently that at least five water molecules were necessary to observe dissociation of HBr. [63] These quasi-spherical cluster compounds can generally speaking provide insight into the influence of geometric confinement on different substrate positionings but especially allow - because of the multitude of different type of equivalent sites - the generation of novel nanoscopic architecture. [10, 64]

[5] However the algorithm of operation of these "cells" are nowhere comparable to their biological analogues

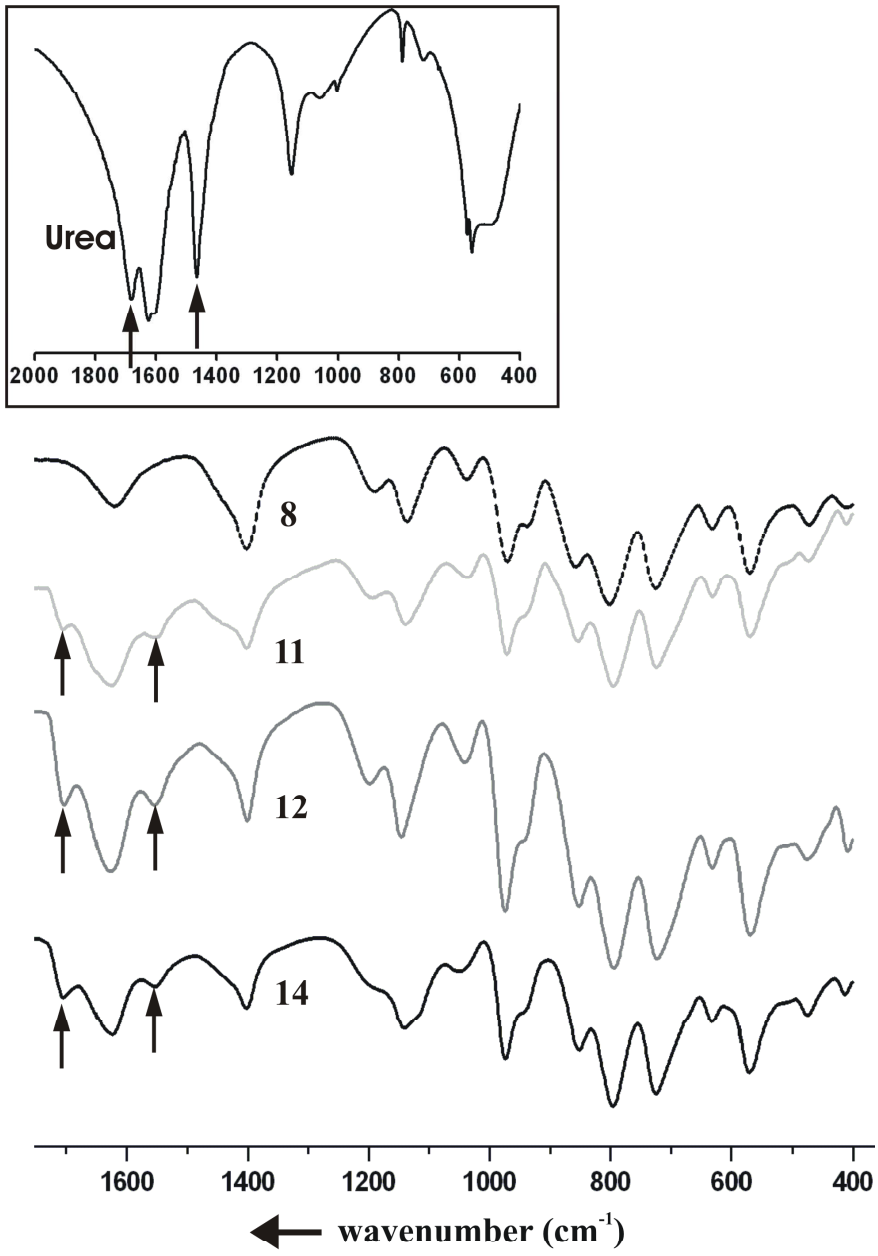

Figure 4.4: *A comparison of infra-red spectra of* ***8***, ***11***, ***12*** *and* ***14*** *with urea and each other. The two bands shown with two black arrows in cases of compounds* ***11***, ***12*** *and* ***14*** *around 1600 cm^{-1}, are vibrational spectroscopic signatures for incorporation of urea in these compounds.*

Chapter 5

'Captive water': Structures of cavity encapsulated 'nanodrops' of water inside $[Mo_{132}]$ type cluster capsules and the influence of encapsulated inorganic ions on them

5.1 Introduction

[1] Water is the fundamental compound for life processes including the biospheres evolution and even for our daily life. [65] It is the most abundant substance on earth, occurs most abundantly as glassy water on tiny grains of interstellar matter [66] and has fascinated philosophers and scientists since the dawn of history. [67] Though many researchers were involved in the development of different models to understand the puzzling properties, no single model can explain all of them. [68] One promising route to obtain additional information would be to look at the structure of H_2O assemblies only 'weakly encapsulated' in cavities with varying size. Until now this phenomenon has only been studied for intrinsically size limited assemblies. [69, 70] In fact, the giant inorganic molybdenum-oxide based spherical clusters of the type $[Mo_{132}]$, could serve as a good starting point in this regard, since they provide the option to investigate the water assemblies encapsulated within them. There is also the additional option to observe the change of the encapsulated water clusters by

1. closing the cluster pores and 'tuning' the microcosm of the cluster cavity (by

[1] Some aspects described in this Chapter have been adapted from reference [55]: A. Müller, H. Bögge, E. Diemann, Inorg. Chem. Commun. 6 (2003) 52.

changing the ligands associated with the 'linkers' of these clusters) (see for instance, ref. [56]) and

2. also the effect of encapsulation of inorganic (alkali metal) cations inside these clusters.

In this Chapter the influence of these parameters will be systematically described by comparing the water assemblies 'captivated' inside the related $[Mo_{132}]$ clusters that span the aforementioned paradigm. The knowledge acquired from this study will then be employed to logically argue the presence of cations like ammonium, encapsulated inside some of the $[Mo_{132}]$ type clusters, which is otherwise difficult to ascertain only from single-crystal X-ray diffraction experiments. The $[Mo_{132}]$ type clusters whose water assemblies will be shortly described have been put into three major groups as following. (For detailed synthetic and structural aspects of these clusters please refer to Chapters 3 and 4.)

Clusters with open pores [2]

$(NH_4)_{42}[(H_2O)_{80}@\{(Mo)Mo_5O_{21}(H_2O)_6\}_{12}\{Mo_2O_4(H_2PO_2)\}_{30}] \cdot ca.220H_2O$ **7**

$(NH_4)_{72-n}[\{(H_2O)_{81-n} + (NH_4)_n\}@\{(Mo)Mo_5O_{21}(H_2O)_6\}_{12}\{Mo_2O_4(SO_4)\}_{30}] \cdot ca.200H_2O$ **8**

Clusters with closed pores[3]

$(GH^+)_{32}[\{(H_2O)_{100} + (GH^+)_{20}\}@\{(Mo)Mo_5O_{21}(H_2O)_6\}_{12}\{Mo_2O_4(H_2PO_2)\}_{20}\{Mo_2O_4(SO_4)\}_{10}] \cdot ca.100H_2O$

9

$(GH^+)(NH_4)_{51-n}[\{(H_2O)_{81/2-n} + (GH^+)_{20} + (NH_4)_n\}@\{(Mo)Mo_5O_{21}(H_2O)_6\}_{12}\{Mo_2O_4(SO_4)\}_{30}] \cdot ca.180H_2O$

10

$(UH^+)_{20}(NH_4)_{32-n}[\{(H_2O)_{81-n} + (UH^+)_{20} + (NH_4)_n\}@\{(Mo)Mo_5O_{21}(H_2O)_6\}_{12}\{Mo_2O_4(SO_4)\}_{30}] \cdot ca.120H_2O$

11

Clusters with closed pores and encapsulated inorganic alkali metal ions [4]

$(UH^+)_{28}Na_{11}[\{(H_2O)_{60} + (UH^+)_{20} + Na_{13}\}@\{(Mo)Mo_5O_{21}(H_2O)_6\}_{12}\{Mo_2O_4(SO_4)\}_{30}] \cdot ca.140H_2O$

12

$(GH^+)_6(NH_4)_{20}Na_{13}[\{(H_2O)_{60} + (GH^+)_{20} + Na_{13}\}@\{(Mo)Mo_5O_{21}(H_2O)_6\}_{12}\{Mo_2O_4(SO_4)\}_{30}] \cdot ca.190H_2O$

13

[2]For synthetic and structural aspects please refer to [13] and [56].

[3]Note here GH^+ and UH^+ stand for $\{(NH_2)_3C^+\}$ and $(NH_3^+CONH_2)$ respectively. For synthetic and structural details of these clusters please refer to Chapter 3 and [47].

[4]For synthetic and structural details please refer to Chapter 4 and [58].

$$(UH^+)_{22}(NH_4)_{16}[\{(H_2O)_{60}+(UH^+)_{20}+Ca_7\}@\{(Mo)Mo_5O_{21}(H_2O)_6\}_{12}\{Mo_2O_4(SO_4)\}_{30}]\cdot ca.140H_2O$$

14

The cluster anions have been abbreviated for the sake of convenience in this Chapter as following:

7a as $[(H_2O)_{80}@Mo_{132}(hypo)_{30}]^{42-}$;

8a as $[\{(H_2O)_{81-n}+(NH_4)_n\}@Mo_{132}(sulph)_{30}]^{(72-n)-}$;

9a as $[\{(H_2O)_{100}+(GH^+)_{20}\}@Mo_{132}(hypo/sulph)_{30}]^{32-}$

10a as $[\{(H_2O)_{81/2-n}+(GH^+)_{20}+(NH_4)_n\}@Mo_{132}(sulph)_{30}]^{(52-n)-}$

11a as $[\{(H_2O)_{81-n}+(UH^+)_{20}+(NH_4)_n\}@Mo_{132}(sulph)_{30}]^{(52-n)-}$

12a as $[\{(H_2O)_{60}+(UH^+)_{20}+Na_{13}\}@Mo_{132}(sulph)_{30}]^{39-}$

13a as $[\{(H_2O)_{60}+(GH^+)_{20}+Na_{13}\}@Mo_{132}(sulph)_{30}]^{39-}$

14a as $[\{(H_2O)_{60}+(UH^+)_{20}+Ca_7\}@Mo_{132}(sulph)_{30}]^{38-}$

5.2 Water-assembly inside $[Mo_{132}]$ type clusters with 'closed' pores

In daily life, opening an envelope usually ends an episode of expectation, whereas in the case of the 'inorganic envelope' it might be just the reverse. Closing an open 'inorganic envelope' or more specifically the pores of a $[Mo_{132}]$ type capsular molecule for example, can be extremely interesting as it can lead to the emergence of new material and/or structural properties. A very simple phenomenon that emerges with such a closure in capsules' pores is the ordering of encapsulated molecules like, water. In fact, inside the 'inorganic envelope' of the cluster $[\{(H_2O)_{100}+(GH^+)_{20}\}@Mo_{132}(hypo/sulph)_{30}]^{32-}$, in case of special linkers, a structurally well-defined $(H_2O)_{100}$ 'nanodrop' of water with icosahedral symmetry is found. [55] The molecules within this water cluster are arranged in three concentric shells with radii of 3.88-4.2, 6.76-7.16 and 7.38-7.7 $\mathring{A}$ spanned by 20, 20, and 60 molecules, forming two dodecahedra and a highly distorted Archimedean solid $(H_2O)_{60}$ respectively. Each of the H_2O molecules of the second (dodecahedral) shell connects molecules from three different pentagons of the third shell and one molecule of the central dodecahedron. This shell structure is nicely illustrated in the distance histogram depicted in Figure 5.1. An important aspect in this context is that the tetrahedrality i.e., the O atoms with two donor and acceptor sites, according to Pauling [44] is fulfilled. The $(H_2O)_{100}$ water cluster represents the centre of a "tetrahedrally centred" icoshedral type $(H_2O)_{280}$ assembly obtained by molecular modeling and was hypothetically expected to explain several feature of liquid water.

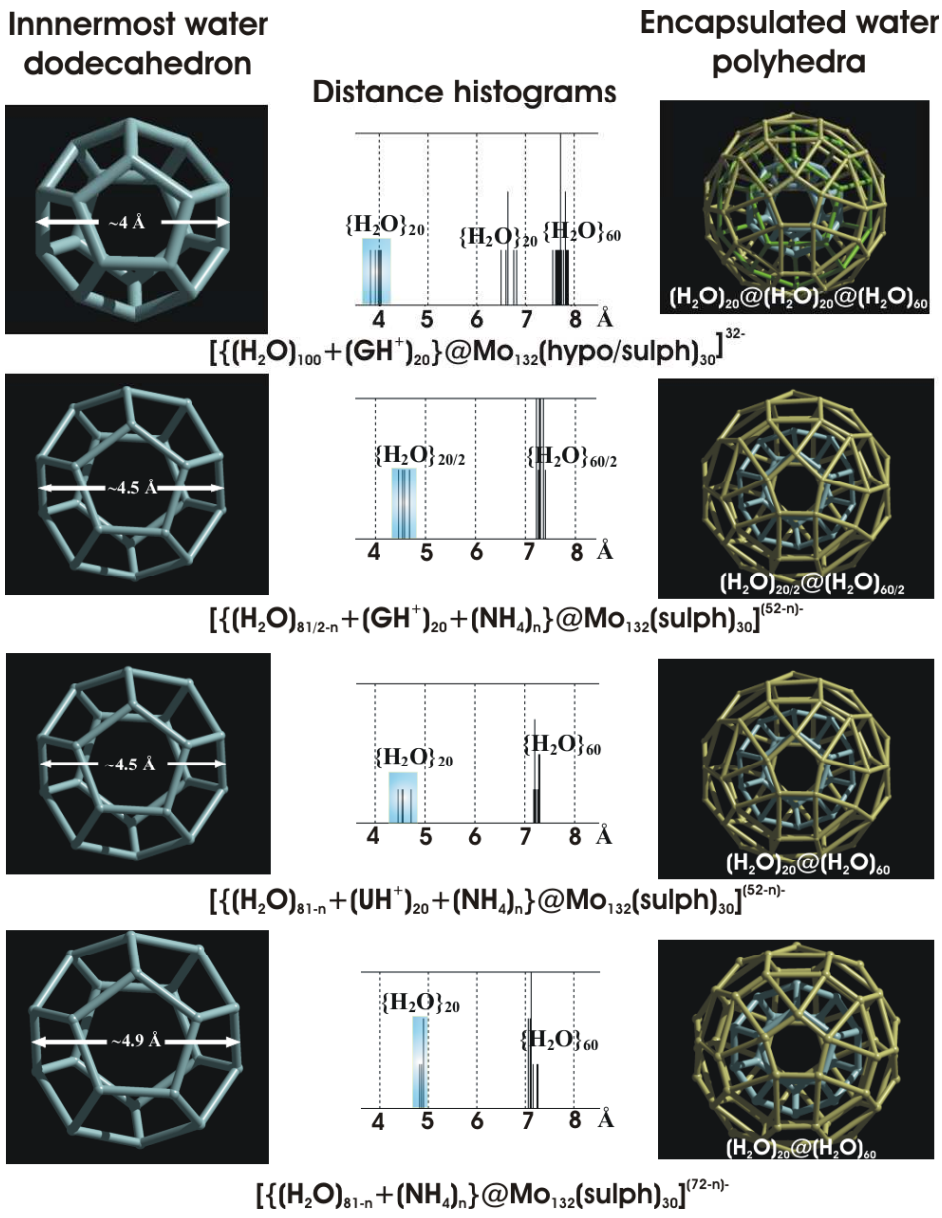

Figure 5.1: *The 'captive water' of* [Mo_{132}] *type polyoxomolybdates - four different encapsulated water-assemblies are depicted in wire-frame representation: The complete water-assemblies are shown on the right hand side while the innermost dodecahedra are shown on the left in light blue for all the cluster capsules. The related distance histograms (in the middle) show a clear 'inflation' of the central dodecahedron as one moves top-down along the Figure. For synthetic and more structural details on these clusters please refer to Chapter 3, [47] and [56]. The distances depicted in the histograms are measured from the centre of the cluster capsules. Adapted from references [55, 56].*

[68] Changing the ligands coordinated to the linkers, also affects the nature of the water-nanodrop inside the cluster capsule. (This holds good even if the capsule pores are not closed, an issue to be discussed in the next section.)

For instance, the cluster $[\{(H_2O)_{81/2-n}+(GH^+)_{20}+(NH_4)_n\}@Mo_{132}(sulph)_{30}]^{(52-n)-}$ (note the change of ligands from mixed hypophosphite/sulfate to only sulfate) shows $(H_2O)_{80}$ assembly comprising of two concentric shells of radii 4.4 - 4.7 $\mathring{A}$ and 7.22 - 7.4 $\mathring{A}$ spanned by 20 and 60 molecules, forming a dodecahedral $(H_2O)_{20}$ and a highly distorted rhombicosidodecahedral $(H_2O)_{60}$ respectively. Likewise another cluster anion having the pores 'closed' with urea; or $[\{(H_2O)_{81-n} + (UH^+)_{20} + (NH_4)_n\}@Mo_{132}(sulph)_{30}]^{(52-n)-}$, shows a similar if not identical $(H_2O)_{80}$ assembly. Here the two concentric shell-solids ($(H_2O)_{20}$ and $(H_2O)_{60}$) have radii of 4.46 - 4.74 $\mathring{A}$ and 7.2 - 7.3 $\mathring{A}$ respectively. (Figure 5.1)

A quick comparison of these three closed shell $[Mo_{132}]$ type cluster capsules reveal not only the 'structuring' of water upon pore closing but also a possibility of cation encapsulation.

- It is worthy to note that the second dodecahedral ($(H_2O)_{20}$) of $[\{(H_2O)_{100} + (GH^+)_{20}\}@Mo_{132}(hypo/sulph)_{30}]^{32-}$ is absent in case of the last two clusters i.e., $[\{(H_2O)_{81/2-n} + (GH^+)_{20} + (NH_4)_n\}@Mo_{132}(sulph)_{30}]^{(52-n)-}$ and $[\{(H_2O)_{81-n} + (UH^+)_{20} + (NH_4)_n\}@Mo_{132}(sulph)_{30}]^{(52-n)-}$ with sulfate as ligands.
- The disruption of the second dodecahedron might be due to encapsulation of cations like ammonium in these clusters.
- It is also interesting to note the 'inflated' innermost dodecahedron of $[\{(H_2O)_{81/2-n}+ (GH^+)_{20} + (NH_4)_n\}@Mo_{132}(sulph)_{30}]^{(52-n)-}$ and $[\{(H_2O)_{81-n}+(UH^+)_{20}+(NH_4)_n\}@Mo_{132}(sulph)_{30}]^{(52-n)-}$ (shell-radius ca. 4.4-4.7 $\mathring{A}$) as compared to that of $[\{(H_2O)_{100}+(GH^+)_{20}\}@Mo_{132}(hypo/sulph)_{30}]^{32-}$ (shell-radius 3.84 - 4.04 $\mathring{A}$). (Figure 5.1)
- Such an inflation together with the disruption of a dodecahedral water structure might be interpreted as a signature of encapsulated cations like ammonium.

Apart from ammonium encapsulation the story here also demonstrates the underlying influence of the ligands on the encapsulated water structure. The influence of the ligands is marked on the water assemblies in case of clusters with 'open-pores' like $[(H_2O)_{80}@Mo_{132}(hypo)_{30}]^{42-}$ and $[\{(H_2O)_{81-n} + (NH_4)_n\}@Mo_{132}(sulph)_{30}]^{(72-n)-}$. But encapsulated ammonium ions there also play an important role as will be seen shortly.

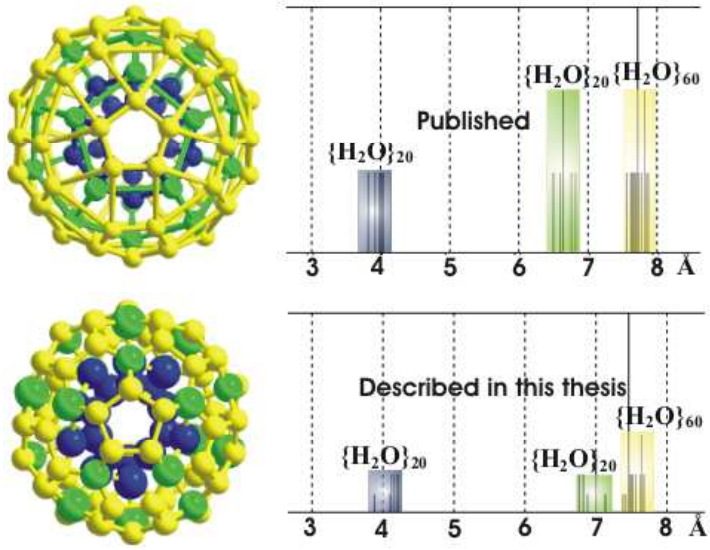

Figure 5.2: *The problem with the reproducibility of the water clusters with 'closed' pores. Note the difference in distance histograms and the corresponding thermal ellipsoids of the* $[\{(H_2O)_{100} + (GH^+)_{20}\}@Mo_{132}(hypo/sulph)_{30}]^{32-}$ *cluster published before [47] and reported in this dissertation. Also note the published* $(H_2O)_{100}$ *shown above is clearly more well-defined than the one given in this dissertation. The ellipsoids of each of the three shells are shown in three different colour for better visualization. For more details on the synthesis and structure of the cluster see Chapter 3, and also [47, 55]. The distances depicted in the histograms are measured from the centre of the cluster capsules. Adapted from reference [55].*

A note on problem of reproducing water-structure in the capsules with closed pores

Important to note in this context that although the 'aqua-architecture' in open cluster systems can easily be obtained and 'freeze-framed' with single crystal X-ray structure analysis, however for 'closed' systems it appears that the time of cluster 'closing', influence the formation of water assembly inside, thereby complicating reproduction. For instance, the cluster $[\{(H_2O)_{100} + (GH^+)_{20}\}@Mo_{132}(hypo/sulph)_{30}]^{32-}$ as described in this thesis differs from its published counter-part slightly in the matter of positioning of the water clusters. The published cluster has a more well-defined $(H_2O)_{100}$ water structure comprising 20, 20, and 60 molecules as three concentric shells with radii 3.84 - 4.04 $\mathring{A}$, 6.51 - 6.83 $\mathring{A}$ and 7.56-7.88 $\mathring{A}$, these distances are slightly different from that of the cluster described in this thesis (where the second dodecahedron is a bit more inflated). This is clearly demonstrated in the distance histogram given in Figure 5.2. Also note the thermal ellipsoids in the case of the cluster described in this thesis are a bit more inflated than the published one, which in turn means that the water structure of the cluster $[\{(H_2O)_{100} + (GH^+)_{20}\}@Mo_{132}(hypo/sulph)_{30}]^{32-}$ described in this dissertation is not as well-defined as the published one. (Figure 5.2) So in a way there is a problem

within the context of the complete reproducibility of the highly symmetrical water structure in these cases, the reasons for which is not very clear.

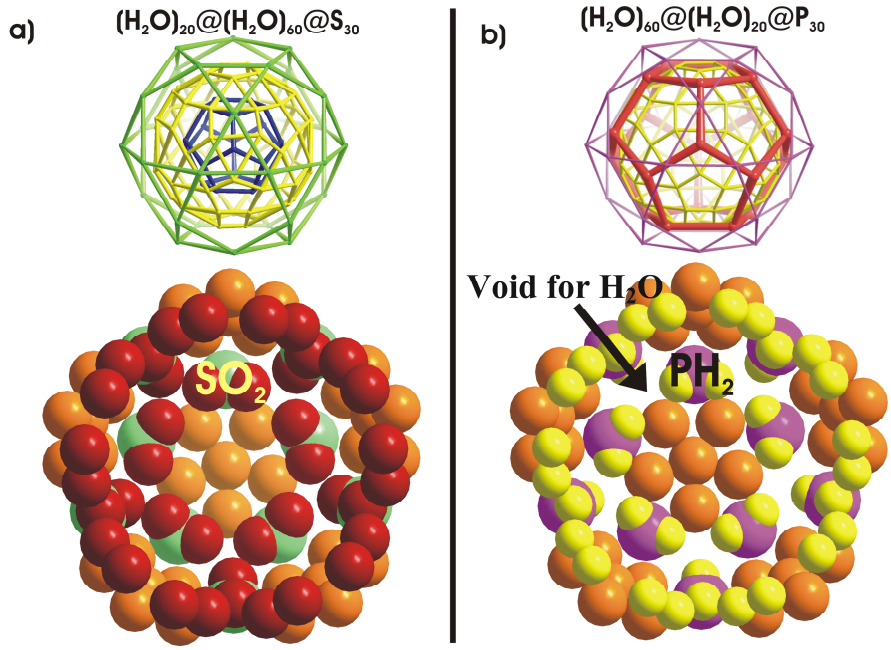

Figure 5.3: *Two different $(H_2O)_{80}$ assemblies with the related inner environment. a) Above: The encapsulated water cluster of $[\{(H_2O)_{81-n}+(NH_4)_n\}@Mo_{132}(sulph)_{30}]^{(72-n)-}$: the inner $(H_2O)_{20}$ shell (blue) together with the rhombicosidodecahedron formed by $60H_2O$ molecules (yellow) inside the S_{30} icosidodecahedron (in green) formed by the cluster's 30 sulfate groups. Below: The related internal shell surface of the spherical nanocapsule is demonstrated by models. b) Above: The encapsulated water cluster of $[(H_2O)_{80}@Mo_{132}(hypo)_{30}]^{42-}$: the inner $(H_2O)_{60}$ shell (yellow) together with the $20H_2O$ molecules (red)- embedded inside P_{30} icosidodecahedron (in lilac) formed by the cluster's 30 hypophosphite groups. Below: The perforated hydrophilic surface spanned by 3×20 H (P) atoms forming 20 holes/voids in which 20 H_2O molecules are integrated is also shown. (Colour code: $O_2(S)$, dark red-brown; S, green; ligands to Mo of the clusters which are mostly H_2O, in light brown; PH_2, lilac/yellow). Adapted from reference [56].*

5.3 Water-assembly inside $[Mo_{132}]$ type clusters with 'open' pores

Introducing $30(O_2)PH_2^-$ in $[(H_2O)_{80}@Mo_{132}(hypo)_{30}]^{42-}$ instead of $30(O_2)SO_2^{2-}$ ligands as in $[\{(H_2O)_{81-n}+(NH_4)_n\}@Mo_{132}(sulph)_{30}]^{(72-n)-}$, i.e., replacing 60 O by 60 terminal H atoms - leads to a remarkable situation with uncovered internal shell - where 20 H_2O molecules can be "fixed" in a well-defined way in 20 trigonal holes (generated by the $30(O_2)PH_2^-$ instead of $30(O_2)SO_2^{2-}$ groups). (Figure 5.3) The

20 trapped H_2O molecules, which of course do not interact with one another, show strong hydrogen bonds to the next $(H_2O)_{60}$ or 12 $(H_2O)_5$ pentagonal shells spanning a strongly distorted Archimedean solid while creating a novel $(H_2O)_{80}$ cluster, which might be written as $(H_2O)_{60}@(H_2O)_{20}$ (O...O: ca. 2.70 $\mathring{A}$). On the other hand the water-assembly inside $[\{(H_2O)_{81-n} + (NH_4)_n\}@Mo_{132}(sulph)_{30}]^{(72-n)-}$ cluster though can be formally written as $(H_2O)_{80}$, is in fact different and can be only described as $(H_2O)_{20}@(H_2O)_{60}$.

In this case of the ammonium salt of $[\{(H_2O)_{81-n}+(NH_4)_n\}@Mo_{132}(sulph)_{30}]^{(72-n)-}$, there is an internal shell built up by 132 hydrophilic ingredients, i.e. O and H_2O ligands (Figure 5.3) which leads to a two-shell water structure with integrated NH_4^+ ions: the first shell, i.e. the central dodecahedron, is similar in shape to the "normal" $(H_2O)_{20}$ dodecahedron - as for instance that in the case of $[\{(H_2O)_{100} + (GH^+)_{20}\}@Mo_{132}(hypo/sulph)_{30}]^{32-}$ (O...O: ca. 2.85 $\mathring{A}$) with 'pure water'- but "blown up" due to the abundance of NH_4^+ ions probably at its centre as well as the peripheral $(H_2O)_{20}$ shell: a situation also known for cluster systems in gas phase. [5] Also note the shell-radius of this 'inflated' innermost dodecahedron is ca., 4.8-4.9 $\mathring{A}$, which is much larger than its encapsulated counter-parts in clusters $[\{(H_2O)_{100} + (GH^+)_{20}\}@Mo_{132}(hypo/sulph)_{30}]^{32-}$, $[\{(H_2O)_{81/2-n}+(GH^+)_{20}+(NH_4)_n\}@Mo_{132}(sulph)_{30}]^{(52-n)-}$ or $[\{(H_2O)_{81-n}+(UH^+)_{20}+(NH_4)_n\}@Mo_{132}(sulph)_{30}]^{(52-n)-}$. Furthermore remarkable is the behaviour of encapsulated ammonium ions as they are tremendously protected against decomposition upon heating. (For further details please look up ref. [56] and also Figure 5.3.) Now an imminent question arises. What happens to the water assembly inside these $[Mo_{132}]$ type clusters when they 'uptake' inorganic or especially smaller alkali metal cations before closing their pores with larger organic corks like protonated urea or guanidinium?

5.4 Water-assembly inside 'cation encapsulating' $[Mo_{132}]$ type clusters and also with 'closed' pores

There is a remarkable resemblance in the water-assemblies of the inorganic (or more precisely alkali metal) cation encapsulating cluster capsules having pores closed with organic 'corks'. Be it $[\{(H_2O)_{81-n} + (UH^+)_{20} + (NH_4)_n\}@Mo_{132}(sulph)_{30}]^{(52-n)-}$, $[\{(H_2O)_{60} + (UH^+)_{20} + Na_{13}\}@Mo_{132}(sulph)_{30}]^{39-}$, $[\{(H_2O)_{60} + (GH^+)_{20} + Na_{13}\}@Mo_{132}(sulph)_{30}]^{39-}$ or $[\{(H_2O)_{60} + (UH^+)_{20} + Ca_7\}@Mo_{132}(sulph)_{30}]^{38-}$, each of them have *only* a rhombicosidodecahedral $(H_2O)_{60}$ water assembly of shell-radius 6.74-7.22$\mathring{A}$ inside. This water-assembly as shown in Figure 5.4, is however built up by 20 × 3 H_2O, indispensable for the O_h coordination geometry of the encapsulated alkali metal cations,

[5] Such an observation supports the proposal of ammonium encapsulation based on inflation of the central 'innermost' water dodecahedron in cases of clusters $[\{(H_2O)_{81/2-n} + (GH^+)_{20} + (NH_4)_n\}@Mo_{132}(sulph)_{30}]^{(52-n)-}$ and $[\{(H_2O)_{81-n} + (UH^+)_{20} + (NH_4)_n\}@Mo_{132}(sulph)_{30}]^{(52-n)-}$, described in the preceding section.

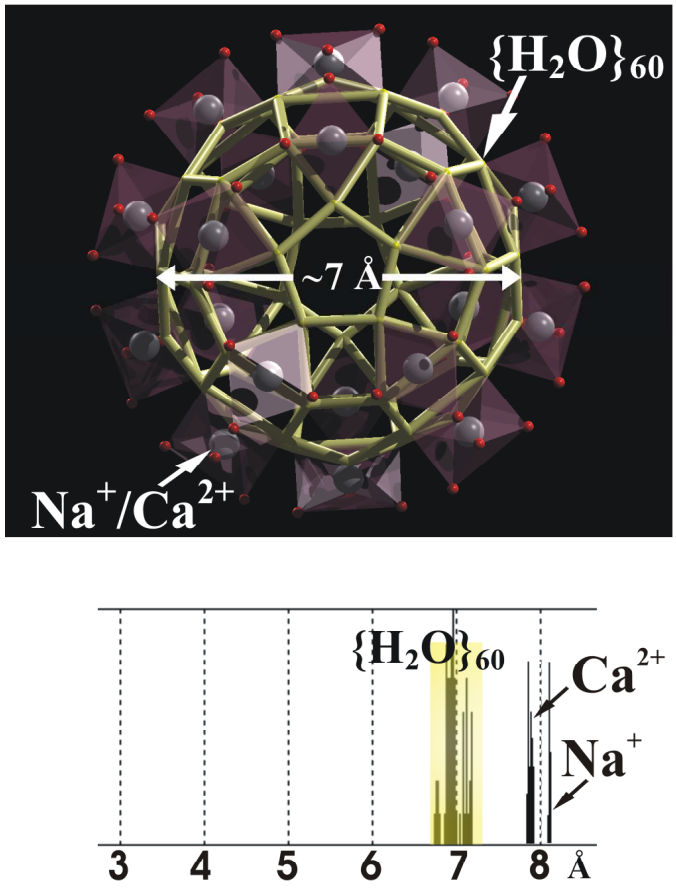

Figure 5.4: *Cation uptake and disruption of water assembly. Above: A representative rhombicosidodecahedral $(H_2O)_{60}$ assembly of Na^+ and/or Ca^{2+} cation encapsulating cluster anion with 'closed' pores showing the oxygen atoms (in red) 'indispensable' to fulfill the metal ions (in light grey) O_h coordination sphere (in pink). Below: The related distance histogram also speaks in favour of the encapsulated cations abhorrence for any structuring of water inside the cluster anions and alludes to the clustering of electron densities around 7 Å from the centre of the cluster capsule, where the depicted $(H_2O)_{60}$ water-assembly is found. These water molecules can be thought of as ligands necessary for the completion of the coordination environment of the encapsulated cations Na^+ and/or Ca^{2+} whose electron densities are also found lying very close to this water-assembly in the histogram. Note the small difference in the distance of disposition of Na^+ and Ca^{2+} inside the capsules from this histogram. The distances in the histogram are from the capsule centre. For synthetic and other structural details on the cluster compounds themselves, please refer to Chapter 4 and [58]. Adapted from reference [58].*

and are usually positioned at the centres of the C_3 faces of the cluster capsules. (The remaining three coordination sites of the metal cation are usually fulfilled by three oxygen atoms of the ligands, i.e., in these cases, of the sulfates.) From the absence of any other structured water-assembly it might also be argued that, encapsulated

cations abhor structuring of water inside these cluster capsules. [6]

5.5 Discussion and perspectives

A proposal for encapsulation of ammonium cations inside some specific $[Mo_{132}]$ **type cluster capsules**

[7]

Putting the pieces of the puzzle together the following picture emerges.

1. Encapsulation of cations (or alkali metal cations) disrupts the water-assembly inside the giant $[Mo_{132}]$ type cluster capsules.
2. Encapsulation of cations like ammonium results in two effects, within the context of water assemblies inside the $[Mo_{132}]$ type clusters. viz.,

   a) It disrupts the water-assembly inside the $[Mo_{132}]$ type clusters. (Note: the absence of second dodecahedral water-shell in ammonium encapsulated clusters. It seems that presence of the second dodecahedral water cluster and encapsulation of ammonium ions are mutually exclusive.)

   b) It also 'blows-up' the central (innermost) dodecahedral water-assembly.

   Since, the shell-radius of the central (innermost) dodecahedral water assembly progressively increases from
   $[\{(H_2O)_{100} + (GH^+)_{20}\}@Mo_{132}(hypo/sulph)_{30}]^{32-}$, (ca. 4 $\mathring{A}$) via
   $[\{(H_2O)_{81/2-n} + (GH^+)_{20} + (NH_4)_n\}@Mo_{132}(sulph)_{30}]^{(52-n)-}$ (ca. 4.5 $\mathring{A}$) or
   $[\{(H_2O)_{81-n} + (UH^+)_{20} + (NH_4)_n\}@Mo_{132}(sulph)_{30}]^{(52-n)-}$, (ca. 4.5 $\mathring{A}$) and reaches a maxima in the cluster anion
   $[\{(H_2O)_{81-n}+(NH_4)_n\}@Mo_{132}(sulph)_{30}]^{(72-n)-}$ (ca. 4.9 $\mathring{A}$) it might be said that this order reflects an ***ascending sequence of ammonium incorporation*** inside these $[Mo_{132}]$ type cluster capsules.

With this end in view a possibility of ammonium encapsulation inside $[(H_2O)_{80}@Mo_{132}(hypo)_{30}]^{42-}$ cannot be completely excluded.

[6] This observation further supports the proposal of ammonium encapsulation in the clusters $[\{(H_2O)_{81/2-n} + (GH^+)_{20}+(NH_4)_n\}@Mo_{132}(sulph)_{30}]^{(52-n)-}$ and $[\{(H_2O)_{81-n}+(UH^+)_{20}+(NH_4)_n\}@Mo_{132}(sulph)_{30}]^{(52-n)-}$, by demonstrating that incorporation of cations disrupts the structuring of water. Needless to say these clusters in spite of having closed pores like $[\{(H_2O)_{100} + (GH^+)_{20}\}@Mo_{132}(hypo/sulph)_{30}]^{32-}$ lack a 3-shell water structure.

[7] See also the argumentation for ammonium encapsulation in [56].

Chapter 6

Stability investigation of four selected $[Mo_{132}]$ type spherical polyoxomolybdate cluster anions

6.1 Introduction

"The procedures required to produce, characterize and probe the properties of a new compound obviously depend very much on the compound's stability, a property which is often not a simple one to define" wrote Sir Harold Kroto. [71] Indeed the word stability although essential in the context of synthetic studies is illusive as well. The imminent questions in this context are: stability against what and for how long?

Recent studies have shown interesting structuring of molybdenum oxide based nanoobjects (like wheel-shaped $[Mo_{154}]$, or spherical $[Mo_{72}Fe_{30}]$) in aqueous solution. [72, 73, 74] A detailed study of such nanoobjects in solution requires an insight into their solution-stability. The stability study of $[Mo_{132}]$ type nanoobjects in aqueous solution described in this Chapter was undertaken keeping in view the increasing importance of their behaviour in solution, especially in water. Hence this study might serve as a vignetted prelude to the ongoing investigations of related nanoobjects in solution of various solvents (primarily water). This Chapter deals with the question of stability of four selected spherical nanoobjects. viz.,[1]

$$(NH_4)_{42}[\{(Mo)Mo_5O_{21}(H_2O)_6\}_{12}\{Mo_2O_4(CH_3COO_)\}_{30}] \cdot ca.300H_2O \cdot 10CH_3COONH_4 \ \mathbf{6}$$

$$(NH_4)_{72-n}[\{(H_2O)_{81-n} + (NH_4)_n\}@\{(Mo)Mo_5O_{21}(H_2O)_6\}_{12}\{Mo_2O_4(SO_4)\}_{30}] \cdot ca.200H_2O \ \mathbf{8}$$

$$(GH^+)_{32}[\{(H_2O)_{100} + (GH^+)_{20}\}@\{(Mo)Mo_5O_{21}(H_2O)_6\}_{12}\{Mo_2O_4(H_2PO_2)\}_{20}\{Mo_2O_4(SO_4)\}_{10}] \cdot ca.100H_2O \ \mathbf{9}$$

$$(UH^+)_{28}Na_{11}[\{(H_2O)_{60} + (UH^+)_{20} + Na_{13}\}@\{(Mo)Mo_5O_{21}(H_2O)_6\}_{12}\{Mo_2O_4(SO_4)\}_{30}] \cdot ca.140H_2O \ \mathbf{12}$$

[1] As always GH^+ and UH^+ stand for $\{(NH_2)_3C^+\}$ and $(NH_3^+CONH_2)$ respectively.

For convenience, in this Chapter **6a**, **8a**, **9a** and **12a** are denoted as $[Mo_{132}(ac)_{30}]$, $[Mo_{132}(sulph)_{30}]$, $[(Gua)@Mo_{132}(hypo/sulph)_{30}]$ and $[(Na+Urea)@Mo_{132}(sulph)_{30}]$ respectively.

The stability study has been performed principally by Raman spectroscopy and in water, and also with DMSO as an external standard. In course of such investigations it was found like all other polyoxometalates stability of these giant nanoobjects is influenced by aerial oxygen, temperature, pH and effect of the electrolytes present in the solution. A detailed investigation to find the exact regime of stability of these nanoobjects, together with the influence of these factors on their stability have been addressed in this Chapter. The Chapter begins with the question: what does the word 'stability' within this context stand for?

Stability Investigation: What it means? How it is done?

The term stability as mentioned before is illusive in itself. For instance, in the field of reaction kinetics even a 'stable' intermediate can survive only for few femtoseconds; [75] whereas for nuclear chemists a 'stable' isotope can have a half-life in the order of 10^{10} years! [76] So the term 'stability' can be misleading. To avoid any such misconception it is necessary to define what is meant by the stability of the nanoobjects. The meaning of this term essentially in this framework of investigations has been addressed with four questions. Do these cluster capsules retain their molecular integrity upon dissolution in water? How long is that integrity retained if the solution is left open in air? Up to what temperature do they retain this integrity? Are they able to stand pH changes? Overarching these questions the meaning and implications of 'stability' obviously depend further on the technique that has been used for these investigations. Raman spectroscopy has been used as a tool here, and any change in the characteristic Raman spectral fingerprint of the clusters has been taken as a sign of their destabilization. (See also the section on: Working hypothesis.) The reasons for the choice of Raman spectroscopy as a tool are described in the next section.

Why Raman spectroscopy?

The answer to this question is the easy detection of the cluster integrity from the Raman fingerprint. The quasi-spherical (icosahedral) construction of these clusters not only enhances their stability but also provides an easy Raman spectroscopic 'finger-print' for studying their stability. Owing to the high I_h symmetry of such clusters, only a few well-defined Raman lines are observed (note the presence of a five-fold degeneracy, and that only A_g and H_g vibrations are Raman allowed). And these lines under varying conditions, allow an easy detection of their possible decomposition.

The Raman spectrum of a $[Mo_{132}]$ type cluster shows four bands: 950 cm^{-1} $[\nu(Mo=O_t)]$, 880 cm^{-1} $[\nu(O_{bri}breathing)]$, 374 cm^{-1} $[\delta(Mo=O_t)]$ and 314 cm^{-1} $[\delta(Mo-O-Mo)]$. (For details on assignments of these bands see the section on the

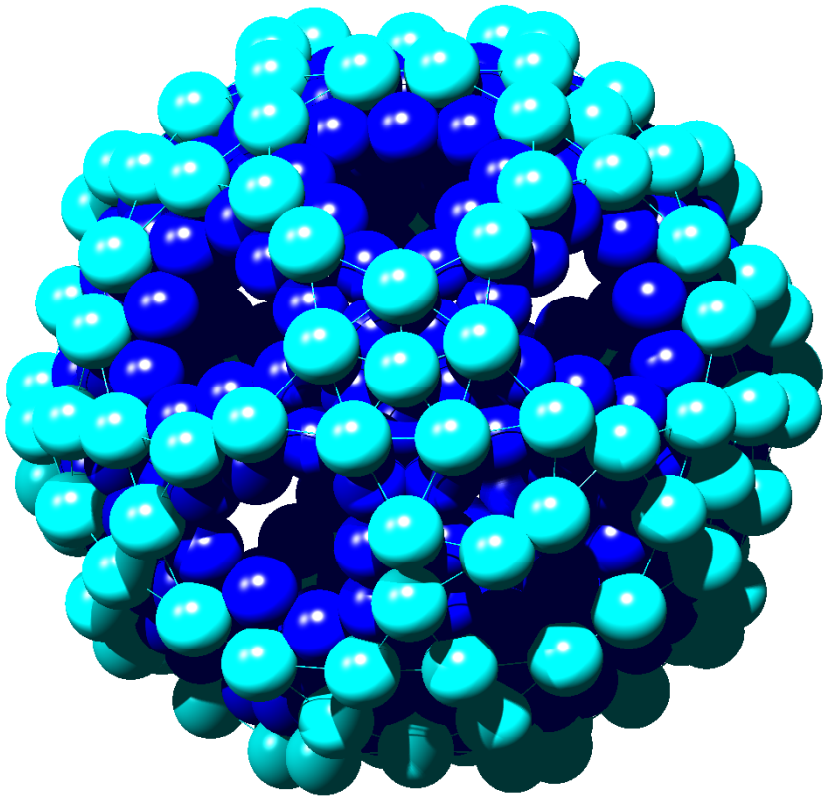

Figure 6.1: $[O_{372}]$ *framework of an* $[Mo_{132}]$ *cluster type. The* $[Mo_{132}]$ *type clusters' decomposition is detected by the change in Raman spectrum induced by the change of the normal coordinates of* $[O_{372}]$ *framework shown here, which preferably contribute to the breathing vibration of the oxomolybdate skeleton. Note: the most intense band at 880* cm^{-1} *corresponds to the totally symmetric* A_{1g} *breathing vibration of the capsule involving predominantly* $60\mu_3-O(Mo_3)$ *and probably also* $180\mu_2-O$ *atoms shown here in blue. 132 terminal oxygen atoms of the cluster are shown in cyan (responsible for giving rise to high frequency Raman lines).*

Raman spectroscopic signatures of the $[Mo_{132}]$ *clusters* later.)

Here it is also perhaps worth mentioning, that the $[Mo_{132}]$ type clusters also have an $[O_{372}]$ framework (comprising 132 terminal and 240 bridging oxygen atoms) associated with them. (Figure 6.1) The high atomic masses of the Mo atoms result in their inertial reluctance to change position with small variation in the cluster configuration (like protonation). Consequently, the importance of this $[O_{372}]$ framework is increased manifold in the matter of these clusters' stability study by Raman spectroscopy. This is so because unlike the heavier molybdenum-atom skeleton the lighter $[O_{372}]$ framework is more sensitive to subtle changes in cluster configuration say due to protonation in the context of Raman spectroscopic studies of the cluster and any change in cluster configuration is reflected in the corresponding Raman band

due to the change in the related normal coordinates.

Moreover the high water solubility of these clusters allow investigation at considerably higher concentration range (around 1 mM). All these factors make Raman spectroscopy a suitable tool for studying the stability of the clusters.

Why not other techniques?

The electronic absorption spectroscopy might have been a good choice as it is a bit more quantitative than Raman spectroscopy, however the problem in this technique is that only very low concentration (in μmol) has to be used because of the correspondingly high value of absorption coefficient around $3 \times 10^6 mol^{-1} cm^{-1}$.

Raman spectroscopic signatures of the $[Mo_{132}]$ clusters and the choice of clusters for stability study

Four different clusters as mentioned before were chosen for stability study in solution. The reasons for their choice are the different charges hence nucleophilicities (as in case of $[Mo_{132}(ac)_{30}]$ and $[Mo_{132}(sulph)_{30}]$) different cluster-surface topologies (closed spherical of $[Gua@Mo_{132}(hypo/sulph)_{30}]$ or bumpy irregular $[(Na + Urea)@Mo_{132}(hypo/sulph)_{30}]$) and also the host-guest relationship among them. For instance $[Mo_{132}(ac)_{30}]$ and $[Mo_{132}(sulph)_{30}]$) are the basic parent host clusters, while $[Gua@Mo_{132}(hypo/sulph)_{30}]$ and $[(Na+Urea)@Mo_{132}(sulph)_{30}]$ are first and second-order [2] host-guest complexes of $[Mo_{132}(sulph)_{30}]$. Hence a detailed and a comparative account of their stability study is necessary not only for the ongoing investigations of various related nanoobjects in aqueous solution, but also to understand the complex interaction dynamics between the empty hosts and their guest containing analogues.

Discussion on the assignment of bands observed in the Raman spectra of $[Mo_{132}]$ cluster type by comparing the spectra of related oxomolybdate clusters with varying charge

In this study, the assignments of the important bands to the characteristic normal modes of vibration have been qualitatively discussed by comparing the important Raman spectral feature of three different spherical cluster types with varying charge.

The Raman spectrum of a $[Mo_{132}]$ type cluster shows four bands, which have been assigned as following. 950 cm^{-1} $[\nu(Mo = O_t)]$, 374 cm^{-1} $[\delta(Mo = O_t)]$, 314 cm^{-1} $[\delta(Mo - O - Mo)]$ and the most intense band at 880 cm^{-1} $[\nu(O_{bri} breathing)]$ that corresponds to the totally symmetric A_{1g} breathing vibration of the capsule which involve predominantly $60\mu_3 - O(Mo_3)$ and $180\mu_2 - O$ surface atoms. [74] (Figure 6.2) [3] The assignments seem to be logical in the sense that, the bond strength for $Mo = O_t$

[2] Note: $[Gua@Mo_{132}(hypo/sulph)_{30}]$ has only one guest type hosted on the cluster surface, so we call it a primary or a first-order host-guest complex of $[Mo_{132}(sulph)_{30}]$whereas $[(Na+Urea)@Mo_{132}(sulph)_{30}]$ in addition to having urea on the surface has sodium ions below the pore channels, so it is proposed to be called as a second-order host-guest complex of $[Mo_{132}(sulph)_{30}]$

[3] The author gratefully acknowledges the help of Prof. A. Müller, in the assignment of various bands in this Chapter. See also: [77, 78]

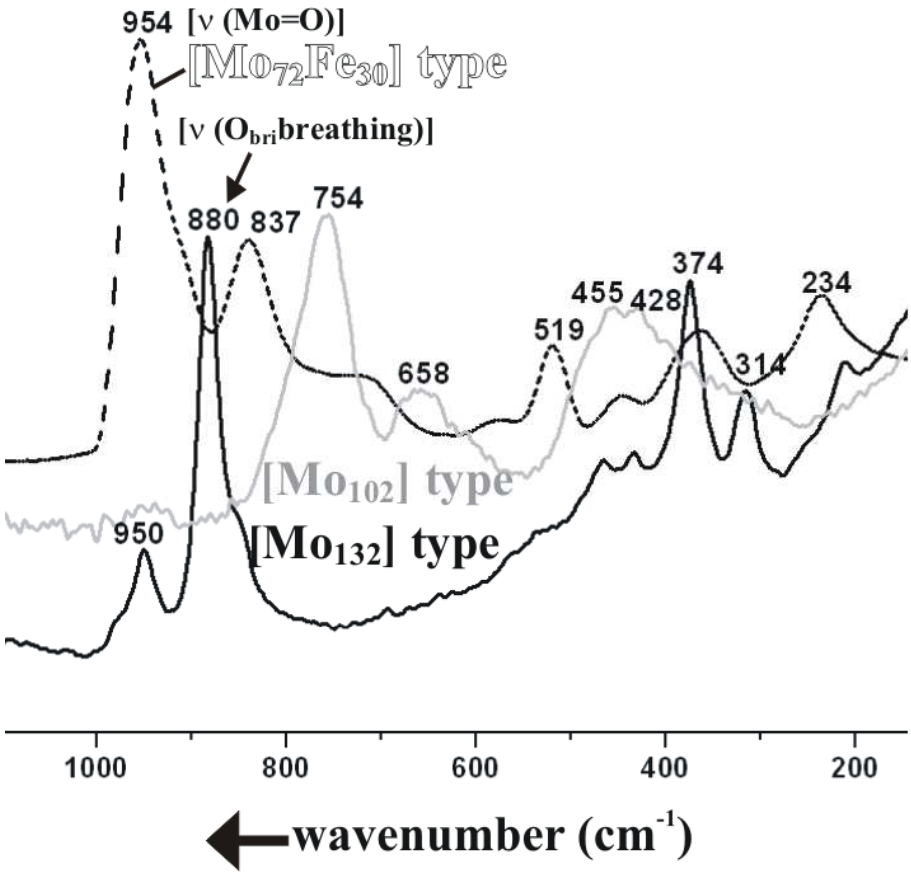

Figure 6.2: *Different cluster capsules show different Raman spectra. Top: The spectrum in black with broken line refers to* $[Mo_{72}Fe_{30}]$ *type cluster [19] while that in grey corresponds to resonance Raman spectrum of* $[Mo_{102}]$ *type cluster [20]. The spectrum in black refers to that of* $[Mo_{132}]$ *type cluster. All the spectra are measured in solid-state and their intensities are not to the scale.*

being higher, is expected to appear at higher frequency (950 cm^{-1}) than that due to symmetric A_{1g} breathing vibration of the capsule involving predominantly Mo-O-M type bonds (880 cm^{-1}) (M is the corresponding metal-centre from the linker of the cluster) and it obviously follows that the bending vibrations will have lower wavenumber than the corresponding stretching vibrations.

These *a priori* assignments can also be verified by the comparison of the corresponding bands in the Raman spectrum of $[Mo_{72}M_{30}]$ type clusters having very low or zero charge. (Figure 6.2.)

It is observed that the relative intensity of the band at 950 cm^{-1} is much higher for $[Mo_{72}Fe_{30}]$ in comparison to that of $[Mo_{132}]$ cluster type. This alteration of intensity can be realized in the framework of the above assignment. Because of the electrical neutrality of the $[Mo_{72}Fe_{30}]$ cluster, the polarizability of the Mo=O bonds in this case

is much higher as compared to that of the negatively charged $[Mo_{132}]$ type cluster. On the other hand, the band around 880 cm^{-1}, resulting from totally symmetric A_{1g} breathing vibration of the capsule which involve predominantly $60\mu_3 - O(Mo_3)$ and $180\mu_2 - O(MoM)$ surface atoms, denoted as $\nu(O_{bri}breathing)$, is less intense in case of $[Mo_{72}Fe_{30}]$ as compared to $[Mo_{132}]$. This perhaps stems from low polarizability of the concerned Mo-O-Fe bonds of the $180\mu_2 - O(MoM)$ (M=Mo or Fe^{3+}) surface atoms of $[Mo_{72}Fe_{30}]$ that give rise to this band than the corresponding Mo-O-Mo bonds of $[Mo_{132}]$ due to the higher electronegativity of the Fe^{3+} centres.

In case of the neutral $[Mo_{102}]$ the relative intensity pattern is same as that of $[Mo_{72}Fe_{30}]$, with the only exception that both the bands are a bit 'red-shifted', and appear at 770 cm^{-1} $[\nu(Mo = O_t)]$ and 670 cm^{-1} $[\nu(O_{bri}breathing)]$ respectively. Such a red shift might be explained in the light of the relatively increased population in the anti-bonding MO of $[Mo_{102}]$ over $[Mo_{132}]$ causing a decrease in the related bond-order. This might be due to the fact that in $[Mo_{102}]$, 30 electrons are delocalized over the available ABOs (note the blue colour of the cluster) whereas in $[Mo_{132}]$ instead of such delocalization every two of the sixty electrons are preferentially localized over the BOs of each of the 30 dinuclear $[Mo_2]$ groups. (Also note the brown colour of the cluster.)

6.2 Working hypothesis

In this study the four most-intense band pattern, characteristically observed in the Raman spectrum of $[Mo_{132}]$ type polyoxomolybdates at: 950 cm^{-1}, 880 cm^{-1}, 374 cm^{-1} and 314 cm^{-1} in solid state is taken as a fingerprint of the cluster's integrity. As a working hypothesis the retention of this spectral fingerprint was taken as an evidence of retention of the integrity of the cluster. Whenever and wherever necessary this study was augmented by the use of an external standard. (See later.)

6.3 Stability in water

First of all, are the cluster capsules stable in water? Do they retain their polyoxomolybdate skeletal integrity when dissolved in it? The solution Raman spectra were obtained using 1 mM solution of the respective cluster compounds, whereas the solid-state spectra were obtained using KBr matrices. As far as Raman spectroscopy is concerned we observe that the spectral patterns of all the four clusters in solid-state are reproduced when dissolved in water. (Figure 6.3) This implies that the clusters retain their molybdenum-oxide skeleton (i.e., their basic structure) although a slight opening of the clusters like formation of a 'basket' might not be ruled out. [79]

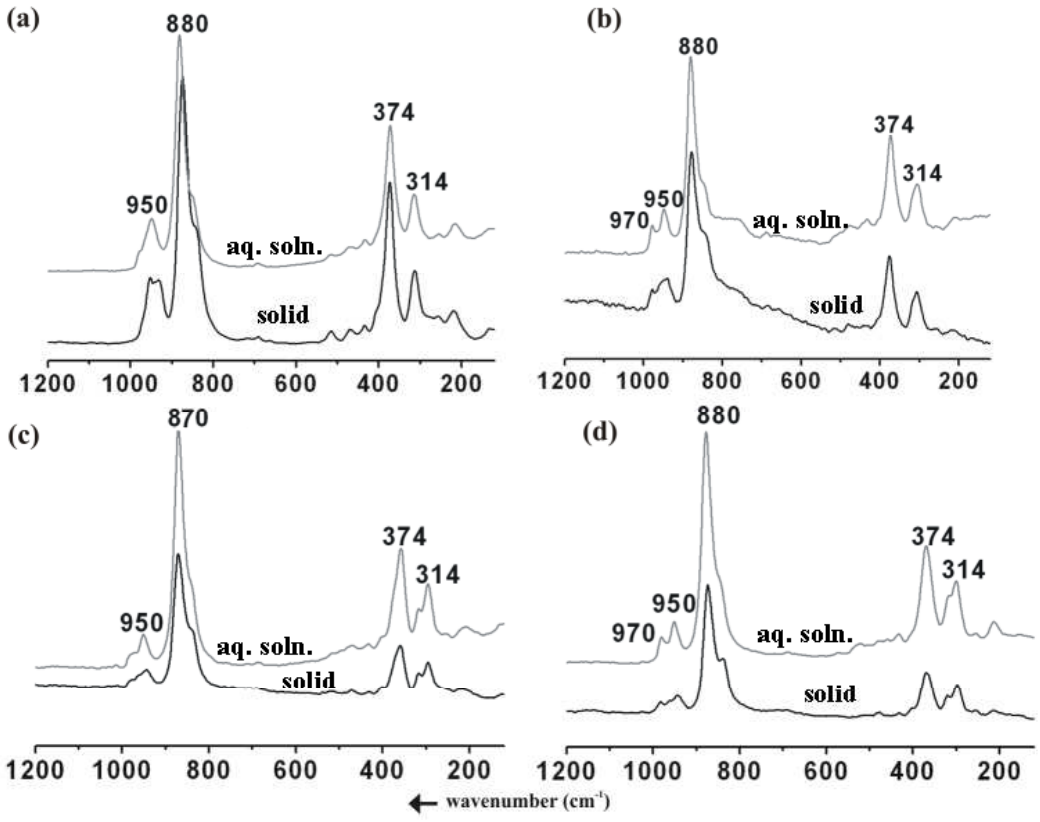

Figure 6.3: *The Raman spectra of $[Mo_{132}(ac)_{30}]$ (a), $[Mo_{132}(sulph)_{30}]$ (b), $[Gua@Mo_{132}(hypo/sulph)_{30}]$ (c) and $[(Na + Urea)@Mo_{132}(sulph)_{30}]$ (d) in solid-state and in aqueous solutions. The intensities of the spectra are not to the scale.*

Implications:

- The cluster capsules retain their integrity in aqueous solution.

External standard

Why an external standard?

The external standard was used for investigating the stability of the clusters against aerial oxidation, temperature and pH change (semi-quantitatively).

Criteria of a suitable external standard

1. It must be water soluble/miscible.
2. The external standard should be non-interacting with the clusters in the context. Hence, commonly used cationic or anionic complexes were not chosen.
3. The standard should be stable under the conditions in which the stability of the clusters are to be probed.
4. The spectra of the standard should not overlap with the major 'informative' window of the cluster.
5. The most intense band of the standard must be of comparable intensity to that of the cluster.

Cluster compound	Conc. (in mM)	$I_{677}ofDMSO$	$I_{880}ofcluster$	$\frac{I_{880}ofcluster}{I_{677}ofDMSO}$
$[Mo_{132}(ac)_{30}]$	1	0.04	0.04	1
	2	0.05	0.09	2
$[Mo_{132}(sulph)_{30}]$	1	0.02	0.02	1.1
	2	0.02	0.03	1.7
$[Gua@Mo_{132}(hypo/sulph)_{30}]$	1	0.04	0.05	1.3
	2	0.04	0.08	2.1
$[(Na+Urea)@Mo_{132}(sulph)_{30}]$	1	0.04	0.05	1.3
	2	0.05	0.02	2.2

Table 6.1: Variation of I_{880}/I_{677} with change in concentration of the cluster capsules. Note intensities are in arbitrary relative units.

Choice of external standard

DMSO (20% by volume) was chosen as an external standard, as it fulfilled all the requirements listed above. The most intense band of DMSO (at 677 cm^{-1}), [4] was used for comparing the intensities of the Raman bands of the clusters. The ratio of the intensity of the most intense band of the clusters (i.e., the band around 880 cm^{-1}) [5] to that of DMSO (at 677 cm^{-1}) showed a nearly linear correspondence to the cluster concentration in solution. (See Table 6.1 and also Figures 6.4 and 6.5).

[4] This band might be due to ν_1, the symmetric vibration with respect to the C_{2v} axis of rotation of DMSO.

[5] Please note that the small variations, in the wavenumber of the major Raman bands of the cluster capsules, (being within the error limits) have been ignored in this Chapter.

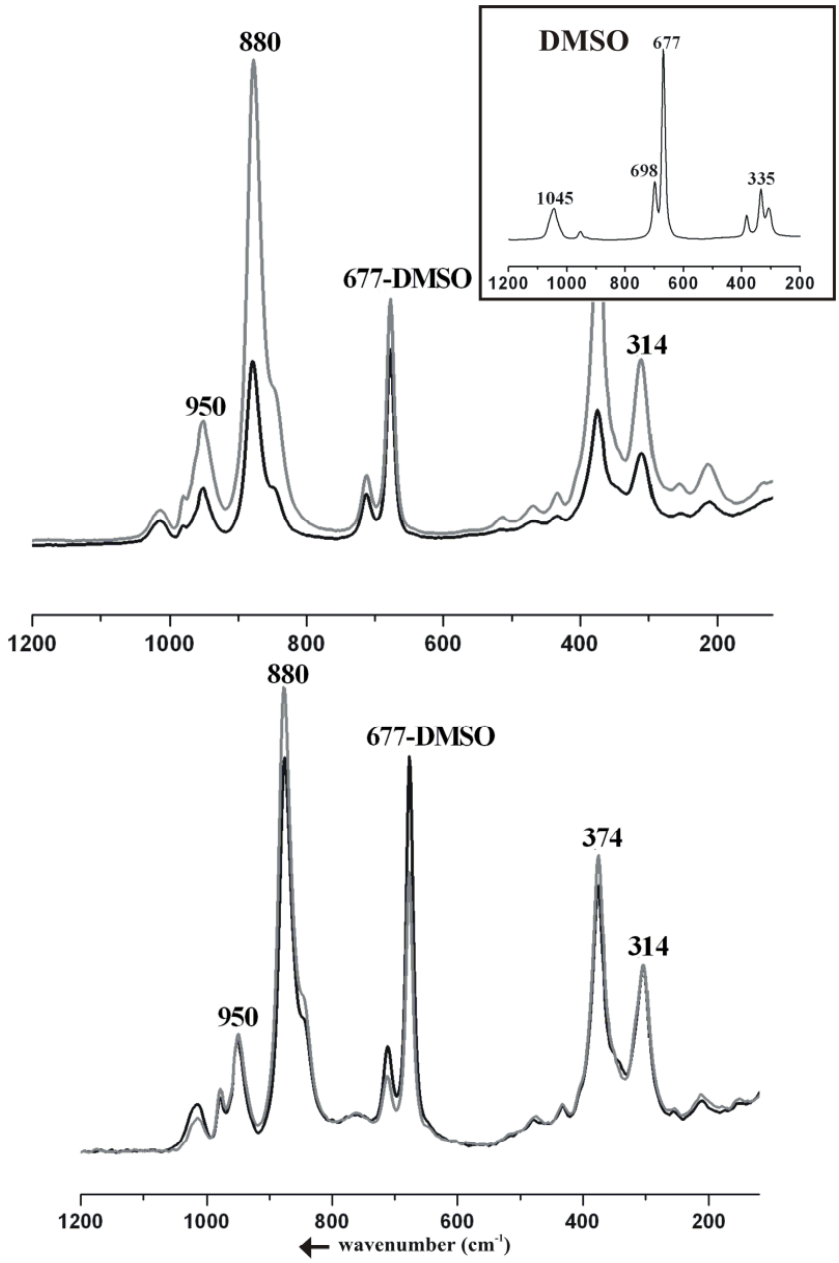

Figure 6.4: *Capsule concentration indexed with an external standard - I: The Raman spectra of $[Mo_{132}(ac)_{30}]$ (above) and $[Mo_{132}(sulph)_{30}]$ (below). The spectra in black refer to 1 mM concentration of cluster compounds and those in grey correspond to 2 mM. The spectra are measured in water containing DMSO 20% by volume. The inset shows the Raman spectrum of the external standard DMSO.*

Hence if cluster decomposition was not otherwise manifested by the complete

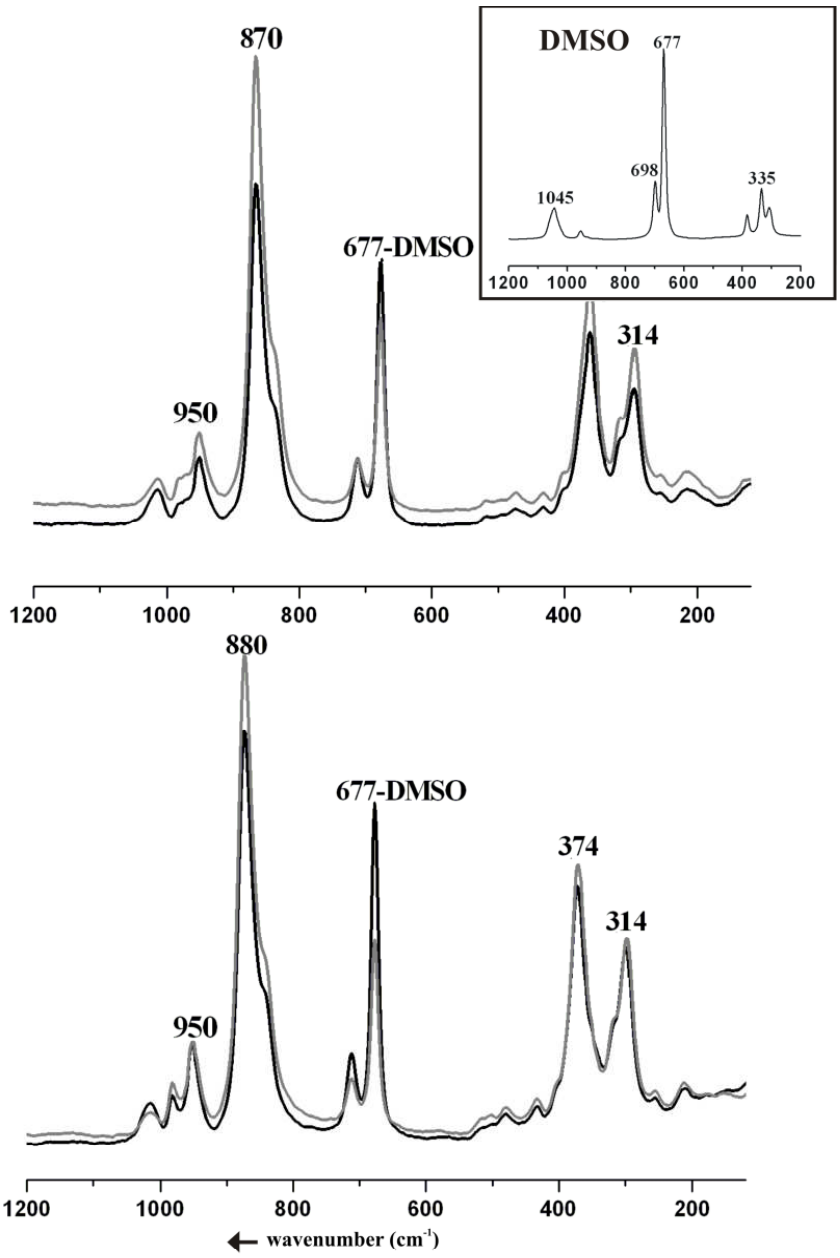

Figure 6.5: *Capsule concentration indexed with an external standard - II: The Raman spectra of* $[Gua@Mo_{132}(hypo/sulph)_{30}]$ *(above) and* $[(Na + Urea)@Mo_{132}(sulph)_{30}]$ *(below). The spectra in black refer to 1 mM concentration of cluster compounds while those in grey correspond to 2 mM. The spectra are measured in water containing DMSO 20% by volume. The inset shows the Raman spectrum of the external standard DMSO. Note: only the most intense band of DMSO has been marked in the figure from now onwards.*

change of the spectral pattern, any alteration of the intensity ratio I_{880}/I_{677} was considered as an indication of cluster decomposition.

Implications:

- External standard like DMSO can provide an insight into the concentration of a cluster capsule in solution, given the cluster's intactness is already manifested by the retention of its solid-state Raman spectral pattern upon dissolution.
- The concentration of the cluster capsules corresponds linearly to the I_{880}/I_{677} ratio. Higher the cluster concentration, greater is this ratio.
- The ratio I_{880}/I_{677} hence provides information on the concentration of intact cluster and serves as a semi-quantitative measure of cluster stability.

6.4 Stability and aerial oxidation

Taking into account that these cluster capsules retain their spectral pattern when dissolved in water, the next imminent questions were: if so, how long? Does the presence or absence of aerial oxygen make a difference in the stability of these cluster capsules? These questions were also investigated by Raman spectroscopy. As per our working hypothesis any decomposition will induce a change in spectral pattern.

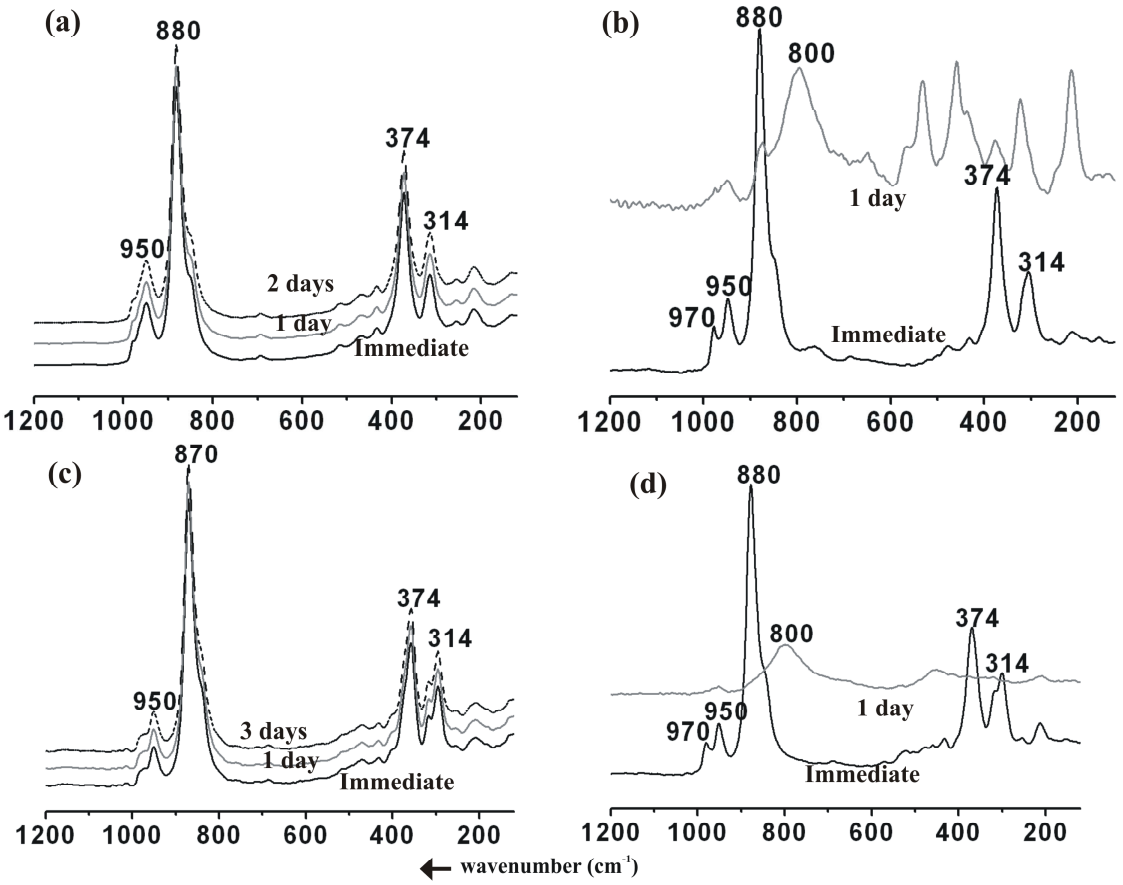

Figure 6.6: *Time dependence of cluster stability in the presence of aerial oxygen (without an external standard): The Raman spectra of* $[Mo_{132}(ac)_{30}]$ *(a),* $[Mo_{132}(sulph)_{30}]$ *(b),* $[Gua@Mo_{132}(hypo/sulph)_{30}]$ *(c) and* $[(Na + Urea)@Mo_{132}(sulph)_{30}]$ *(d) with time. The intensities of the spectra are not to the scale.*

It was observed that ***in the presence of aerial oxygen***, 1 mM solution of $[Mo_{132}(ac)_{30}]$ and $[Gua@Mo_{132}(hypo/sulph)_{30}]$ are stable at least for 2 and 3 days respectively, as signatured by their retained spectral patterns. (Figure 6.6) On the other hand, 1 mM solution of the other two clusters viz., $[Mo_{132}(sulph)_{30}]$ and $[(Na+Urea)@Mo_{132}(sulph)_{30}]$ show the emergence of a new spectral pattern, after 1 day, implying decomposition.

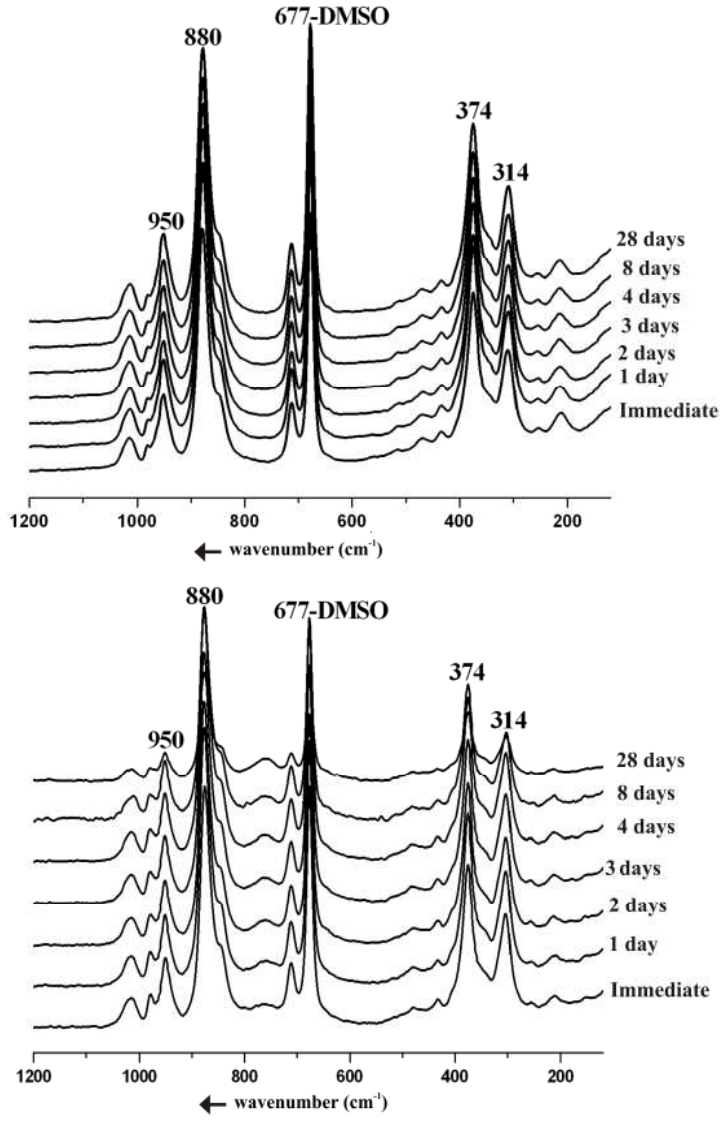

Figure 6.7: *Time dependence of cluster stability, in the absence of aerial oxygen, indexed with an external standard (DMSO) - I: Raman spectra of* $[Mo_{132}(ac)_{30}]$ *(above) and* $[Mo_{132}(sulph)_{30}]$ *(below) [indexed with 20% (v/v) DMSO] in the absence of aerial oxygen with time are shown.*

Whereas in ***the absence of aerial oxygen*** [6] the overall stability of the cluster compounds in solution is significantly increased. In order to have a semi-quantitative idea on the extent of stabilization of the cluster compounds the time dependent Raman spectra of the four different cluster compounds were measured. In each case 1 mM solution of the cluster compound containing DMSO (20% v/v) as an

[6] To ensure the exclusion of aerial oxygen, all the experiments were carried out by dissolving the cluster compounds with deionized, degassed water and flushed with argon for 10 minutes.

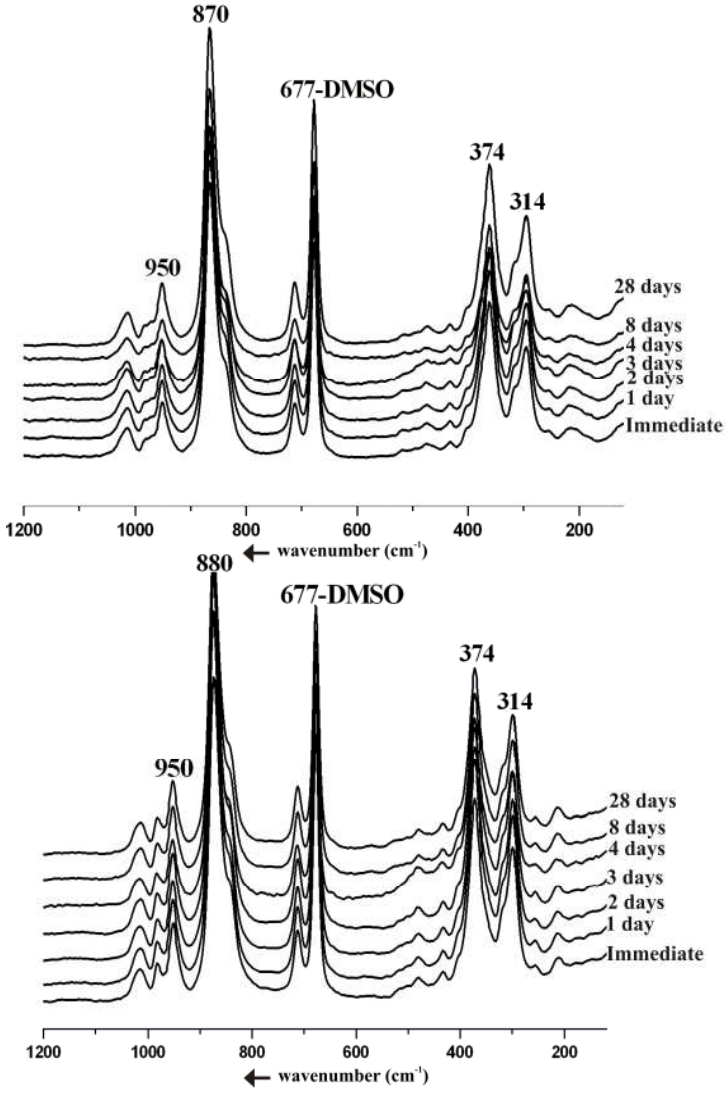

Figure 6.8: *Time dependence of cluster stability, in the absence of aerial oxygen, indexed with an external standard (DMSO) - II: Raman spectra of* $[Gua@Mo_{132}(hypo/sulph)_{30}]$ *(above) and* $[(Na + Urea)@Mo_{132}(sulph)_{30}]$ *(below) [indexed with 20% (v/v) DMSO] in the absence of aerial oxygen with time are shown.*

external standard was used. The spectra remained unaltered for weeks, indicating their stability in solution lasts for weeks (or at least for a month). All four clusters showed a nearly identical pattern as depicted in Figure 6.7 and 6.8.

Implications:

- The cluster capsules are destabilized by aerial oxidation.
- The higher the overall negative charge of the cluster capsule more prone it

becomes towards aerial decomposition.

6.5 Stability against temperature rise

How stable are these cluster capsules against the rise of temperature? What information do their Raman spectra give in this context? The experiments were performed both with and without external standards.[7]

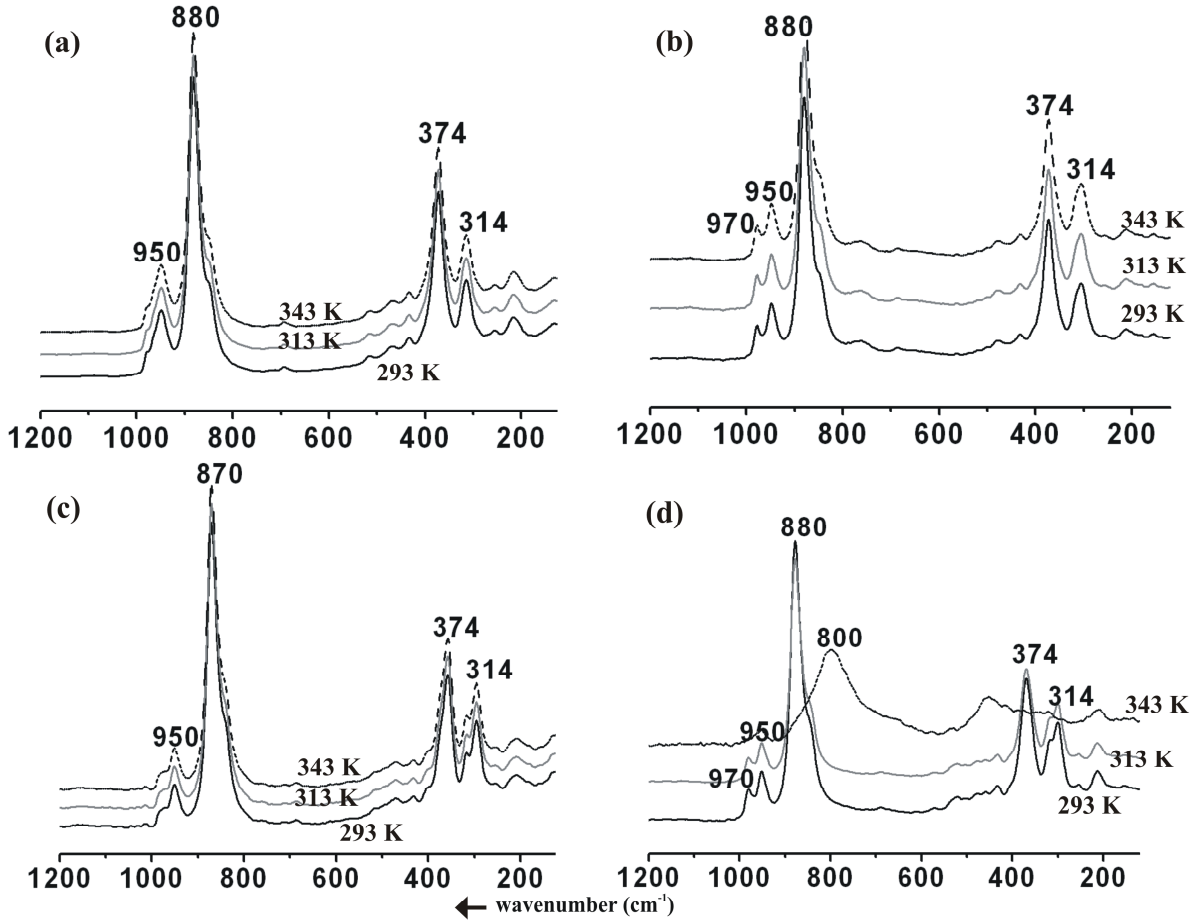

Figure 6.9: *The Raman spectra of $[Mo_{132}(ac)_{30}]$ (a), $[Mo_{132}(sulph)_{30}]$ (b), $[Gua@Mo_{132}(hypo/sulph)_{30}]$ (c) and $[(Na + Urea)@Mo_{132}(sulph)_{30}]$ (d) at different temperature in the absence of aerial oxygen, recorded in aqueous solution. The intensities of the spectra are not to the scale.*

[7]These experiments were carried out with 1 mM aqueous solution of the cluster capsules up to a temperature of 343K, further heating to higher temperature was avoided.

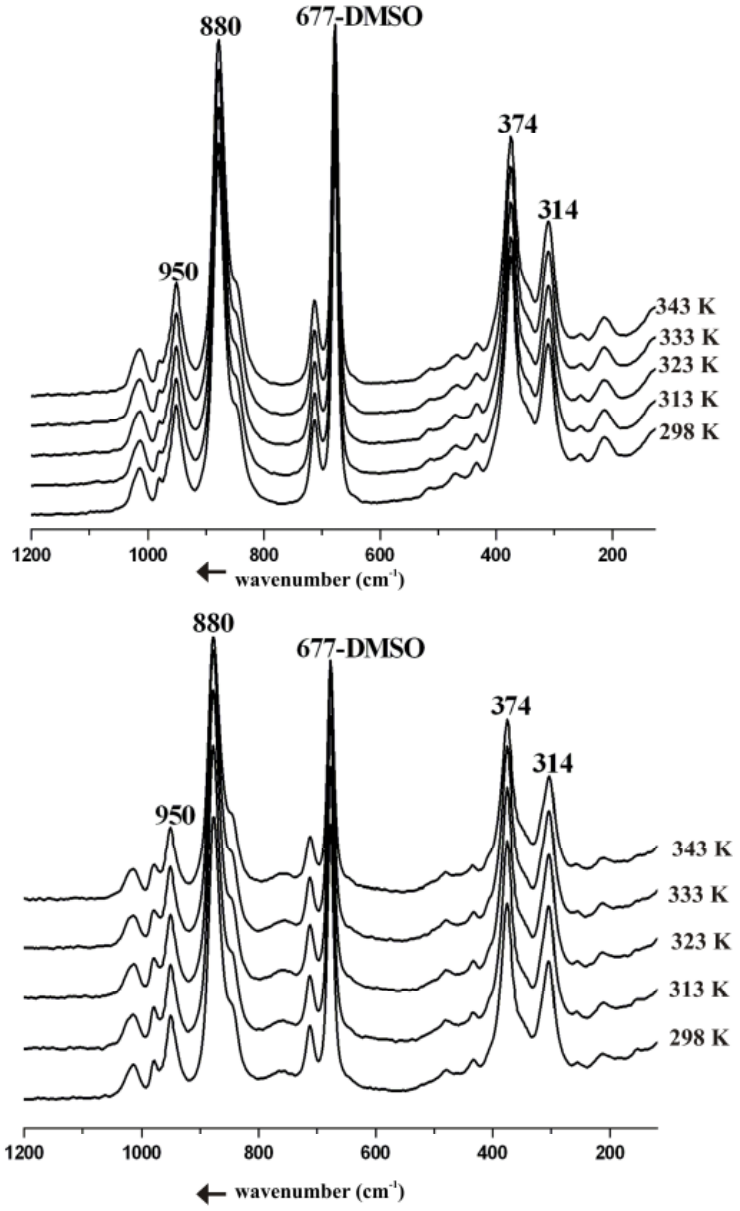

Figure 6.10: *Temperature and stability studies - I: Raman spectra of* $[Mo_{132}(ac)_{30}]$ *(above) and* $[Mo_{132}(sulph)_{30}]$ *(below) in the absence of aerial oxygen with the rise in temperature are shown, using DMSO 20% (v/v) as an external standard.*

Without an external standard

The effect of temperature on the stability of the four clusters in question were first carried out under the exclusion of aerial oxygen, using an aqueous 1 mM

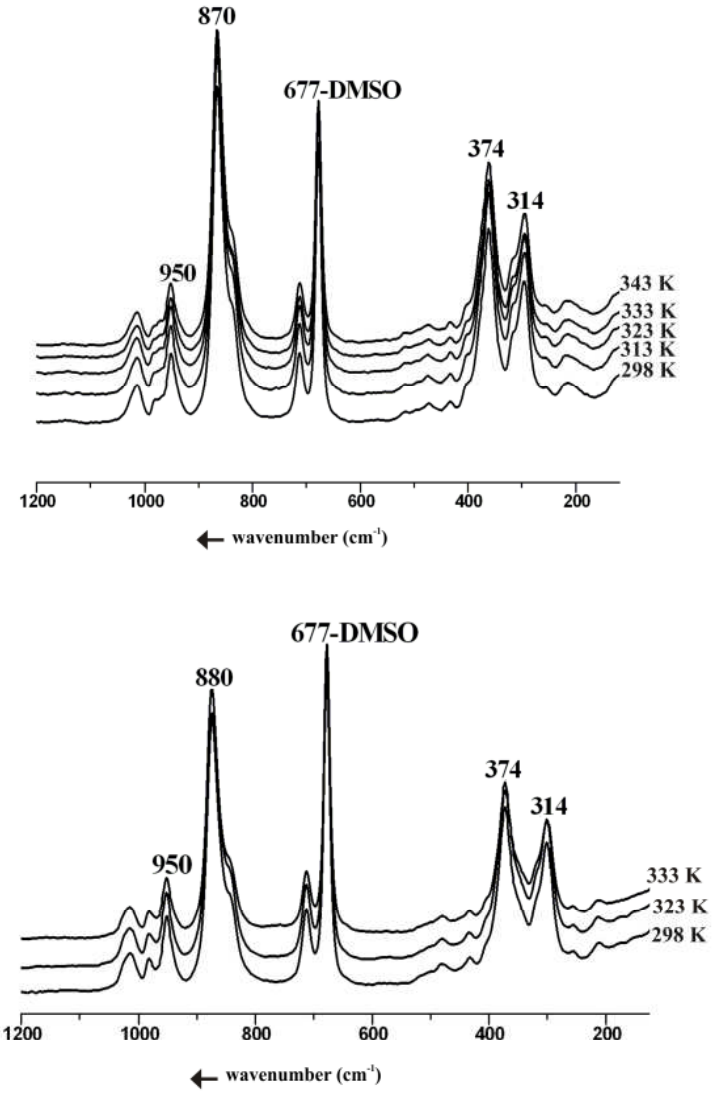

Figure 6.11: *Temperature and stability studies - II: Raman spectra of* $[Gua@Mo_{132}(hypo/sulph)_{30}]$ *(above) and* $[(Na + Urea)@Mo_{132}(sulph)_{30}]$ *(below) in the absence of aerial oxygen with the rise in temperature, using DMSO 20% (v/v) as an external standard, are shown.*

solution in each case, without an external standard. [8] The spectral patterns were retained in three of the four cases i.e., $[Mo_{132}(ac)_{30}]$, $[Mo_{132}(sulph)_{30}]$ and $[Gua@Mo_{132}(hypo/sulph)_{30}]$ up to a temperature of 343 K. It implies that only the remaining cluster $[(Na+Urea)@Mo_{132}(sulph)_{30}]$ is relatively less stable and decomposes beyond 333 K. (Figure 6.9)

[8] A slight drop in the temperature during the acquisition of the spectral data cannot be ruled out. Also note in each case the probes were kept at the said temperature for 10 mins.

With an external standard

The same experiments were repeated with 20% DMSO (by volume) as an external standard. The spectra were recorded and they showed the same behaviour as obtained before without the use of any external standard. (See Figures 6.10 and 6.11.) All the cluster compounds showed an enormous stability at least up to a temperature as high as 333K.

Implications:

- All the cluster capsules are stable at least up to a temperature of 333 K (at least for 10 mins).
- The capsule $[(Na + Urea)@Mo_{132}(sulph)_{30}]$ is less stable relative to the others against temperature rise.

6.6 pH and stability

Polyoxometalates are in general sensitive to pH alterations. For every given polyoxometalate there is a given regime of pH stability. In this section a comparative account of the pH stability of the four nanoobjects/clusters is described.

Generally the polyoxometalates decompose at alkaline pH. On dissolution of the four nanoobjects in discussion it was observed that the pH of the resulting solution was somewhere in the acidic range (around pH 3 to pH 5). Hence the pH dependent stability studies were divided into two parts: one at the higher pH range (i.e., the pH attained by alkalization of the solution generated by dissolution of the cluster in question) and the other at lower pH range (attained by acidification of the aqueous solution). The experiments in this case were performed with 1 mM solution and in the absence of aerial oxygen, with and without external standard. All the experiments described here were performed under exclusion of aerial oxygen.

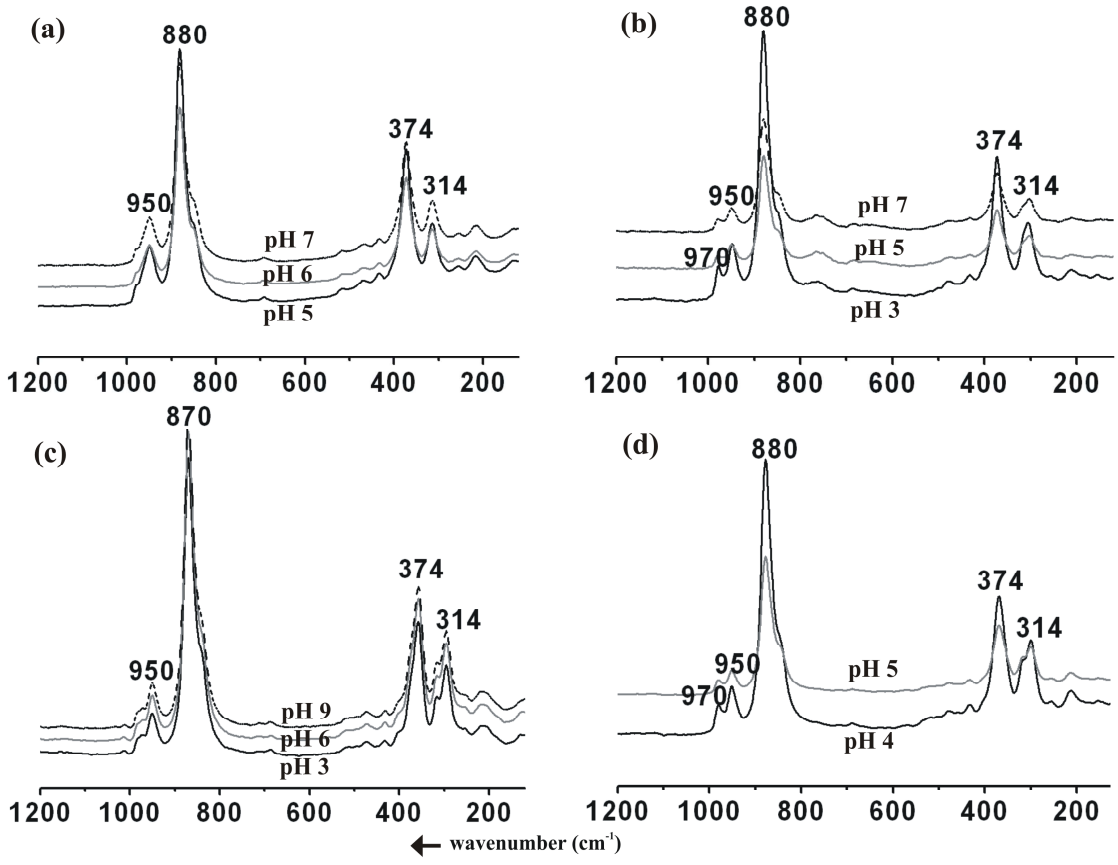

Figure 6.12: *The Raman spectra of* $[Mo_{132}(ac)_{30}]$ *(a),* $[Mo_{132}(sulph)_{30}]$ *(b),* $[Gua@Mo_{132}(hypo/sulph)_{30}]$ *(c) and* $[(Na + Urea)@Mo_{132}(sulph)_{30}]$ *(d) with increase in pH in the absence of aerial oxygen. The intensities of the spectra are not to the scale.*

6.6.1 Stability at high pH

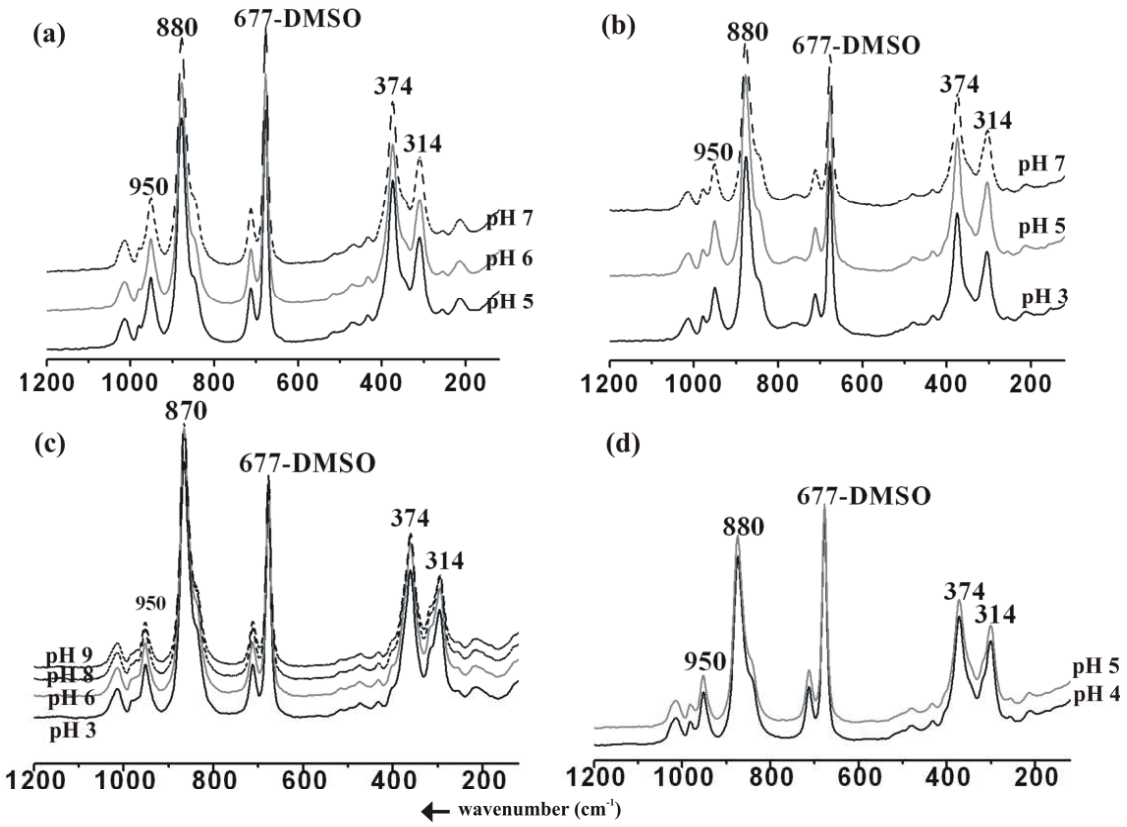

Figure 6.13: *The Raman spectra of $[Mo_{132}(ac)_{30}]$ (a), $[Mo_{132}(sulph)_{30}]$ (b), $[Gua@Mo_{132}(hypo/sulph)_{30}]$ (c) and $[(Na + Urea)@Mo_{132}(sulph)_{30}]$ (d) with increase in pH of the aqueous solution of the cluster, indexed with 20% v/v DMSO (as an external standard) in the absence of aerial oxygen.*

Without external standard

The alkalization of the 1 mM aqueous solution of the cluster capsules was carried out by drop-wise addition of 1 M NaOH under the exclusion of aerial oxygen. The spectra showed that the cluster $[Mo_{132}(ac)_{30}]$ is stable from a pH 5 (the pH of the solution immediately after dissolution of the cluster) to 7. Likewise, $[Mo_{132}(sulph)_{30}]$ is stable from a pH 3 (the starting pH) to 7. The cluster anion $[Gua@Mo_{132}(hypo/sulph)_{30}]$ is rather stable and retains integrity over a wide range of pH from 3 (the pH of the starting solution) to 9. Whereas $[(Na + Urea)@Mo_{132}(sulph)_{30}]$ seems to be the least stable and decomposes even at a pH as low as 5. (Figure 6.12.)

With an external standard

In order to have a semi-quantitative idea on the cluster stability these experiments were repeated with 20% v/v DMSO (as an external standard) and same trend in the context of pH dependence of the stability of the clusters were observed as the respective solutions were alkalized. (See Figure 6.13).

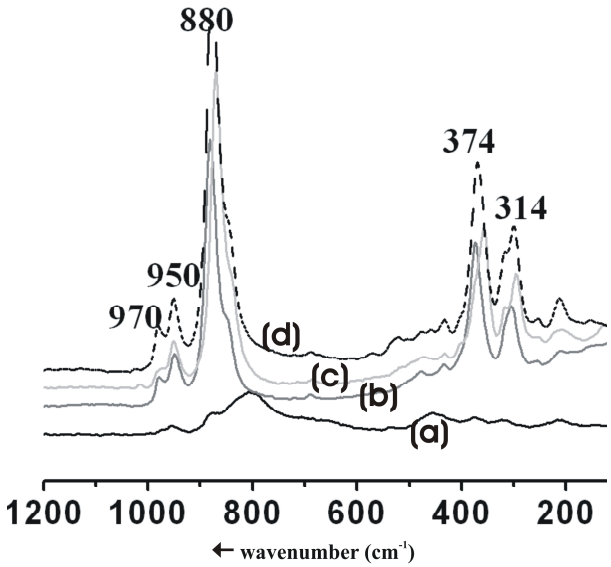

Figure 6.14: *Destabilization of* $[Mo_{132}(ac)_{30}]$ *(a) at low pH (<* 2*). The other clusters like* $[Mo_{132}(sulph)_{30}]$ *(b);* $[Gua@Mo_{132}(hypo/sulph)_{30}]$ *(c) and* $[(Na + Urea)@Mo_{132}(sulph)_{30}]$ *(d) are however stable at such pH. The intensities of the spectra are not to the scale. (For details please refer to the text.)*

6.6.2 Stability at low pH and effect of cations in stabilization

Stability of the cluster capsules in the absence of cations/electrolytes as stabilizing agents at low pH

In this series of experiments an interesting phenomenon emerged. It was observed that except $[Mo_{132}(ac)_{30}]$ cluster all the other three clusters in question were stable even under very low pH. (Figure 6.14) [9]

This observation was in a sense unusual from the standpoint of overall cluster charges. For instance, of the parent clusters $[Mo_{132}(ac)_{30}]$ and $[Mo_{132}(sulph)_{30}]$, the overall negative charge for the former (42-) is much lower than that of the latter

[9]These experiments were carried out using 1mM solution of the cluster compounds in water and acidification was done using 1M HCl, without addition of cations or electrolytes.

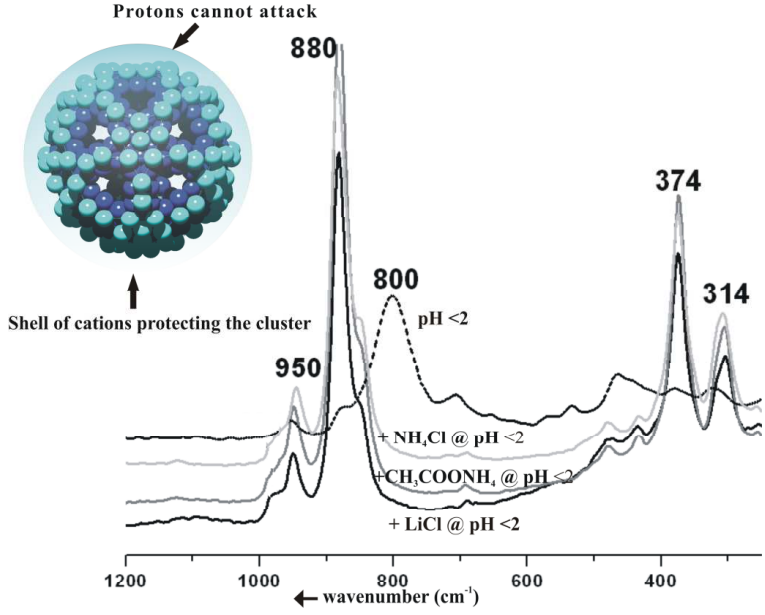

Figure 6.15: *Cations protecting the cluster anion* $[Mo_{132}(ac)_{30}]$ *at low pH (< 2). The Figure shows that in the presence of* Li^+, NH_4^+ *the cluster retains its integrity as evidenced from an unchanged Raman spectroscopic fingerprint. In each case 1 mM solution of the cluster compound was used. The Raman spectrum of the decomposed cluster not protected by cations/electrolytes at pH < 2 (in dotted line) is also given for reference. A model of* $[O_{372}]$ *framework 'protected' by cation shell (in light blue surrounding sphere) is shown for better visualization. Colour code: terminal oxygen atoms in cyan and bridging oxygen atoms in blue. For details see the text.*

(72-). So it might be expected that the latter is more susceptible to protonation than the former, but the experimental results showed just the reverse tendency.

On the other hand taking into account the number density of the counter-cations around the afore-mentioned two clusters, it is obvious that $[Mo_{132}(sulph)_{30}]$ has 72 ammonium ions whereas $[Mo_{132}(ac)_{30}]$ has only 42. Could it be that these cations 'wrap' the clusters and 'protect' them from destruction? The proposition would then also require the stabilization of the cluster $[Mo_{132}(ac)_{30}]$ in consideration at low pH in the presence of other cations and hence other electrolytes. This is tested in the next section.

Stability of the cluster capsules in the presence of cations/electrolytes as stabilizing agents at low pH

It is known since a while that cations/electrolytes facilitate the precipitation of the clusters by disrupting their solvation shell. [11] But as proposed above do the cations/electrolytes also affect the stability of the clusters? This was studied using $[Mo_{132}(ac)_{30}]$ as a model.

It was observed that in the presence of electrolytes such as $LiCl, NH_4Cl, CH_3COONH_4$, the cluster was stabilized at $pH < 2$; i.e., under acidic conditions. [10] This in turn vindicates the above proposal that the cations from the electrolytes perhaps somehow 'wrap' the cluster and thereby 'protect' the cluster from the scavenging protons. (Figure 6.15) The stoichiometric excesses required for such protection varies also for each cations but a rough range can be mentioned. Protection with CH_3COONH_4 requires only 100 fold excess whereas that for $LiCl, NH_4Cl$ is 250 fold (in each case). The 'protection' of the cluster by 100 fold stoichiometric excess CH_3COONH_4 might be due to the inhibition in formation of the acetic acid as leaving group. It might also be mentioned here that $NaCl$ 'fails' to protect the $[Mo_{132}(ac)_{30}]$ cluster against protonation. The reason(s) for which is not clear.

Implications:

- Cluster capsule with less negative charge and also with a closed 'isotropic' surface e.g., $[Gua@Mo_{132}(hypo/sulph)_{30}]$ is least prone to destabilization by pH change, both in alkaline or in acidic range.
- Except cluster capsule $[Mo_{132}(ac)_{30}]$ the other three capsules investigated are stable at low pH. Note: $[Mo_{132}(ac)_{30}]$ decomposes at a $pH < 2$ in absence of any electrolyte or cation.
- However the cluster capsule $[Mo_{132}(ac)_{30}]$ is stabilized at low pH in the presence of cations/electrolytes.

[10] These experiments were carried out with 1 mM solution of the cluster and different electrolyte concentrations, under the the exclusion of aerial oxygen. The solutions were acidified using conc. HCl.

6.7 A short note on 'cation uptake'

Having shown that the clusters are stabilized at low pH by different cations it is only natural to ask, are these cations taken up by the cluster like $[Mo_{132}(sulph)_{30}]$ [11] in aqueous solution? If yes, then is it also possible to have an idea about the 'site' of cation 'uptake'?

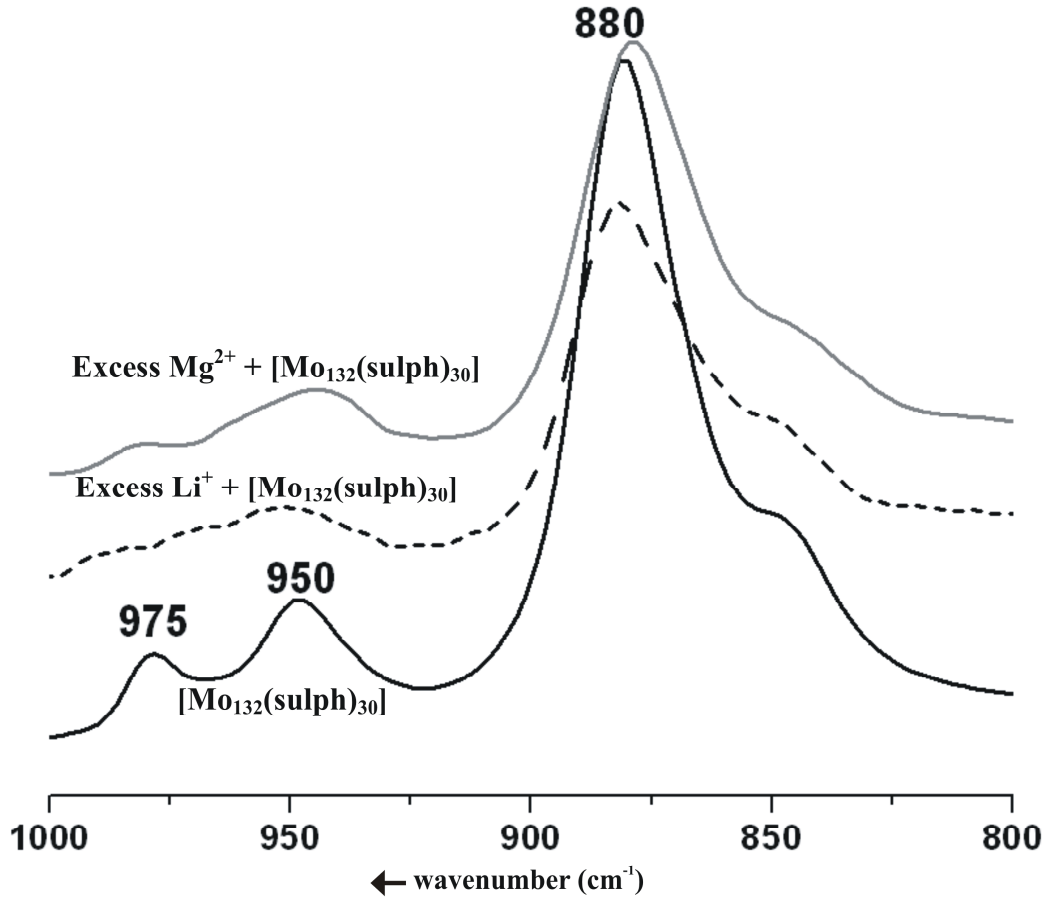

Figure 6.16: *Cation 'up-take' by the cluster anion $[Mo_{132}(sulph)_{30}]$. The Figure shows that in the presence of excess of Li^+, Mg^{2+} the Raman spectrum of the cluster is significantly changed. The band at 880 cm^{-1} $[\nu(O_{bri}breathing)]$, is broadened and diminished in intensity. The bands at 950 cm^{-1} $[\nu(Mo = O_t)]$ and 970 cm^{-1} $[\nu(SO_4)]$ are also broadened in both cases. For details see text.*

As mentioned earlier the Raman spectrum of the cluster $[Mo_{132}(sulph)_{30}]$ comprise of four intense bands. 950 cm^{-1} $[\nu(Mo = O_t)]$, 880 cm^{-1} $[\nu(O_{bri}breathing)]$, 374 cm^{-1} $[\delta(Mo = O_t)]$ and 314 cm^{-1} $[\delta(Mo - O - Mo)]$. Additionally there is another

[11] The other parent cluster anion $[Mo_{132}(ac)_{30}]$ was not used owing to its lower nucleophilicity.

band at 970 cm^{-1}. The intensification of this band - upon addition of a large excess [12] of ammonium sulfate implied - it is a $[\nu(SO_4)]$ band. Interestingly addition of $LiCl$, $BeCl_2$ or $MgCl_2$ in smaller amounts (in the mole ratio of up to 1:1000 with respect to the cluster concentration) did not alter the Raman spectral pattern. However when a very high excess (i.e., in the mole ratio of 1:10000 with respect to the cluster concentration) of these electrolytes were used the aforesaid 970 cm^{-1} $[\nu(SO_4)]$ band together with the bands at 950 cm^{-1} $[\nu(Mo = O_t)]$, 880 cm^{-1} $[\nu(O_{bri}breathing)]$, were broadened, implying interaction of the Li^+, Be^{2+} or Mg^{2+} cations with the 132 terminal, 180 μ_2- and 60 μ_3- O atoms of the cluster (see also the section on assignment of the cluster's Raman bands). (Figure 6.16)

The need for a high excess of cation concentration might be due to the relative extreme affinity of these cations to water. Only when all or a major part of the water is used up, the cations 'take recluse' in the residual 'water pockets' of the clusters showing interaction.

[12]Note: 10000 fold excess ammonium sulfate was added to 1 mmol aqueous solution of $[Mo_{132}(sulph)_{30}]$.

6.8 Discussion and perspectives

The investigations described so far in this Chapter unfolds factors essential for the stability of the cluster compounds in aqueous solution and also gives a comparative account of stability of different clusters.

- The cluster capsules are relatively stable in aqueous solution.
- They are more stabilized under the exclusion of aerial oxygen.
- The clusters are stable up to a temperature as high as 333 K.
- Except for cluster anion $[Gua@Mo_{132}(hypo/sulph)_{30}]$ (which is stable up to a $pH \sim 9$) all the other cluster anions investigated are decomposed at pH > 7.
- Only cluster capsule $[Mo_{132}(ac)_{30}]$ is not stable at low pH (< 2).
- Presence of electrolytes like $LiCl, NH_4Cl, CH_3COONH_4$ however can prevent this cluster from decomposition at low pH.
- Addition of cations like Li^+ or Be^{2+}, Mg^{2+} in large excess to a solution of $[Mo_{132}(sulph)_{30}]$ results in their 'uptake' by the cluster.
- Among the parent hosts $[Mo_{132}(ac)_{30}]$ and $[Mo_{132}(sulph)_{30}]$ it is observed that $[Mo_{132}(ac)_{30}]$ is more stable than $[Mo_{132}(sulph)_{30}]$, within the context of aerial oxidation which is expected as per the overall cluster charge, however in the matter of protonation the order is just the reverse.
- Among the host-guest complexes $[Gua@Mo_{132}(hypo/sulph)_{30}]$ and $[(Na+Urea)@Mo_{132}(sulph)_{30}]$, the latter is less stable than the former against aerial oxidation, temperature rise, alkalization or protonation.

6.8.1 Probable explanation for the order of stability

The stability of the hosts only: $[Mo_{132}(ac)_{30}]$ **and** $[Mo_{132}(sulph)_{30}]$

$[Mo_{132}(ac)_{30}]$ and $[Mo_{132}(sulph)_{30}]$ cluster capsules are negatively charged mixed-valent species. So a major reason for their decomposition has to be oxidants and protons. It is obvious that higher the negative charge of the cluster capsule the greater is its tendency to 'give away' electrons and to get oxidized. Similar behaviour of the clusters is expected towards an electrophilic agent like proton. Since the negative charge of cluster $[Mo_{132}(sulph)_{30}] > [Mo_{132}(ac)_{30}]$, so it is expected that $[Mo_{132}(sulph)_{30}]$ is more prone to react than $[Mo_{132}(ac)_{30}]$ and hence the former is less stable than the latter. This expectation is fulfilled in the case of aerial oxidation but in case of protonation/acid hydrolysis the order is just the reverse. Such an anomaly can only be argued in the light of higher number density of the ammonium cations (72) in the case of $[Mo_{132}(sulph)_{30}]$ in comparison to that of $[Mo_{132}(ac)_{30}]$, with 42 ammonium cations, enhancing the stability of the former against lowering of pH. Such a proposal of cationic 'protection' is buttressed by the observation that the less stable $[Mo_{132}(ac)_{30}]$ cluster can be stabilized against pH drop, in the presence of

externally added cations/electrolytes. From this it might also be proposed that the cations play a significant role in stabilizing the clusters. (See also later under the rubric: Cations and stability.) Also note that in addition to the 'cation-effect' the presence of substrates like CH_3COONH_4 can further stabilize $[Mo_{132}(ac)_{30}]$ cluster by inhibiting the formation of the acetic acid as leaving group ('common-ion effect').

The stability of the host-guest complexes: $[Gua@Mo_{132}(hypo/sulph)_{30}]$ **and** $[(Na+Urea)@Mo_{132}(sulph)_{30}]$

$[Gua@Mo_{132}(hypo/sulph)_{30}]$ and $[(Na + Urea)@Mo_{132}(sulph)_{30}]$ are stable at low pH, at higher concentration (1 mM). But in the matter of aerial oxidation or exposure to high pH, $[Gua@Mo_{132}(hypo/sulph)_{30}]$ is more stable than $[(Na+Urea)@Mo_{132}(sulph)_{30}]$. These differences could be explained as following. The difference in the structure of $[Gua@Mo_{132}(hypo/sulph)_{30}]$ and $[(Na + Urea)@Mo_{132}(sulph)_{30}]$ in this context is worth noting. In case of $[(Na + Urea)@Mo_{132}(sulph)_{30}]$ the oxygen atom of protonated urea cations at the periphery of $\{Mo_9O_9\}$ rings is likely to have a repulsive interaction with the $\mu_2 - O$ of the ring and perhaps destabilizes the cluster more easily in comparison to that of $[Gua@Mo_{132}(hypo/sulph)_{30}]$ in general. Since in case of the latter similar position is occupied by protonated nitrogen atom and this being capable of forming strong hydrogen bonds with the $\mu_2 - O$s of the ring stabilizes the cluster instead of destabilizing it. (Note also the N...O electronegativity difference.)

More specifically speaking the destabilization of $[(Na + Urea)@Mo_{132}(sulph)_{30}]$ at higher pH can be attributed to the deprotonation of urea, which leaves the cluster unprotected and hence facilitating its decomposition. Such a question of deprotonation does not arise in case of $[Gua@Mo_{132}(hypo/sulph)_{30}]$, since the pK_a of guanidine (around 13) is comparatively higher than urea, which is around 5.

6.8.2 Cations and stability

It has been proposed in the preceding section that the cations 'protect' the clusters against decomposition. Here a very short argument for such a proposal is outlined.

At higher pH, cations like guanidinium/protonated urea/ammonium of the clusters are deprotonated. [13] It is logical to think that the deprotonation of these ions at higher pH induces cluster decomposition. Likewise at lower pH it is observed $[Mo_{132}(sulph)_{30}]$ is more stable than $[Mo_{132}(ac)_{30}]$. The observation also alludes to cations role in cluster stability (here the cations are ammonium). The higher the number density of cations around the cluster, more 'protected' is the cluster from protonation/acid hydrolysis. $[Mo_{132}(sulph)_{30}]$ has a 'clothing' of 72 ammonium cations whereas for $[Mo_{132}(ac)_{30}]$ the number is only 42. Hence the later is less protected than the former against protonation/acid hydrolysis at low pH.

This proposal of 'cationic protection' of the clusters also draws support from the observation that on addition of electrolytes the less stable $[Mo_{132}(ac)_{30}]$, is also stabi-

[13] It might be mentioned that electron densities are found in the vicinity of the $\{Mo_9O_9\}$ rings of the clusters. These densities might be attributed to that of ammonium ions, as in case of $[Mo_{132}(ac)_{30}]$ or $[Mo_{132}(sulph)_{30}]$.

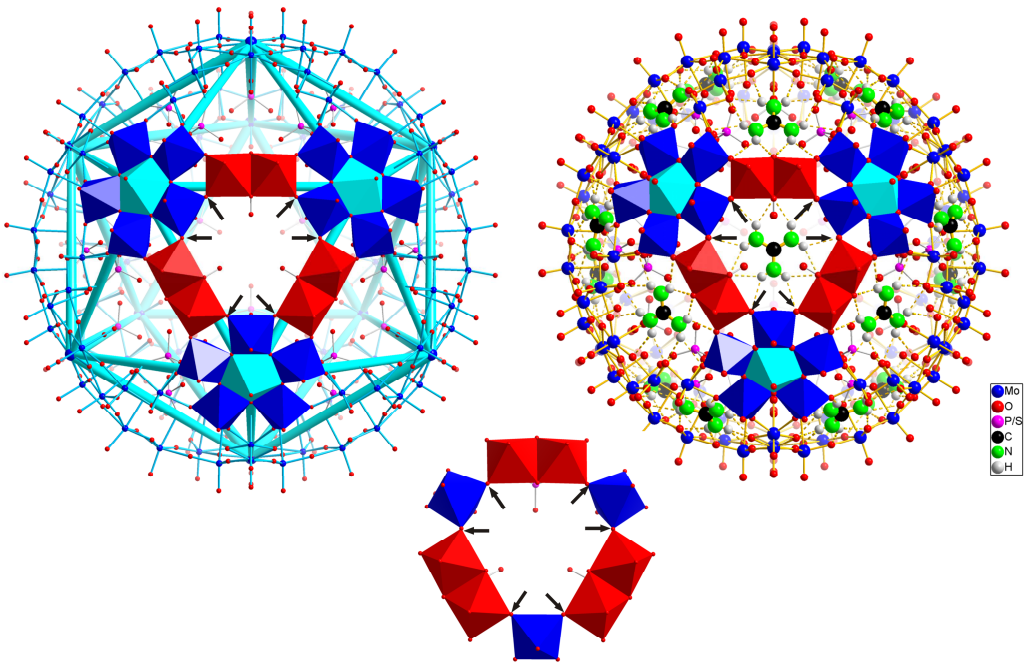

Figure 6.17: *Probable sites of decomposition: $[Mo_{132}]$ type cluster anion shown schematically. Highlighted with arrows are the proposed sites of 'attack': 6 μ_2-O lining the $\{Mo_9O_9\}$ rings of a $[Mo_{132}]$ type cluster with open (left) and closed (with guanidinium) $\{Mo_9O_9\}$ rings (right) in mixed polyhedral and ball-stick representation. The environment of an isolated $\{Mo_9O_9\}$ ring is shown in polyhedral representation with the related sites marked below for clarity.*

lized even at low pH (< 2). An electrolyte addition in such case most likely increases the number density of 'protecting' cations around the cluster and consequently the protons cannot attack the cluster and correspondingly the cluster is stabilized.

Also note that in presence of substrates like CH_3COONH_4 which inhibits the formation of the acetic acid, additionally the inhibition in formation of the leaving group plays an important role in stabilizing the $[Mo_{132}(ac)_{30}]$ cluster.

Likewise the 'higher' the affinity of the cations to the cluster more stable are the corresponding clusters. Guanidinium cations by the virtue of having highest binding affinity toward the cluster, (as every cation 'fits' perfectly in the pore and forms 6 H-bonds,) renders $[Gua@Mo_{132}(hypo/sulph)_{30}]$ with highest stability.

6.8.3 A proposal for decomposition site

The cations can 'sit' on the $\{Mo_9O_9\}$ pore openings/'nanowindows of the cluster capsules. It might be proposed that the 6 $\mu_2 - O$ atoms lining the $\{Mo_9O_9\}$ pore openings/nanowindows, (bridging the $[Mo_2]$ and $[(Mo)Mo_5]$ groups of the cluster)

are vulnerable to 'attack' by decomposing reagents: be it protons or oxygen. In case this site is unavailable for the decomposing reagent, (i.e., when occupied by a cation with very high affinity to the $\{Mo_9O_9\}$ nanowindow) the cluster becomes inert or attains stability. This proposal is vindicated in the observed order of stability. For instance, $[Mo_{132}(sulph)_{30}]$ with 'available' μ_2-O lining of the $\{Mo_9O_9\}$ rings is much less stable than for example, $[Gua@Mo_{132}(hypo/sulph)_{30}]$ where the aforementioned sites are 'blocked' by guanidinium cations with very high affinity to the cluster's $\{Mo_9O_9\}$ nanowindows. (Figure 6.17)

In other words, it emerges that the cations are crucial for stabilizing these clusters against decomposition. They do so by 'protecting' the clusters in general or more specifically as in some cases, like that of $[Gua@Mo_{132}(hypo/sulph)_{30}]$, the vulnerable $\mu_2 - O$ atoms lining the $\{Mo_9O_9\}$ pore openings/nanowindows.

Chapter 7

Summary and conclusion

Large complex molecules of the nanocosmos - like proteins - can do things like activating, storing, transferring complex information, transporting, scavenging, and separating substrates and related functions iteratively with a high precision. The unusual and absolutely unique chemistry of oxomolybdates - under reducing conditions - offers the option to generate related nanosystems. In the solution of oxoanions of the early transition metals (like molybdenum)- controlled linking of metal-oxide building blocks from a 'virtual library' - provides the option to get exquisite molecular architecture. Such architecture constitute two broad classes: the molybdenum 'blues' and 'browns'. [13] In this dissertation some clusters of these two classes have been isolated, characterized and studied in detail.

It is said that in science we enter future backwards. This dissertation was no exception. Synthetic investigation of the known systems opened up new avenues, which when systematically studied, transcending the known regime of covalent chemistry crystallized at the 'supramolecular frontier'. New effects were observed, those understood were exploited and have been described here. Unanswered questions remain. After describing the problems which were answered this thesis will conclude with a perspective asking some unanswered questions. First, the story of a synthetic optimization.

While investigating the synthesis of a 'defect' polyoxomolybdate $[Mo_{138}]$ wheel type cluster, [28] from the so-called 'molybdenum blue' solution, the conditions (like pH, temperature, use of electrolyte, etc.) were systematically varied. On one such variation the use of a reagent like urea, at low pH resulted in early precipitation of a crystalline solid from the 'molybdenum blue' solution. The crystalline precipitate on analysis showed an interesting aspect. It consisted of a covalently connected molecular chain of wheel-shaped $[Mo_{154}]$ clusters, more precisely, **1**. [33]

$$^{1}_{\infty}\{(UH^{+})_{14}[Mo^{VI}_{126}Mo^{V}_{28}O_{462}H_{14}(H_2O)_{68}]\} \cdot ca.350H_2O \equiv \mathbf{1}$$

It was further observed that urea, in addition to disrupting the hydration shell, [11] also showed 'guest' behaviour thereby pointing to some of the potential host

sites on the cluster surface: $\{Mo_6O_6\}$ rings. [40]

Within the context of host-guest chemistry the presence of related $\{Mo_9O_9\}$ crown-ether type rings in the $[Mo_{132}]$ type spherical clusters did not escape attention. This dissertation demonstrated (with the collaboration of many colleagues of the group) that clusters, like **6a**, **7a** and **8a** with appropriate ($\{Mo_9O_9\}$) pore size could for instance bind, large organic cations like guanidinium/protonated urea present in the solution leading to the formation of **9a**, **10a** and **11a**. [47] Because of such substrate specific behaviour, the parent hosts like **6a**, **7a** and **8a** were proposed to be called guanidinium/urea 'nanosponges'. [1]

$$(NH_4)_{42}[\{(Mo)Mo_5O_{21}(H_2O)_6\}_{12}\{Mo_2O_4(CH_3COO)\}_{30}]\cdot ca.300H_2O\cdot 10CH_3COONH_4 \ \mathbf{6}$$

$$(NH_4)_{42}[(H_2O)_{80}@\{(Mo)Mo_5O_{21}(H_2O)_6\}_{12}\{Mo_2O_4(H_2PO_2)\}_{30}]\cdot ca.220H_2O \ \mathbf{7}$$

$$(NH_4)_{72-n}[\{(H_2O)_{81-n}+(NH_4)_n\}@\{(Mo)Mo_5O_{21}(H_2O)_6\}_{12}\{Mo_2O_4(SO_4)\}_{30}]\cdot ca.200H_2O \ \mathbf{8}$$

$$(GH^+)_{32}[\{(H_2O)_{100}+(GH^+)_{20}\}@\{(Mo)Mo_5O_{21}(H_2O)_6\}_{12}\{Mo_2O_4(H_2PO_2)\}_{20}\{Mo_2O_4(SO_4)\}_{10}]\cdot ca.100H_2O$$
9

$$(GH^+)(NH_4)_{51-n}[\{(H_2O)_{81/2-n}+(GH^+)_{20}+(NH_4)_n\}@\{(Mo)Mo_5O_{21}(H_2O)_6\}_{12}\{Mo_2O_4(SO_4)\}_{30}]\cdot ca.180H_2O$$
10

$$(UH^+)_{20}(NH_4)_{32-n}[\{(H_2O)_{81-n}+(UH^+)_{20}+(NH_4)_n\}@\{(Mo)Mo_5O_{21}(H_2O)_6\}_{12}\{Mo_2O_4(SO_4)\}_{30}]\cdot ca.120H_2O$$
11

It also emerged from these investigations that the extent of larger guest cation uptake is not only governed by the overall negative charge of the cluster capsule but also by the maximum available space in the crystal lattice of the precipitated host-guest complex. For instance, it seems that the space in the lattice of the host-guest complex is limited to a maximum of 52 large monopositive organic cations like protonated urea or guanidinium. (Note: total number of guanidinium or protonated urea is always found to be less than or equal to 52, even if the overall cluster charge is higher (72-) as in **10a** or **11a**.)

In the matter of host-guest chemistry involving these 'nanosponges', it was also observed that there exist other sites beneath the cluster surface, lined by the negatively charged ligands to the linkers (like sulphates) where smaller inorganic cations, like Na^+, Ca^{2+}, etc. could be placed. The formation of **12a**, **13a** and **14a** from **8a** (generated *in-situ*) proved such expectation. [58]

[1] As always, here also GH^+ and UH^+ stand for $\{(NH_2)_3C^+\}$ and $(NH_3^+CONH_2)$ respectively.

$(UH^+)_{28}Na_{11}[\{(H_2O)_{60} + (UH^+)_{20} + Na_{13}\}@\{(Mo)Mo_5O_{21}(H_2O)_6\}_{12}\{Mo_2O_4(SO_4)\}_{30}] \cdot ca.140H_2O$

12

$(GH^+)_6(NH_4)_{20}Na_{13}[\{(H_2O)_{60} + (GH^+)_{20} + Na_{13}\}@\{(Mo)Mo_5O_{21}(H_2O)_6\}_{12}\{Mo_2O_4(SO_4)\}_{30}] \cdot ca.190H_2O$

13

$(UH^+)_{22}(NH_4)_{16}[\{(H_2O)_{60} + (UH^+)_{20} + Ca_7\}@\{(Mo)Mo_5O_{21}(H_2O)_6\}_{12}\{Mo_2O_4(SO_4)\}_{30}] \cdot ca.140H_2O$

14

All these host-guest clusters from **9a** to **14a** have 'nanodews'/'nanodrops' of water within. [55, 56] The nature of these 'nanodrops' of water though different in different clusters, however shows an informative structural patterning. Presence of one guest type and suitable ligands seem to favour a three-shell water structuring: $(H_2O)_{20}@(H_2O)_{20}@(H_2O)_{60}$ as in the case of **9a**. But in cases of **12a** - **14a**, where a second type of guest is present, only the outer-most $(H_2O)_{60}$ cluster was observed. It implied that incorporation of inorganic cations like Na^+, Ca^{2+}, etc. could disrupt the structuring of water inside these capsules. This implication was then extrapolated in cases of clusters like, **10a** and **11a**, with water structured in 2 shells: $(H_2O)_{20}@(H_2O)_{60}$. Here the second dodecahedral water shell was missing and the innermost dodecahedral cluster (in comparison to **9a**) was also 'inflated'. These implications were proposed to be a signature of encapsulation of ions inside those clusters. And it was proposed that these clusters have encapsulated ammonium ions inside. See also: [55, 56] [2]

The phenomena within the context of host-guest chemistry related to 'uptake' of cationic species described so far have been observed by the precipitation of crystals of the corresponding complexes. But what is the dynamic nature of these processes in solution? Is it possible to study those processes at least qualitatively? The present is promising, [72, 73, 74] but the future holds perhaps a better, if not a complete answer. The solution state although more promising is extremely complex as well. So as a closing theme of this dissertation a ground work for future solution investigations was carried out. The ground work being: the stability study of four selected clusters **6a**, **8a**, **9a** and **12a**.

The stability studies were performed principally by Raman spectroscopy in water and it was observed that the clusters investigated retain their molybdenum-oxide skeleton *when dissolved in water* [3] and remain stable up to a temperature as high as around 333K. However they *are destabilized by aerial oxidation*, but remain stable at least for a month in the absence of aerial oxygen. It was also observed that the cluster **6a** is more stable than the more negative **8a**, in the matter of aerial oxidation among the parent host structure but the trend is just the reverse within the context of protonation. Such an anomaly alluded to the role of the cations in stabilizing the clusters. This was further supported by the observation that the host-guest complex

[2] Please note the difficulty if not impossibility of locating ammonium ions experimentally.

[3] Although a slight opening of the clusters like formation of a 'basket' might not be ruled out. [79]

9a with strongly binding guanidinium cations as guests was more stable than **12a** with less tightly bound protonated urea and sodium cations. It was also separately shown that presence of cations as electrolytes enhanced the stability of the complexes. When present in extreme excess the cations were also found to be taken up by the suitable clusters.

These observations, in turn, pointed to the most vulnerable regions of the spherical clusters from the standpoint of their decomposition. These sites/points are eventually those where cations find 'recluse' in these clusters: the $\{Mo_9O_9\}$ pores/rings. To be more precise they are the $\mu_2 - O$ atoms lining those rings (bridging the $[Mo_2]$ and $[(Mo)Mo_5]$ groups of the cluster). The more protected these sites are with the guests, (like guanidinium as in case of **9a**) or electrolytes in general, more stable are the clusters. When left empty (as in the parent clusters **6a**, **8a**) or in the absence of added electrolytes the clusters are comparatively less stable since the aforementioned vulnerable sites (the $\mu_2 - O$ lining of the $\{Mo_9O_9\}$ rings/pores) are then 'open' to attack by destabilizing agents.

Chapter 8

Perspective

Making a detour from destruction to construction, many interesting questions emerge. What prompts the crystallization of these unusually giant clusters? What might be the starting point for nucleation? Is the nucleation centre an aggregate of few molecular clusters? Or are there parallel pathways for formation of the crystalline precipitate? These questions remain unanswered. The emergence of elegant molecular architecture from a 'soup'of ionic ingredients perhaps alludes to the operation of an 'evolutionary selection process' operating on a molecular level by which more symmetric species 'evolve' predating on less symmetric 'building blocks' in a 'virtual library'. [80] However a complete understanding of all such questions is still incomplete! Perhaps future has the key.

Rewinding back to the beginning, sharing Feynmann's view, one can only "wonder at wondering" and humbly contemplate the creative prowess of ***Nature***.

Chapter 9

Appendix I

9.1 Experimental methods

9.1.1 Elemental analysis

C,H,N analyses were completed by the Analytical services unit at the Universität Bielefeld using a LECO CHNS-932 instrument.

Na analysis were carried out by flame emission spectroscopy (Pye Unicam SP1900 Spectrophotometer).

Mo^V centers were determined by potentiometric titration with 0.01 M cerium sulphate solution under argon, using a Pt / Calomel electrode.

The crystal water contents of all compounds were determined in an argon atmosphere (50 ml/min) with a Shimadzu DTG 50 DTA-TG instrument.

9.1.2 Vibrational spectroscopy

Vibrational spectra were recorded with a Bruker IFS 66/FRAU 106 spectrometer. FT-IR: KBr pellet prepared under argon and Nujol mull (not displayed), recorded in the range 4000-350 cm^{-1}; FT-Raman: KBr matrix, excitation with a Nd: YAG-laser; $\lambda_e = 1064$ nm.

9.1.3 Electronic absorption spectroscopy

UV-Vis spectra were recorded from degassed solutions in the range 200 - 100 nm with a Shimadzu UV-160A spectrophotometer and evaluated with a program associated with the spectrometer. Solid state reflection spectra in the range 250 - 850 nm were measured using bleached cellulose as a white standard.

9.1.4 Single crystal X-ray structure analysis

X-ray diffraction data for the compounds described in this dissertation were collected by the removing the corresponding crystals from the mother-liquor and immediately

cooling them to a temperature around 173 - 193 K on a Bruker AXS SMART diffractometer (three circle goniometer with 1K CCD detector, $Mo-K_\alpha$ radiation, graphite monochromator; hemisphere data collection in ω at 0.3 scan width in three runs with 606, 435 and 230 frames (f = 0, 88 and 180) at a detector distance of 5 cm). In each case empirical absorption correction using equivalent reflections was performed with the program SADABS-2.03. The structures were solved with the program SHELXS-97 and refined using SHELXL-93 to different R values as appended in the tables for corresponding reflections with $I > 2\sigma(I)$. The programs SHELXS/L, SADABS- 2.03 were kindly provided by Prof. G. M. Sheldrick, University of Göttingen; structure graphics were done with DIAMOND 2.1 from Dr. K. Brandenburg, Crystal Impact GbR, 2001. Some of the artworks in this thesis have been prepared using POV-Ray 3.5 freeware from C. J. Cason.

9.1.5 Bond valence sum calculations

The bond valence sums n_j for an atom j were calculated as follows:

$n_j = \sum_i n_{ij} = \sum_i \exp[-(R_{ij} - R_{0,ij})/B_{ij}]$

where: n_{ij}: the bond valence between the atoms i and j; R_{ij}: distance between the atoms i and j; $R_{0,ij}$: single bond distance between the atoms i and j; B_{ij}: empirically determined parameter. [34]

9.2 Spectra of synthesized compounds

All the Infra-red spectra were measured by preparing KBr disks of the corresponding compounds. The Raman spectra were also measured in solid-state.

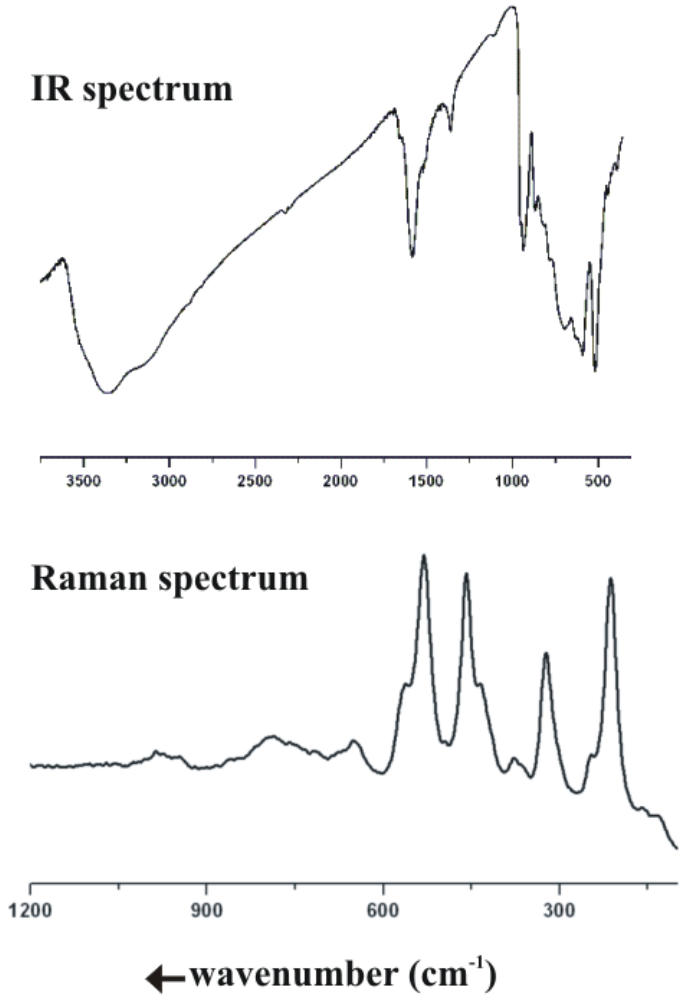

Figure 9.1: *The IR and Raman spectra of* ***1****.*

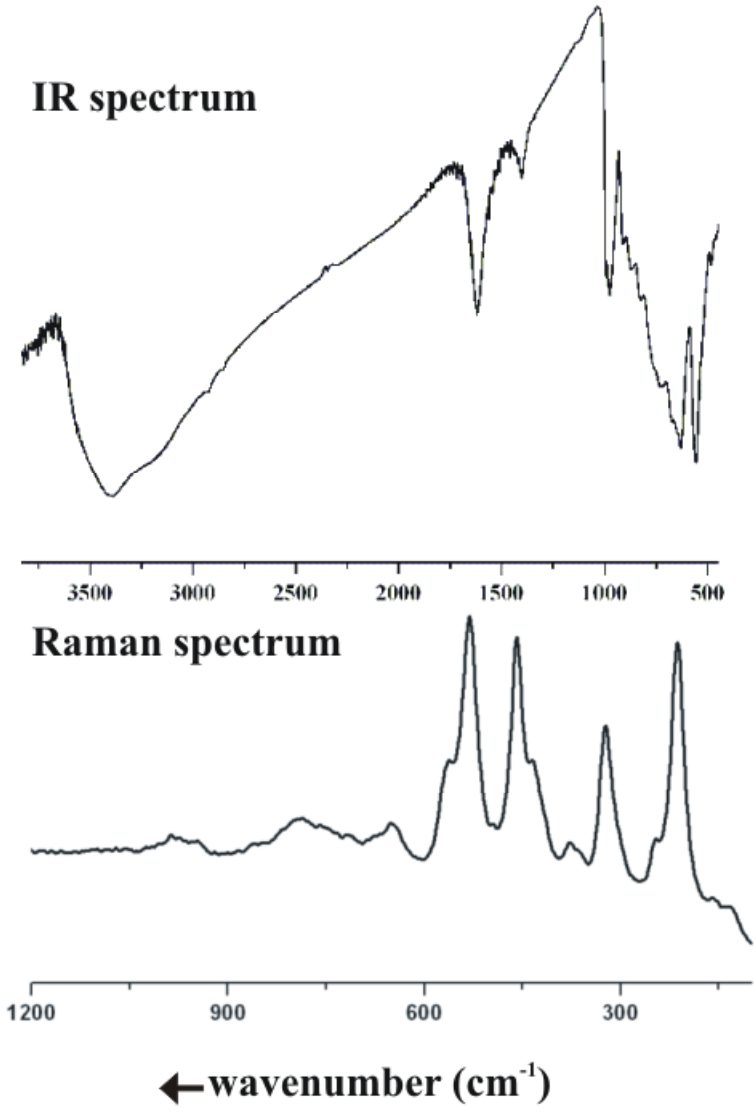

Figure 9.2: *The IR and Raman spectra of* ***2****.*

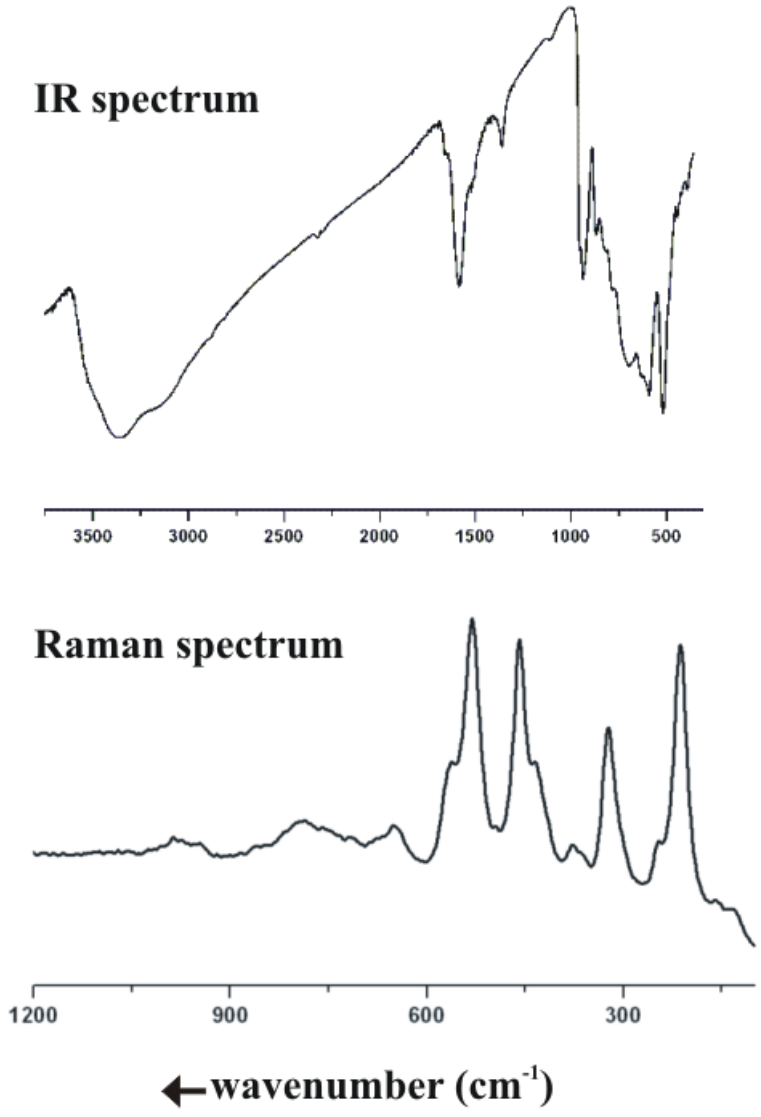

Figure 9.3: *The IR and Raman spectra of* ***3****.*

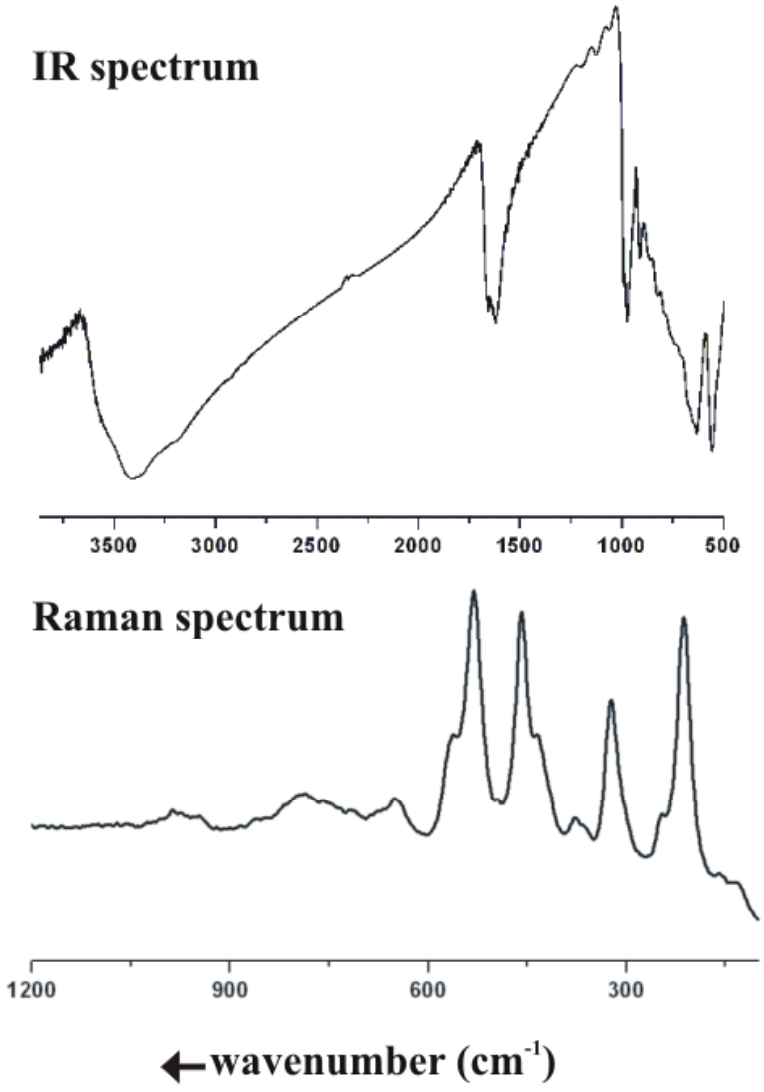

Figure 9.4: *The IR and Raman spectra of* ***4****.*

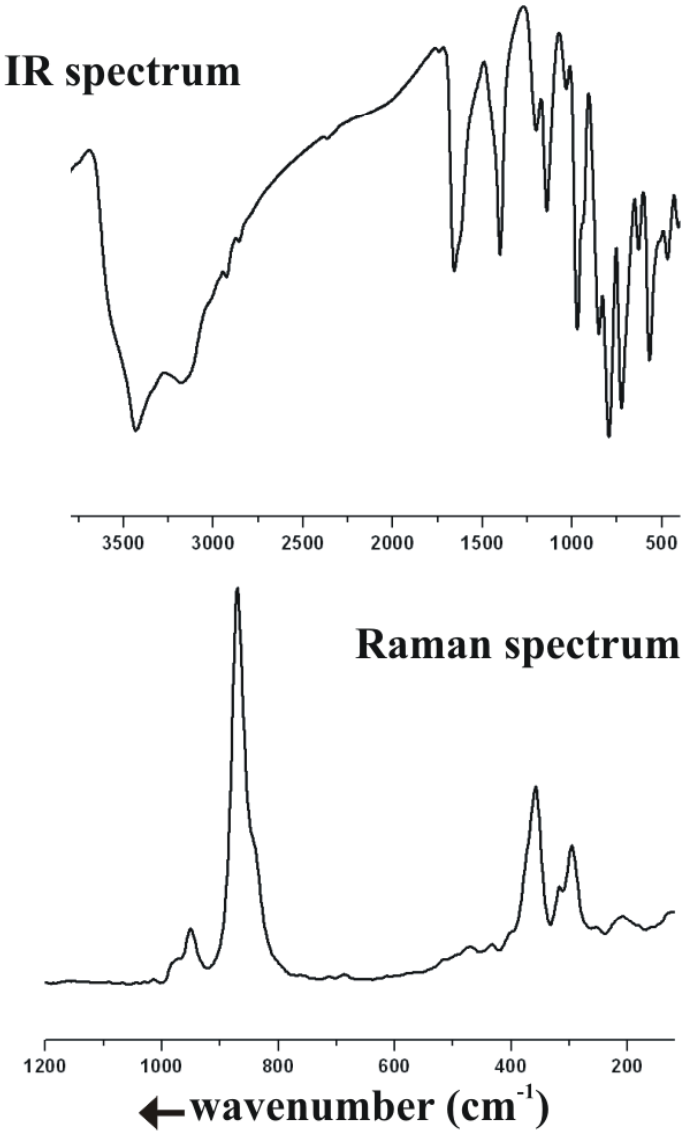

Figure 9.5: *The IR and Raman spectra of* ***9****.*

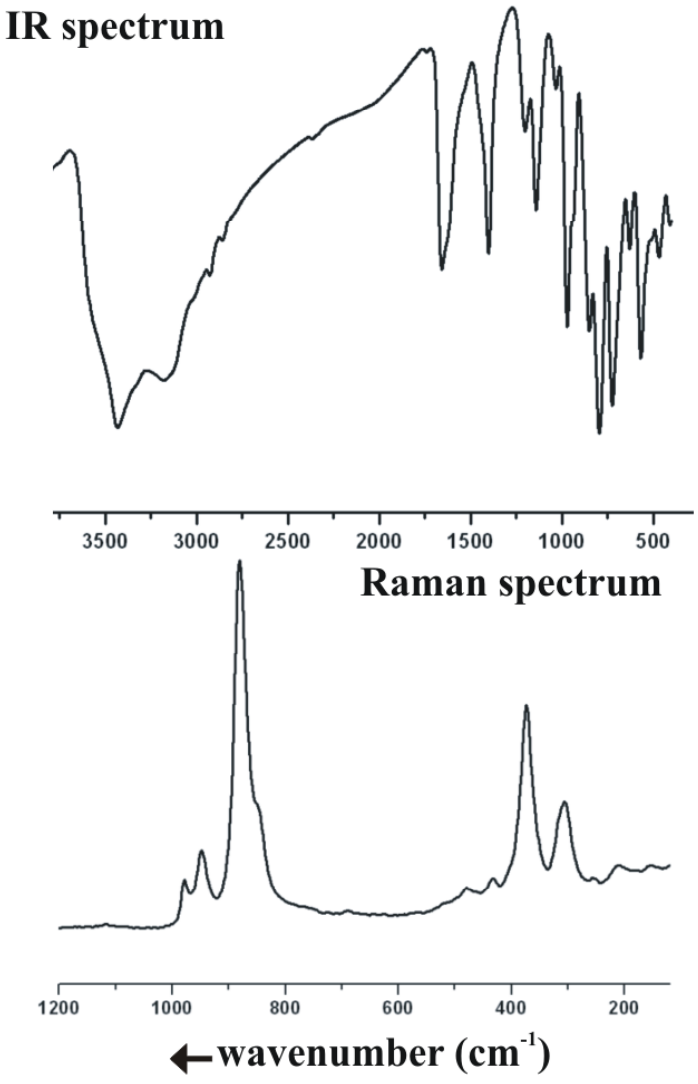

Figure 9.6: *The IR and Raman spectra of* ***10****.*

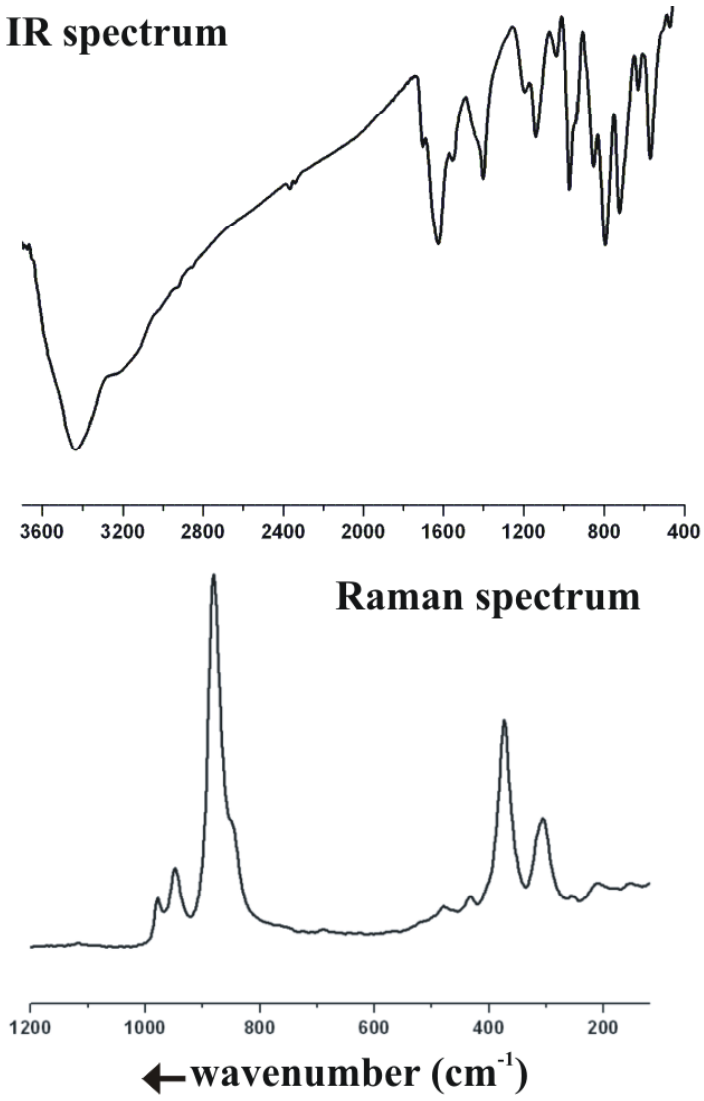

Figure 9.7: *The IR and Raman spectra of* ***11****.*

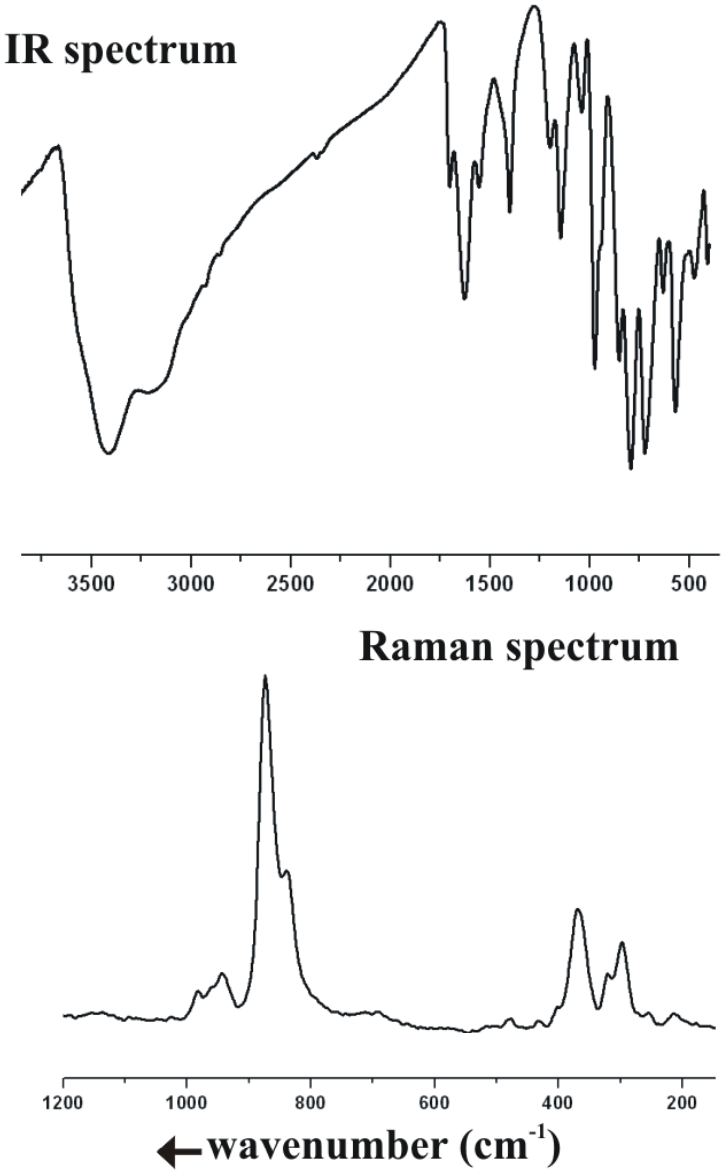

Figure 9.8: *The IR and Raman spectra of* ***12****.*

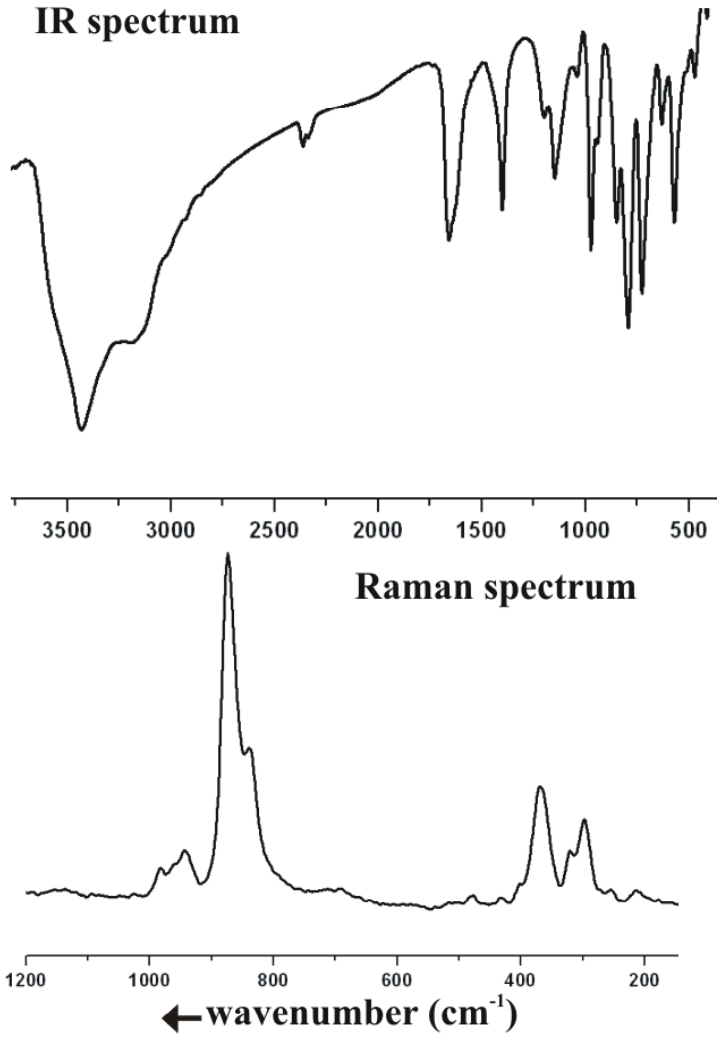

Figure 9.9: *The IR and Raman spectra of* ***13****.*

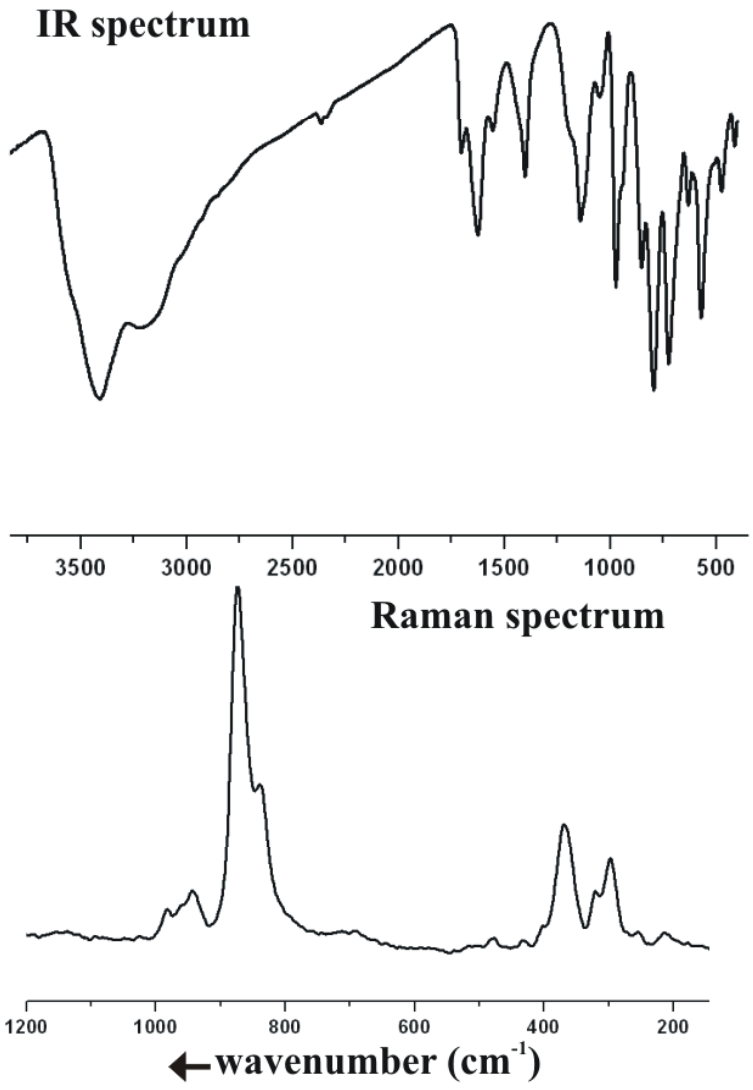

Figure 9.10: *The IR and Raman spectra of* ***14****.*

Chapter 10

Appendix II

10.1 Crystallographic data

Compound	**1**	**2**
Empirical formula	C14 H920 Mo154 N28 O894	H906 Mo154 N14 O880
Formula weight	30566.54	29964.15
Space group	C2/m	C2/m
Temperature, K	183(2)	188(2)
Crystal system	monoclinic	monoclinic
Crystal size	0.40 x 0.20 x 0.10 mm^3	0.25 x 0.20 x 0.08 mm^3
a, Å	33.447(1)	33.469(2)
b, Å	53.320(2)	53.191(3)
c, Å	27.064(1)	26.915(1)
$\alpha,^0$	90	90
$\beta,^0$	107.532(1)	107.368(1)
$\gamma,^0$	90	90
Volume, $\AA^3$	46024.4(3)	45731(4)
Z	2	2
$\rho, calc.gcm^{-3}$	2.206	2.176
μ, mm^{-1}	2.139	2.149
Reflections collected	136742	115405
Θ range	0.74^o to 27.03^o	1.53^o to 25.00^o
F(000)	29640	29024
Unique reflections	50307	40621
Observed reflections	34050	23869
$[I > 2\sigma(I)]$		
Final R indices	R_1=0.0523	R_1=0.0784
$[I > 2\sigma(I)]$	wR_2=0.1412	wR_2=0.2012

Table 10.1: Crystallographic data for compounds **1** and **2**.

Note: The *.cif files of the compounds reported in this thesis can be obtained by quoting the formula and the compound number as given in this dissertation on request from Prof. A. Müller by e-mail: a.mueller@uni-bielefeld.de

Compound	**4**
Empirical formula	C8 H779 Mo146 N24 Na14 O800.50
Formula weight	28354.65
Space group	P2(1)/n
Temperature, K	188(2)
Crystal system	monoclinic
Crystal size	0.35 x 0.35 x 0.10 mm^3
a, Å	30.528(2)
b, Å	43.781(3)
c, Å	33.113(2)
$\alpha,^0$	90
$\beta,^0$	95.735(1)
$\gamma,^0$	90
Volume, $\mathring{A}^3$	44036(5)
Z	2
$\rho, calc.gcm^{-3}$	2.138
μ, mm^{-1}	2.120
Reflections collected	175000
Θ range	1.54 to 22.49^o
F(000)	27370
Unique reflections	57407
Observed reflections	28951
$[I > 2\sigma(I)]$	
Final R indices	R_1=0.1048
$[I > 2\sigma(I)]$	wR_2=0.2501

Table 10.2: Crystallographic data for compound **4**.

Compound	**9**	**11**
Empirical formula	C52 H896 Mo132 N156 O724 P20 S10	C40H872Mo132N112O804S30
Formula weight	28901.33	29418.38
Space group	R-3m	R-3
Temperature, K	188(2)	183(2)
Crystal system	rhombohedral	rhombohedral
Crystal size	0.30 x 0.30 x 0.10 mm^3	0.40 x 0.30 x 0.25 mm^3
a, Å	62.947(2)	32.837(6)
b, Å	62.947(2)	32.837(6)
c, Å	76.393(3)	73.911(2)
$\alpha,^0$	90	90
$\beta,^0$	90	90
$\gamma,^0$	120	120
Volume, $\AA^3$	262144(15)	69018(3)
Z	12	3
$\rho, calc.gcm^{-3}$	2.197	2.123
μ, mm^{-1}	2.002	1.918
Reflections collected	454074	187852
Θ range	1.52^o to 25.00^o	1.53^o to 29.99^o
F(000)	169152	43056
Unique reflections	52824	44604
Observed reflections	454074	36340
$[I > 2\sigma(I)]$		
Final R indices	R_1=0.0744	R_1=0.0424
$[I > 2\sigma(I)]$	wR_2=0.1816	wR_2=0.1188

Table 10.3: Crystallographic data for compounds **9** and **11**.

Compound	**12**	**13**
Empirical formula	C48H784Mo132N96Na24O812S30	C26H880Mo132N98Na26O814S30
Formula weight	29881.35	29819.90
Space group	R-3	R-3
Temperature, K	183(2)	188(2)
Crystal system	rhombohedral	rhombohedral
Crystal size	0.25 x 0.25 x 0.15 mm^3	0.30 x 0.25 x 0.20 mm^3
a, Å	32.803(5)	33.004(8)
b, Å	32.803(5)	33.004(8)
c, Å	73.948(2)	74.027(3)
$\alpha,^0$	90	90
$\beta,^0$	90	90
$\gamma,^0$	120	120
Volume, $\AA^3$	68909.6(2)	69830(3)
Z	3	3
$\rho, calc.gcm^{-3}$	2.160	2.127
μ, mm^{-1}	1.933	1.908
Reflections collected	190772	194529
Θ range	0.77^o to 30.02^o	1.55^o to 29.99^o
F(000)	43584	43632
Unique reflections	44749	45168
Observed reflections	36437	41877
$[I > 2\sigma(I)]$		
Final R indices	R_1=0.0395	R_1=0.0339
$[I > 2\sigma(I)]$	wR_2=0.1091	wR_2=0.0916

Table 10.4: Crystallographic data for compounds **12** and **13**.

Compound	**14**
Empirical formula	C42H818Mo132N100Ca7O806S30
Formula weight	29532.40
Space group	R-3
Temperature, K	188(2)
Crystal system	rhombohedral
Crystal size	0.30 x 0.20 x 0.20 mm^3
a, Å	32.822(1)
b, Å	32.822(1)
c, Å	73.925(4)
$\alpha,^0$	90
$\beta,^0$	90
$\gamma,^0$	120
Volume, $\AA^3$	68968(5)
Z	3
$\rho, calc.gcm^{-3}$	2.133
μ, mm^{-1}	1.958
Reflections collected	136651
Θ range	1.54^o to 26.99^o
F(000)	43146
Unique reflections	33326
Observed reflections	28169
$[I > 2\sigma(I)]$	
Final R indices	R_1=0.0378
$[I > 2\sigma(I)]$	wR_2=0.1099

Table 10.5: Crystallographic data for compound **14**.

A short biography

Soumyajit Roy, born in Calcutta, India, on July 30, 1976, completed graduation with a first class honours in Chemistry, from the University of Calcutta, (1999). After completing Master of Science from the Indian Institute of Technology, Delhi, (2001), he started his Ph. d under the supervision of Prof. Dr. Dr. h. c. mult. Achim Müller at the University of Bielefeld, Germany, with a fellowship from 'Graduiertenkolleg Strukturbildungsprozesse' of the university. Recipient of National Scholarship (in India), and recently, the best speaker award in GDCh-JCF: Euroregionale 2003 (in Germany), he is now completing his doctoral dissertation.

List of publications

1. A. Müller, S. Roy, M. Schmidtmann and H. Bögge, **"Urea as deus ex machina in giant molybdenum blue type cluster synthesis: an unusual hybrid compound with perspectives for related nano, supramolecular and extended structures."** Chem. Commun. (2002) 2000.

2. A. Müller, S. Roy, **"Quest for beauty through lenses of molecules."** Desh (Bengali literary magazine), 22 (2002) 44.

3. A. Müller, S. Roy, **"Metal-oxide based nanoobjects: reactivity, building blocks for polymeric structures and structural variety."** Russ. Chem. Revs. 71 (2002) 981.

4. A. Müller, E. Krickemeyer, H. Bögge, M. Schmidtmann, S. Roy, A. Berkle, **"Changeable pore sizes allowing effective and specific recognition by a molybdenum-oxide based nanosponge: en route to sphere-surface and nanoporous-cluster chemistry."** Angew. Chem. Int. Ed. 41 (2002) 3604.

5. A. Müller, S. K. Das, S. Talismanov, S. Roy, E. Beckmann, H. Bögge, M. Schmidtmann, A. Merca, A. Berkle, L. Allouche, Y. Zhou, L. Zhang, **"Trapping cations in specific positions in tunable artificial cell channels: new nanochemistry perspectives."** Angew. Chem. Int. Ed. 42 (2003) 5039.

6. A. Müller, S. Roy, **"En route from the mystery of molybdenum blue via the related manipulateable building blocks to aspects of materials science."** Coord. Chem. Rev. 245 (2003) 153.

7. A.Müller, S. Roy, **"Oxomolybdates: From structures to functions in a new era of nanochemistry"** in: C. N. R. Rao, A. Müller, A. K. Cheetham (Eds) Recent Advances in the Chemistry of Nanomaterials, Wiley-VCH, Weinheim, 2004.

8. A. Müller, S. Roy, **"Metal-oxide based porous capsules/artificial cells with unprecedented material properties."** J. Mater. Chem. (submitted).

9. A. Müller, S. Roy, **"Nanoobjects can behave differently - but how and why?"** Angew. Chem.Int. Ed. (Mini Rev.) (to be submitted shortly).

10. A. Müller, S. Roy, **"Linking giant novel polyoxomolybdates in solid-state, solution and gas-phase."** Eur. J. Inorg. Chem. (to be submitted shortly).

11. A. Müller, S. Roy, **"Molybdenum oxide based nanoobjects getting linked to form extended structure in solution and even in solid-state."** Sol. St. Sc. (to be submitted).

12. A. Mix, H. Bögge, D. Rehder, S. Roy, T. Mitra, R. Tomsa, M. Schmidtmann, A. Stammler and A. Müller, **"Opening and closing artificial cell pores influence on encapsulated guests: a super-supramolecular species phenomenon."** (in preparation).

13. A. Müller, S. Roy, A. Merca, H. Bögge, M. Schmidtmann, **"Linking wheel-shaped giant polyoxomolybdates to chains."** (in preparation).

Bibliography

[1] R. P. Feynman, The Pleasure of Finding Things Out, Penguin, London, 2001, p. 144.

[2] P. Ball, Stories of the Invisible: A Guided Tour of Molecules, Oxford University Press, Oxford, 2001, p. 37-39.

[3] Scientific American, Special issue on Nanotech, September (2001). See also reference [62].

[4] (a) J.-M. Lehn, Supramolecular Chemistry, Concepts and Perspectives, Wiley-VCH, Weinheim, 1995;
(b) J.W. Steed, J.L. Atwood, Supramolecular Chemistry, Wiley, Chichester, 2000;
(c) F. Vögtle, Supramolecular Chemistry, Wiley, Chichester, 1991;
(d) J.-P. Behr (Ed) Perspectives in Supramolecular Chemistry, Vol. 1: The Lock and Key Principle (The State of the Art - 100 Years on), Wiley, Chichester, 1994;
(e) A. D. Hamilton (Ed) Perspectives in Supramolecular Chemistry, Vol. 3: Supramolecular Control of Structure and Reactivity, Wiley, Chichester, 1996;
(f) L. F. Lindoy, The Chemistry of Macrocyclic Ligand Complexes, Cambridge University Press, Cambridge, 1989;
(g) J. Simon, P. Bassoul, Design of Molecular Materials: Supramolecular Engineering , Wiley, Chichester, 2000.

[5] J.-P. Sauvage, Acc. Chem. Res. 31 (1998) 611.

[6] T. R. Kelly, H. D. Silva, R. A. Silva, Nature 401 (1999) 150.

[7] (a) S. Mann, Biomineralization: Principles and Concepts in Bioinorganic Chemistry, Oxford University Press, Oxford, 2001;
(b) S. Mann, Angew. Chem. Int. Ed. 39 (2000) 3392;
(c) L. Addadi, S. Weiner, Nature 411 (2001) 753.

[8] M.T. Pope, A. Müller, Angew. Chem. Int. Ed. Engl. 30 (1991) 34.

[9] A. Müller, E. Beckmann, H. Bögge, M. Schmidtmann, A. Dress, Angew. Chem. Int. Ed. 41 (2002) 1162.

[10] A. Müller, Science, 300 (2003) 749.

[11] A. Müller, C. Serain, Acc. Chem. Res. 33 (2000) 2.

[12] A. Müller, S. Roy, Coord. Chem. Rev. 245 (2003) 153.

[13] A. Müller, S.K. Das, E. Krickemeyer, C. Kuhlmann, Inorg. Synth. (Ed. J. Shapley) 34 (2004) 191.

[14] A. Müller, J. Meyer, E. Krickemeyer, C. Beugholt, H. Bögge, F. Peters, M. Schmidtmann, P. Kögerler, M.J. Koop, Chem. Eur. J. 4 (1998) 1000.

[15] M.I. Khan, A. Müller, S. Dillinger, H. Bögge, Q. Chen, J. Zubieta, Angew. Chem. Int. Ed. 32 (1993) 1780.

[16] A. Müller, S. Dillinger, E. Krickemeyer, H. Bögge, W. Plass, A. Stammler, R.C. Haushalter, Z. Naturforsch. B. 52 (1997) 1301.

[17] A. Müller, P. Kögerler, C. Kuhlmann, Chem. Commun. (1999) 1347.

[18] A. Müller, F. Peters, M.T. Pope, D. Gatteschi, Chem. Rev. 98 (1998) 239.

[19] (a) A. Müller, S. Sarkar, S.Q.N. Shah, H. Bögge, M. Schmidtmann, Sh. Sarkar, P. Kögerler, B. Hauptfleisch, A.X. Trautwein, V. Schünemann, Angew. Chem. Int. Ed. 38 (1999) 3238;
(b) A. Müller, M. Luban, C. Schröder, R. Modler, P. Kögerler, M. Axenovich, J. Schnack, P. Canfield, S. Bud'ko, N Harrison, ChemPhysChem. (Concepts) 2 (2001) 517.

[20] A. Müller, S.Q.N. Shah, H. Bögge, M. Schmidtmann, P. Kögerler, B. Hauptfleisch, S. Leiding, K. Wittler, Angew. Chem. Int. Ed. 39 (2000) 1614.

[21] A. Müller, E. Krickemeyer, H. Bögge, M. Schmidtmann, F. Peters, Angew. Chem. Int. Ed. 37 (1998) 3359.

[22] A. Müller, S.K. Das, P. Kögerler, H. Bögge, M. Schmidtmann, A.X. Trautwein, V. Schünemann, E. Krickemeyer, W. Preetz, Angew. Chem. Int. Ed. 39 (2000) 3413.

[23] J. Kepler, Mysterium Cosmographicum, 1593 (see also: M. Kemp, Nature 393 (1998) 123).

[24] A. Müller, P. Kögerler, A.W.M. Dress, Coord. Chem. Rev. 222 (2001) 193.

[25] (a) D. G. Kurth, P. Lehmann, D. Volkmer, H. Cölfen, M. J. Koop, A. Müller, A. Du Chesne, Chem. Eur. J. 6 (2000) 385;
(b) D. G. Kurth, D. Volkmer, M. Ruttorf, B. Richter, A. Müller, Chem. Mater. 12 (2000) 2829;
(c) D. G. Kurth, P. Lehmann, D. Volkmer, A. Müller, D. Schwahn, J. Chem. Soc., Dalton Trans. (2000) 3989;
(d) F. Caruso, D. G. Kurth, D. Volkmer, M. J. Koop, A. Müller, Langmuir 14 (1998) 3462;
(e) D. Volkmer, A. Du Chesne, D. G. Kurth, H. Schnablegger, P. Lehmann, M. J. Koop, A. Müller, J. Am. Chem. Soc. 122 (2000) 1995;
(f) S. Polarz, B. Smarsly, C. Göltner, M. Antonietti, Adv. Mater. 12 (2000) 1503;

(g) S. Polarz, B. Smarsly, M. Antonietti, ChemPhysChem. 2 (2001) 457 ;
(h) L. An, J. M. Owens, L. E. McNeil, J. Liu, J. Am. Chem. Soc. 124 (2002) 13688;
(i) D. Gatteschi, L. Pardi, A. L. Barra, A. Müller, J. Döring, Nature 354 (1991) 463;
(j) A. Müller, E. Diemann, C. Kuhlmann, W. Eimer, C. Serain, T. Tak, A. Knöchel, P. K. Pranzas, Chem. Commun. (2001) 1928.

[26] A. Müller, E. Beckmann, H. Bögge, M. Schmidtmann, unpublished results.

[27] A. Müller, C. Beugholt, M. Koop, S. K. Das, M. Schmidtmann, H. Bögge, Z. Anorg. Allg. Chem. 625 (1999) 1960.

[28] A. Müller, R. Maiti, M. Schmidtmann, H. Bögge, S. K. Das, W. Zhang, Chem. Commun. (2001) 2126.

[29] A. Müller, E. Krickemeyer, H. Bögge, M. Schmidtmann, P. Kögerler, C. Rosu, E. Beckmann, Angew. Chem. Int. Ed. 40 (2001) 4034.

[30] A. Müller, L. Toma, H. Bögge, M. Schmidtmann, P. Kögerler, Chem. Commun. (2003) 2000.

[31] A. Müller, C. Beugholt, H. Bögge, M. Schmidtmann, Inorg. Chem. 39 (2000) 3112.

[32] L. Cronin, C. Beugholt, E. Krickemeyer, M. Schmidtmann, H. Bögge, P. Kögerler, T. K. K. Luong, A. Müller, Angew. Chem. Int. Ed. 41 (2002) 2805.

[33] A. Müller, S. Roy, M. Schmidtmann and H. Bögge, Chem. Commun. (2002) 2000.

[34] I. D. Brown in M. O' Keeffe, A. Navrotsky (Eds) Structure and Bonding in Crystals, Vol. 2, Academic Press, New York, 1981, p. 1-30.

[35] T. Yamase and P. Prokop, Angew. Chem. Int. Ed. 41 (2002) 466.

[36] Beyer-Walter Lehrbuch der Organischen Chemie, 23. Aufl., Hirzel, Stuttgart, 1998, p. 378.

[37] A. Müller, E. Krickemeyer, H. Bögge, M. Schmidtmann, C. Beugholt, S. K. Das, F. Peters, Chem. Eur. J. 5 (1999) 1496.

[38] G. A. Jeffrey, An Introduction to Hydrogen Bonding, Oxford University Press, New York, 1997.

[39] T. Steiner, Angew. Chem. Int. Ed. 41 (2002) 48.

[40] A. Müller, M. Koop, H. Bögge, M. Schmidtmann, C. Beugholt, Chem. Commun. (1998) 1501.

[41] J. Chen, S. Körner, S. Craig, D. Rudkevich, J. Rebek Jr., Nature 415 (2002) 385.

[42] D. Jones, Nature 399 (1999) 25.

[43] S. Lee, B. M. Kariuki, A. L. Richardson, K. D. M. Harris, J. Am. Chem. Soc. 123 (2001) 12684.

[44] L. Pauling, The Nature of The Chemical Bond, 3rd Edn., Cornell University Press, New York, 1980.

[45] A. Müller, E. Krickemeyer, H. Bögge, M. Schmidtmann, F. Peters, C. Menke, J. Meyer, Angew. Chem. Int. Ed. 36 (1997) 484.

[46] This cluster was synthesized in collaboration with Ms. A. Merca.

[47] A. Müller, E. Krickemeyer, H. Bögge, M. Schmidtmann, S. Roy, A. Berkle, Angew. Chem. Int. Ed. 41 (2002) 3604.

[48] D. Voet, J. Voet, Biochemistry, 2nd Edn., Wiley, New York, 1995.

[49] a) H. S. M. Coxeter, Regular Polytopes, 3rd Edn., Dover, New York, 1973;
b) L. R. MacGillivray, J. L. Atwood, Angew. Chem. Int. Ed. 38 (1999) 1018.

[50] A. Müller, B. Botar, H. Bögge, P. Kögerler, A. Berkle, Chem. Commun. (2002) 2944.

[51] A compound where the guanidinium cation binds to a monotopic receptor ([27] − O_9 macrocycle through an array of six H-bonds) is known; see: J.-M. Lehn, P. Vierling, R. C. Hayward, Chem. Commun. (1979) 296.

[52] a) Q. Wang, T. Lin, L. Tang, J. E. Johnson, M. G. Finn, Angew. Chem. Int. Ed. 41 (2002) 459;
b) O. Delgado, A. Dress, A. Müller, in M. T. Pope, A. Müller (Eds) Polyoxometalate Chemistry: From Topology via Self-Assembly to Applications, Kluwer, Dordrecht, 2001.

[53] J. Falbe, M. Regitz (Eds) Römpp Lexikon Chemie, 10. Aufl., Thieme, Stuttgart, 1999.

[54] P. J. Bailey, S. Pace, Coord. Chem. Rev. 214 (2001) 91.

[55] A. Müller, H. Bögge, E. Diemann, Inorg. Chem. Commun. 6 (2003) 52.

[56] A. Müller, E. Krickemeyer, H. Bögge, M. Schmidtmann, B. Botar, M. O. Talismanova, Angew. Chem. Int. Ed. 42 (2003) 2085.

[57] H. H. Kung, Transition Metal Oxides: Surface Chemistry and Catalysis, Elsevier, Amsterdam, 1989.

[58] A. Müller, S. K. Das, S. Talismanov, S. Roy, E. Beckmann, H. Bögge, M. Schmidtmann, A. Merca, A. Berkle, L. Allouche, Y. Zhou, L. Zhang, Angew. Chem. Int. Ed. 42 (2003) 5039.

[59] a) F. Schüth, K. S. W. Sing, J. Weitkamp (Eds) Handbook of Porous Solids, Wiley, Chichester, 2002;
b) M. A. White, Properties of Materials, Oxford University Press, New York, 1999, see Chapter on: Inclusion Compounds.

[60] The term stable means here that at least in the final product always the same type of well-defined capsules are found with the expected functionalities after reactions have taken place in solution. But, in principle, it cannot be excluded that in solution the pores, i.e. the $\{Mo_9O_9\}$ rings, are opened slightly. For more details on stability of cluster capsules, please refer to Chapter 6.

[61] For more on related topic please refer to Chapter 18 of [48]: Transport through Membranes.

[62] For related topics see: a) K. E. Drexler, Nanosystems: Molecular Machinery, Manufacturing, and Computation, Wiley, New York, 1992;
b) C. N. R. Rao, A. Müller, A. K. Cheetham (Eds) Recent Advances in the Chemistry of Nanomaterials, Wiley-VCH, Weinheim, 2004;
c) P. Ball, Made to Measure: New Materials for the 21st Century, Princeton University Press, Princeton, 1997; regarding the importance of pores see also:
d) J. Tersoff, Nature 412 (2001) 135.

[63] A. F. Voegele, K. R. Liedl, Angew. Chem. Int. Ed. 42 (2003) 2114.

[64] W. G. Klemperer, G. Westwood, Nature Materials 2 (2003) 780.

[65] a) F. Franks (Ed) Water: A Comprehensive Treatise, Plenum, New York, 1973;
b) D. Eisenberg, W. Kauzmann, The Structure and Properties of Water, Oxford University Press, New York, 1969;
c) C. H. Cho, S. Singh, G. W. Robinson, Farad. Discuss. 103 (1996) 19;
d) G. W. Robinson, S. B. Zhu, S. Singh, M. W. Evans, Water in Biology, Chemistry, and Physics, World Scientific, Singapore, 1996;
d) P. Ball, H_2O: A Biography of Water, Weidenfeld and Nicolson, London, 1999;
e) F. Franks, Water: A Matrix of Life, 2nd Edn., Royal Society of Chemistry, Cambridge, 2000;
f) L. R. Pratt (Ed) Thematic issue on Water (Issue No. 8), Chem. Rev. 102 (2002).

[66] a) P. Jenniskens, D.F. Blake, Science 265 (1994) 758;
b) P. Jenniskens, S. F. Barnhak, D. F. Blake, J. Chem. Phys. 107 (1997) 1232.

[67] A. Müller in A. Müller, H. -J. Quadbeck-Seeger, E. Diemann (Eds) Facetten einer Wissenschaft: Chemie aus ungewöhnlichen Perspektiven, Wiley-VCH, Weinheim, 2004, p. 84.

[68] M. F. Chaplin, Biophys. Chem. 83 (1999) 211.

[69] M. Henry, Chem. Phys. Chem. 3 (2002) 607.

[70] R. Ludwig, Angew. Chem. Int. Ed. 40 (2001) 1808.

[71] H. Kroto, Pure and Appl. Chem. 62 (1990) 407.

[72] T. Liu, E. Diemann, H. Li, A. Dress, A. Müller, Nature 426 (2003) 59.
See also: T. Liu, J. Clust. Sci., 14 (2003) 215;
ibid J. Am. Chem. Soc. 125 (2003) 312; J. Am. Chem. Soc. 124 (2002) 10942;
A. Müller, S. Roy, Eur. J. Inorg. Chem. (minireview to be submitted).

[73] A. Tsuda, E. Hirahara, Y. Kim, H. Tanaka, T. Kawai, T. Aida, Angew. Chem. Int. Ed. 43 (2004) 6327.

[74] A. Müller, D. Rehder, E. T. K. Haupt, A. Merca H. Bögge, M. Schmidtmann, G. Heinze-Brückner, Angew. Chem. Int. Ed. 43 (2004) 4466.

[75] A. Zewail, Angew. Chem. Int. Ed. Engl. 40 (2001) 4371. See also:
a) H. Rabitz, in A. D. Bandrauck (Ed) Atomic and Molecular Processes with Short Intense Laser Pulses, Plenum, New York, 1988.
b) H. Rabitz, R. Vivie-Riedle, M. Motzkus, K. Kompa, Science, 288 (2000) 824.

[76] N. N. Greenwood, A. Earnshaw, Chemistry of Elements, Pergamon, Oxford, 1989.

[77] a) G. W. Chantry, in A. Anderson (Ed) The Raman Effect, Vol. 1, Marcel Dekker, New York, 1971, p. 70.
b) G. Placzek, in E. Marx (Ed) Handbuch der Radiologie, Akademische Verlagsgesellschaft Leipzig, Vol 6, part 2, p. 205.
For a proposal on the assignments of vibrational spectra of C_{60} and related fullerenes, see: K. Nakamoto, M. A. McKinney, J. Chem. Edu. 77 (2000) 775.

[78] M. Ohm, Doctoral Dissertation, Univerity of Bielefeld, 1997.

[79] A. Müller, S. Polarz, S. K. Das, E. Krickemeyer, H. Bögge, M. Schmidtmann, B. Hauptfleisch, Angew. Chem. Int. Ed. 38 (1999) 3241.

[80] A. Müller, S. Roy, Angew. Chem. Int. Ed. (to be submitted).